FUNCTIONAL CHARACTERIZATION OF HUMAN METHYLTRANSFERASE LIKE PROTEIN 8 IN DNA DAMAGE RESPONSE

LIANG JUNXIN

(B.Sc., SHANDONG UNIVERSITY, CHINA)

A THESIS SUBMITTED

FOR THE DEGREE OF DOCTOR OF PHILOSOPHY

DEPARTMENT OF BIOCHEMISTRY

NATIONAL UNIVERSITY OF SINGAPORE

2014

Declaration

I hereby declare that this thesis is original work done by Doctor Liu Xinyu and me with close collaboration and it has been written by me in its entirety.

I have duly acknowledged all the sources of information which have been used in the thesis.

This thesis has also not been submitted for any degree in any university previously.

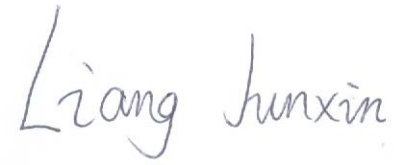

Liang Junxin

20th January 2014

Acknowledgements

First and foremost, I would like to thank my supervisor, Professor Fu Xin-Yuan for his constant support, guidance and encouragement throughout my PhD study.

Next, I would like to thank the members of my Thesis Advisory Committee, Dr. LIM Yoon Pin and Professor Philipp KALDIS (IMCB) for their constructive comments and advice.

Special thanks to my mentor, Dr. Liu Xinyu, for his immediate and continued support of this project and invaluable creative direction. I am extremely grateful for the time he spent mentoring me. It is a great honor working with him. His motivation and enthusiasm in science and research have inspired me greatly. Without his support and guidance, this thesis would not have been possible.

I would like to thank all the current and former members in our lab, for sharing reagents and protocols and for their help in many other ways.

I would like to thank Dr. Lai Kim Peng Mitchell of NUS for help with scintillation counter. Thank Dr. Deng Lih Wen for U2OS and HCT116 cell lines, Dr. Wu Qiang for pPyCAGIP vector, and Dr. Peter Cheung (NTU) for inhibitors and antibodies. Thank Doctor Leilei CHEN (CSI), Doctor Kai Albring (Friedrich-Schiller-University Jena) and Doctor Siew Wee CHAN (IMCB) for their help with soft agar assay.

I would also like to thank the staff in Department of Biochemistry and Cancer Science Institute for their help and assistance throughout my graduate studies.

Last but not least, I'd like to thank my family for their support.

Table of Contents

Summary

Stat3 is an important transcription factor involved in various biological functions. We started our research by a cell line based screening of Stat3 regulated epigenetic factors and identified a novel target of Stat3: methyltransferase like protein 8 (Mettl8). Human Mettl8 is a potential methyltransferase with several featured domains: SANT domain, SAM binding domain for methyltransferase activity, nuclear localization signal, NRB domain and pS/TQ motif, which is a signature of ATM/ATR substrate. Mouse Mettl8 has same domains except pS/TQ motif. Most of our study focused on human Mettl8.

Firstly, we confirmed mouse Mettl8 as a Stat3 target gene by qPCR, ChIP assay, and promoter activity assay, human Mettl8 by ChIP assay.

Secondly, we showed the peculiar localization of overexpressed wildtype and ΔSAM Mettl8 protein in human cells by both biochemical cell fractionation and immunostaining.

Then we validated the SAM binding activity of Mettl8 protein in SAM binding assay *in vitro*. We confirmed that Mettl8 can be specifically phosphorylated by ATM kinase at Serine 405 pSQ motif. Interestingly Mettl8 modulates the activation of ATM itself and its downstream targets such as early DNA damage marker γH2AX, cell cycle checkpoint kinase Chk2, and p53 tumor suppressor in a manner dependent on the SAM binding ability of Mettl8. Triggered by microarray analysis, we found that an

increase of ATM protein level in the ΔSAM Mettl8 mutant cells could be one of the reasons underneath. As a result G2/M checkpoint was activated.

Similar results of ATM pathway activation were observed only with shRNA knockdown of both Mettl8 and its close member Mettl2 in the cells, but not by single knockdown of Mettl8 or Mettl2. Using the new CRISPR/Cas9 technique, we successfully generated cell lines with Mettl8 knocked out, and showed that knocking out Mettl8 alone can induce the ATM pathway activation in a similar manner to that of ΔSAM mutant Mettl8 or double knockdown. Consistently, an increase of ATM protein level was observed in these circumstances. So far the underlining mechanisms of ATM expression level change are unknown; our preliminary data suggested ATM transcription regulation was not the main reason. Despite the similar changes of ATM level and activity, the outcome of cell growth differed significantly between ΔSAM mutant Mettl8, double knockdown and Mettl8 KO cells, implicating more broader and intricate involvement of Mettl8 in other pathways besides ATM.

Taken together, our study revealed a new target of Stat3, a new substrate of ATM and a novel mechanism regulating ATM expression and ATM activation in DNA damage response. Given the essential role of ATM kinase in guarding DNA integrity and in other aspects of cellular life, such as neurogenesis and cancer, this Mettl8-ATM connection could be an attractive therapeutic target in the long term and worth further studies.

List of Tables

List of Figures

List of Symbols

℃	degree Celsius
aa	amino acid
Ala	alanine
ATP	adenosine 5’-triphosphate
bp	base pairs
BRCA	breast cancer susceptibility gene
BSA	bovine serum albumin
CDC	cell-division cycle protein
CDK	cyclin dependent kinase
ChIP	chromatin immunoprecipitation
DAPI	4', 6-diamidino-2-phenylindole
DDR	DNA damage response
DMSO	dimethyl sulfoxide
DNA	deoxyribonucleic acid
DSB	double-strand break
dsDNA	double-stranded DNA
E.coli	*Escherichia coli*

EDTA	ethylenediaminetetraacetic acid
EGTA	ethylene glycol tetraacetic acid
g	gram
GAPDH	glyceraldehyde 3-phosphate dehydrogenase
GFP	green fluorescent protein
Glu	glutamic acid
GST	glutathione-s-transferase
h / hr	hour
HA	haemagglutinin
HEPES	N-2-hydroxyethylpiperazine-N-2-ethane sulfonic acid
HR	homologous recombination
HRP	horseradish peroxidase
IB	immunoblotting
IgG	immunoglobulin g
IP	immunoprecipitation
IR	irradiation
kb	kilobases
KCl	potassium chloride

kD	kilodalton
LB	Luria-Bertani medium
M	molar
M2/Mettl2	methyltransferase like protein 2
M8/Mettl8	methyltransferase like protein 8
MEF	mouse embryonic fibroblast
mg	milligram
$MgCl_2$	magnesium chloride
ml	milliliter
mM	millimolar
Mn	manganese
mRNA	messenger RNA
Na_2PO_4	disodium hydrogen phosphate
NaCl	sodium chloride
NaOH	sodium hydroxide
NHEJ	Non-homologous End Joining
nm	nanometer
NP-40	nonindet-p-40

OD	optical density
PAGE	polyacrylamide gel electrophoresis
PBS	phosphate-buffered saline
PCR	polymerase chain reaction
RNA	ribonucleic acid
SAM	S-adenosylmethionine
SDS	sodium dodecyl sulfate
Ser	serine
ss	single strand
ssDNA	single-stranded DNA
TE	Tris-EDTA buffer
Tris	Tris(hydroxymethyl)aminomethane
UTR	untranslated region
WT	wild type
µg	microgram
µl	microliter
µM	micromolar

Chapter 1 Introduction

1.1 STAT proteins

Our lab has studied STAT (Signal Transducer and Activator of Transcription) proteins, especially Stat3 in different systems for a long time. Stat3 is a well-known transcription factor participating in a wide variety of physiological processes such as ES cell pluripotency maintenance, embryogenesis, cancer and immunity (Levy & Darnell, 2002; Takeda et al., 1997; Ying, Nichols, Chambers, & Smith, 2003; Yu, Pardoll, & Jove, 2009).

STAT proteins are activated by JAK family of receptor-associated tyrosine kinases, which are rapidly activated by autophosphorylation triggered by ligand-induced receptor dimerization. Activated JAK sequentially phosphorylates the receptor to which it has bound, which enables STAT docking to this complex via binding of STAT Src-homology-2 (SH2) domain to the phosphotyrosine residue of the receptor. This leads to phosphorylation of STAT and triggers its release and dimerization. Dimerized phosphorylated STAT proteins rapidly translocate to nucleus and bind to certain gene promoters with specific STAT binding sequences (Figure 1) (Levy & Darnell, 2002). Both cell-type specific transcription and stereotypic mRNA profiles can be induced by STAT signaling in a cell type or tissue specific manner. (Murray, 2007; H. Wang, Chen, He, Zhou, & Luo, 2013), depending on the genomic accessibility of target genes, such as histone modifications or DNA methylations

(Alvarez & Frank, 2004), and possibly on cofactors that further refine gene expression profiles (Murray, 2007).

Stat3 can be activated by a plethora of cytokines, growth factors and peptides. Interleukin-6 family is one of them (Heinrich, Behrmann, Müller-Newen, Schaper, & Graeve, 1998). Oncostatin M (OSM), a member of IL-6 family, is a potent activator of Stat3 and is crucial in hepatic maturation (Kamiya, Kinoshita, & Miyajima, 2001).

Besides transcription factors and signal transduction pathways, the chromatin packaging of the genome is also crucial in setting and maintaining the gene expression pattern of a cell. We are especially interested in the interplay between epigenetics and transcription factors, which in our case is Stat3. Although there are reports about epigenetic genes regulated by Stat3, for example, Stat3 as a major inducer of DNA (cytosine-5-)-methyltransferase 1 (Dnmt1) transcription in malignant T lymphocytes (Q. Zhang et al., 2006), and transcriptional regulation of the histone H3 Lys 27 (H3K27) demethylase Jmjd3 by Stat1 and Stat3 as a novel mechanism for inflammatory gene expression in microglia (Przanowski et al., 2013), it remains largely unappreciated for Stat3 mediated epigenetic regulations.

To explore Stat3 regulated epigenetics, we screened for Stat3 targets from a large number of epigenetics related genes in mouse adult hepatocytes-derived cell lines by qPCR (primers available upon request) and found several candidates, one of which is methyltransferase like protein 8 (Mettl8), which has a predicted Stat3 binding site.

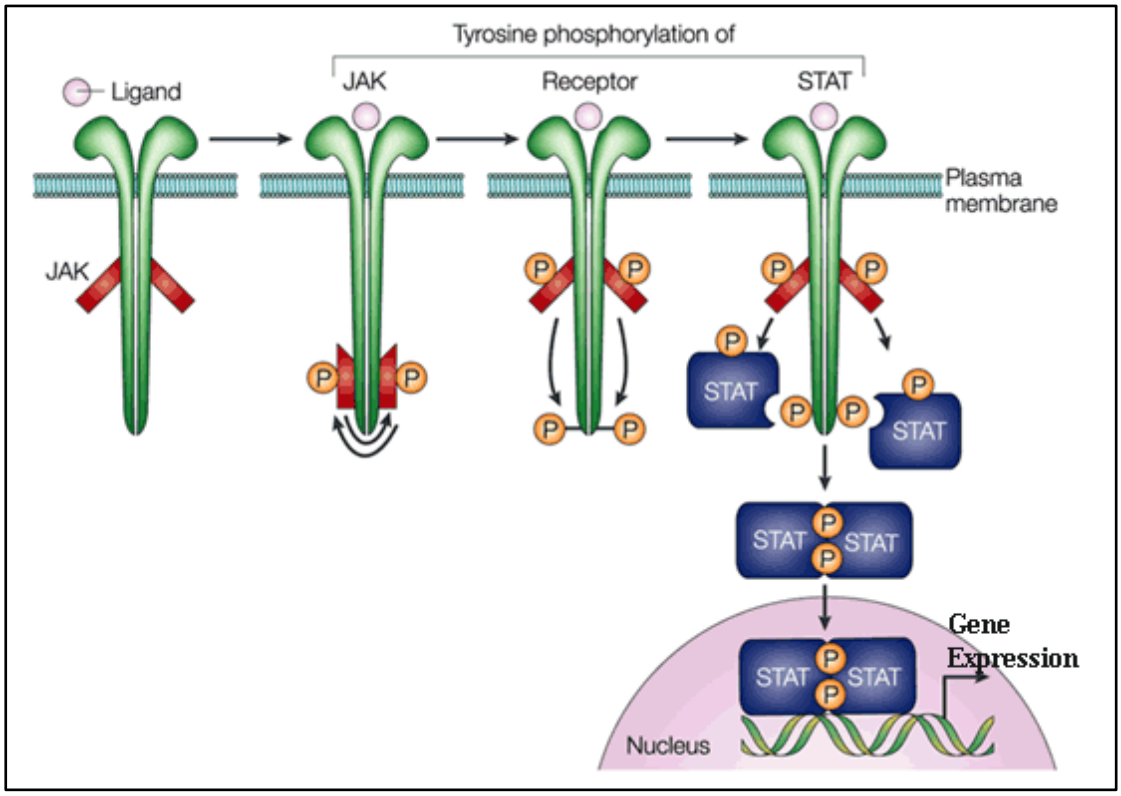

Figure 1. Canonical JAK–STAT pathway.

Sequential tyrosine phosphorylation triggered by cytokine-receptor interaction. Receptor dimerization allows transphosphorylation and activation of Janus Kinase (JAKs). This is followed by phosphorylation of receptor tails and the recruitment of STAT proteins through their SH2 domains. STAT tyrosine phosphorylation then occurs. Dimerization of activated (tyrosine phosphorylated) STAT is followed by nuclear entry and expression of target genes.

Figure and caption adapted from (Levy & Darnell, 2002).

1.2 Methyltransferase like protein 8

1.2.1 Mettl8 gene and protein

Mettl8 was first reported by Schuger group as TIP (tension-induced/inhibited proteins) gene, as splicing isoforms of Mettl8 in mouse were identified in tension induction assay (Jakkaraju, Zhe, Pan, Choudhury, & Schuger, 2005). Two different TIPs were shown to play divergent roles in myogenic versus adipogenic differentiation of lung embryonic mesenchymal cells. Later they claimed that TIP family composed of eight isoforms generated by alternative splicing from a single gene (Mettl8) located in chromosome 2q22-23 in mouse and 2q31.1 in human (Badri, Zhou, Dhru, Aramgam, & Schuger, 2008), although some of these transcripts are regarded as nonsense-mediated decay in Ensembl database. According to NCBI, mouse Mettl8 is a gene with 10 exons across 118kbp genome and human Mettl8 with 10 exons across 153kbp. The full-length mRNA of mouse and human Mettl8 are of 2370 bp and 8154 bp respectively.

Regulatory transcription factor binding site analysis on mouse Mettl8 gene promoter showed that it has binding sites of many important transcription factors, such as Stat3, Oct1 (octamer-binding transcription factor-1, also called Pou2F1), AP-1 (activator protein 1), and Foxa2 (forkhead box protein A2), all of which are also present in human Mettl8 promoter.

Domains of mouse Mettl8 gene were mapped: a SANT (*s*witching-defective protein 3 [Swi3], *a*daptor 2 [Ada2], *n*uclear receptor corepressor [N-CoR], and *t*ranscription

factor IIIB [TFIIIB]) domain, a SAM domain (the D/ExGxGxGx signature motif present in some *S-a*denosyl-L-*m*ethionine-binding proteins), and an NRB domain (*n*uclear *r*eceptor *b*ox, represented by the LXXLL signature motif). A nuclear localization signal (NLS) was also found in moue Mettl8 with the peptide sequence LRFKKGRCL (Badri et al., 2008; Jakkaraju et al., 2005). The corresponding NLS in human is LRFKKGHCL with one amino acid difference.

The Schuger group made an in-depth study of the Mettl8 SANT domain in mouse and found that even the shortest isoform of Mettl8 with only SANT domain could induce adipogenesis via SANT domain dependent p300 recruitment which in turn showed histone acetylation activity on the promoter of PPARγ2, a key adipogenic transcription factor (Badri et al., 2008). Yet they failed to detect the SAM binding ability of TIP3, one isoform of mouse Mettl8 by filter binding assay (Jakkaraju et al., 2005).

So far there were no reports on the physiological role of human Mettl8 protein in PubMed. Human Mettl8 was strongly stained in gastric parietal cells, distal renal tubules, subsets of lymphoid and bone marrow poietic cells in the Human Protein Atlas. In the International Cancer Genome Consortium (ICGC) data portal, 53 mutations of human Mettl8 gene were found in 40 patient donors in 15 cancer projects to date, among which the highest percentage of donor with mutation lies in prostate cancer (37.50%), liver cancer (19.05%) and esophageal cancer (13.64%). All mutations are single base substitutions located across the gene except only one in frame deletion found in ovarian cancer.

Full-length human Mettl8 protein has 407 amino acids. Sequence analysis reveals that similar to mouse Mettl8, it is featured by an N-terminal SANT domain, a middle SAM domain for possible methyltransferase activity, and a C-terminal NRB motif as shown in Figure 2. A unique feature of Mettl8 protein is its pS/TQ motif candidate that sits at the very C-terminus, suggesting Mettl8 may be a substrate of phosphoinositol-3 kinase like kinase (PIKK). Mouse Mettl8 has no pS/TQ motif (Figure 3).

We generated expression vectors with Flag human Mettl8 ΔSANT (52-87aa deleted), ΔSAM (200-208aa deleted), and ΔNRB (295-300aa deleted) mutants (Figure 2). To study the pS/TQ motif, we mutated Ser405 to either nonphosphorylatable Ala (S405A) or phospho-mimic Glu residues (S405E).

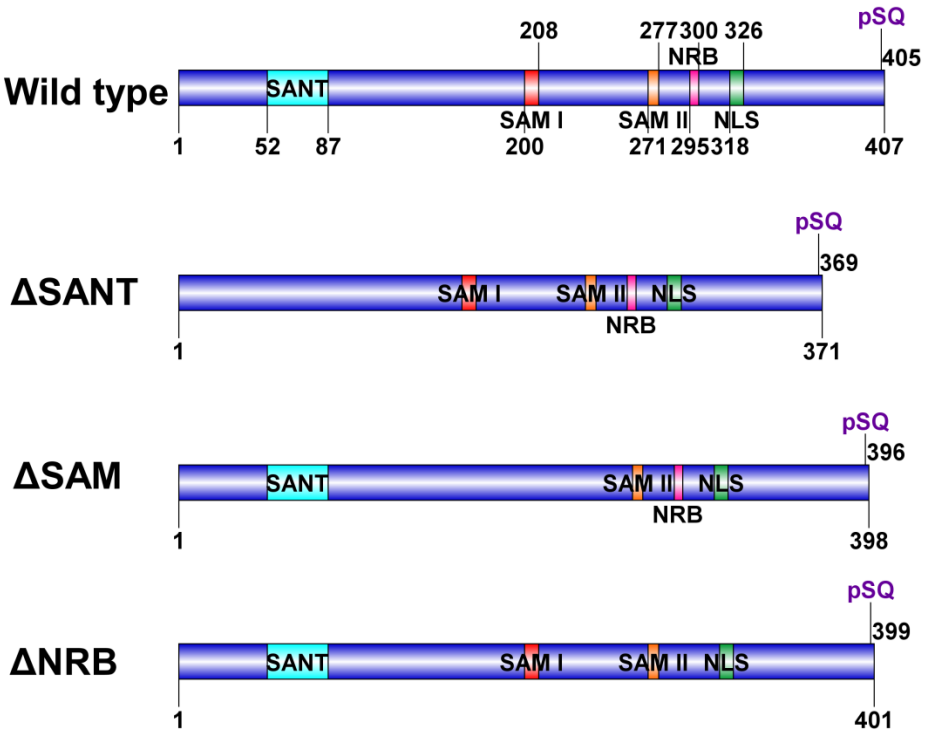

Figure 2. Domain structure of human Mettl8 protein.

Schematic structure of wildtype human Mettl8 protein. Mettl8 is featured with SANT domain, SAM binding domain, NRB domain, NLS and pS/TQ motif, the functions of which are described in detail in the main text. The domain structures of Mettl8 mutants used in this study are also shown.

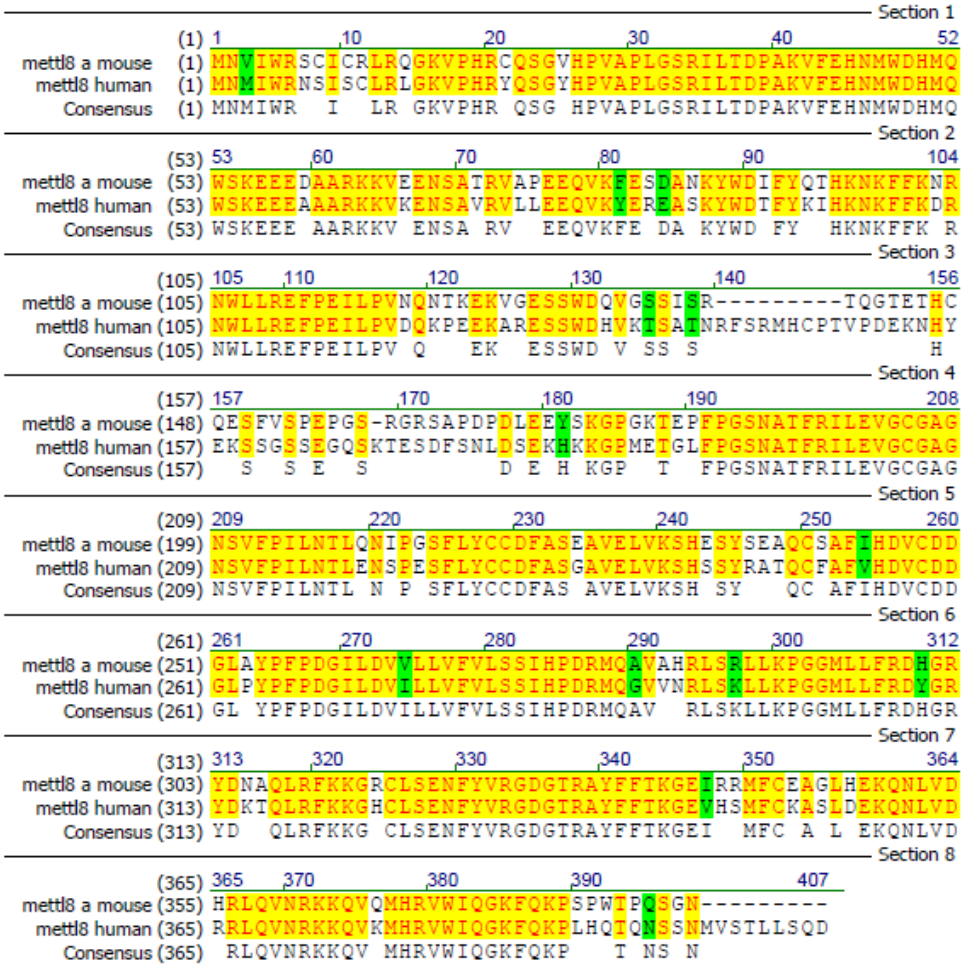

Figure 3. Sequence alignment of human Mettl8 and mouse Mettl8 proteins.

Alignment of human Mettl8 with moue Mettl8 protein sequence using Vector NTI software showed the lack of pS/TQ motif in mouse Mettl8 protein.

Identical aa: red text on a yellow background;
Block of Similar aa: black on a light green background;
Non-similar aa: black on a white background.

1.2.2 Methyltransferase

The most striking feature of Mettl8 is its S-adenosylmethionine (SAM, also known as AdoMet) binding domain. SAM was discovered in 1953 as a conjugate of methionine and the adenosine moiety of ATP (Catoni, 1953). It is involved in a diversity of metabolic reactions and is the second most widely used and versatile small molecule ligand after ATP (Loenen, 2006). The most well-known biological role of SAM is as a methyl donor for the majority of methyltransferases (MTases) (Figure 4a).

Most methyl transfer reactions catalyzed by SAM-dependent MTases are bimolecular nucleophilic substitution (S_N2) reactions, in which one bond is broken and one bond is formed synchronously. The methyl groups are transferred from SAM to a large variety of acceptor substrates, varying from small molecules to macromolecules like protein, nucleic acid, and lipid, generating S-adenosyl-homocysteine (SAH) as the by-product (Figure 4A). SAM-dependent MTase are inhibited by the product, SAH, which can accumulate in the presence of homocysteine because the equilibrium of the SAH hydrolase reaction favors SAH formation (Figure 4B) (Moat & McDowell, 2002).

The SAM-dependent MTases share little sequence identity, but incorporate some highly conserved structural folds (Martin & McMillan, 2002). There are five known families of typical SAM-dependent MTases (Classes I to V) based on their distinct structural features (Schubert, Blumenthal, & Cheng, 2003). A further class of radical SAM-dependent MTases that methylate a range of substrates at unreactive,

non-nucleophilic carbon and phosphorus centers was recently discovered (Q. Zhang, van der Donk, & Liu, 2012).

A)

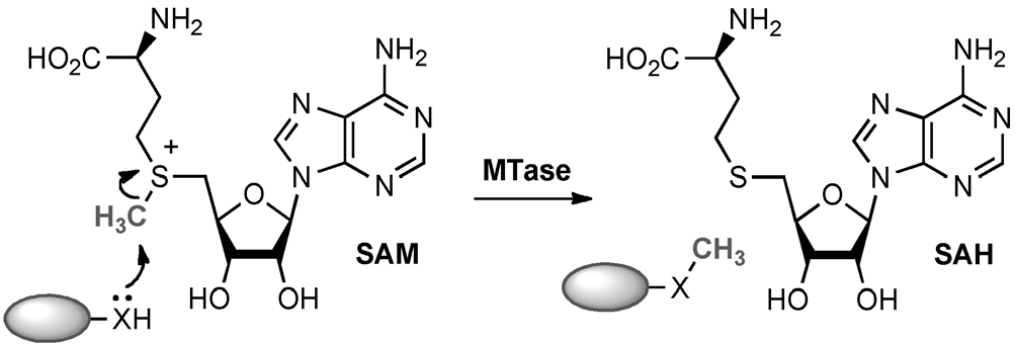

B)

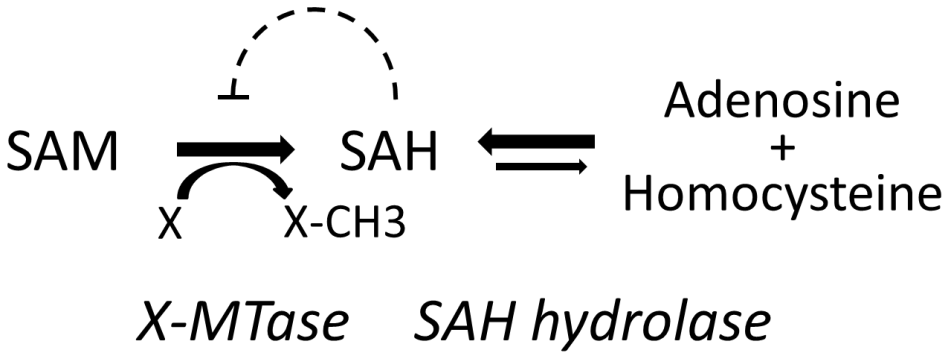

Figure 4. Schematic description of methyl transfer reaction.

A) The S_N2 mechanism common to the SAM-dependent MTases.
Nucleophilic groups of MTase substrates are represented by _XH.
Figure and caption adapted from (Struck, Thompson, Wong, & Micklefield, 2012).
B) Metabolic relationships between SAM, SAH, and homocysteine in mammalian cells. The details are described in the main text. The methyl-accepting substrates are designed X.
Figure and caption adapted from (Moat & McDowell, 2002).

The SAM binding domain of Mettl8 consists of seven-stranded beta sheet with three helices on each side, which defines the Rossmann fold (Figure 5), a hallmark structure of class I methyltransferase (Schubert et al., 2003). The N-terminal region of this core fold contains highly conserved glycine-rich sequence E/DXGXGXG (often referred to as motif I) between the first β-strand (β1) and the α-helix (αA), which interacts with the amino acid portion of SAM (Struck et al., 2012).

Class I MTases with the Rossmann fold are the largest group of MTases, responsible for the majority of methylation reactions in all life forms. Through the S_N2 mechanism (Figure 4), they methylate a very large plethora of small molecules, from simple halide ions to O-, N-, C-, S-, Se and As-centered nucleophiles in bioactive molecules derived from several branches of primary and secondary metabolism (Struck et al., 2012).

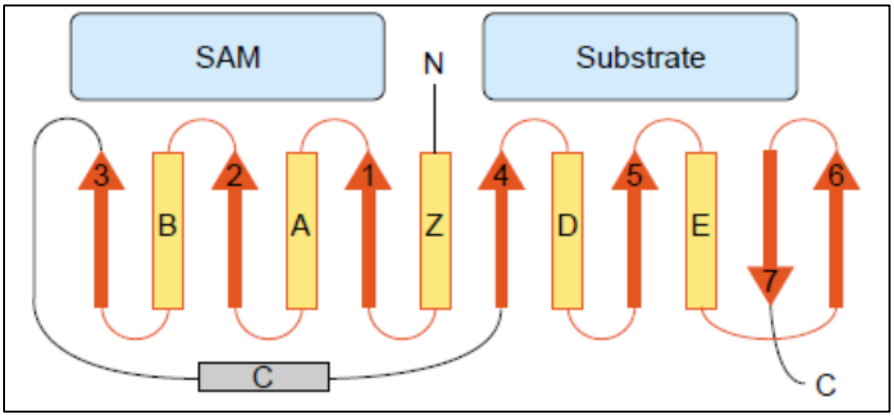

Figure 5. Rossmann fold.

Schematic picture of the topology of the core fold of the Class I SAM-MTases, indicating the SAM- and substrate-binding regions of the fold. Helices are shown as yellow cylinders, strands as red arrows. αC is shown in grey, because it is not always conserved in the core fold. The N and C termini are labeled.

Figure and caption adapted from (Martin & McMillan, 2002).

Besides small molecule methylation, the class I MTases also includes all DNA methyltransferases (Dnmts) (Struck et al., 2012). DNA methylation is essentially involved in a variety of important biological functions including gene expression regulation, mutation repair, gene imprinting, preservation of chromosomal integrity, X-chromosome inactivation, embryo development and diseases. Based on their structure and functions, Dnmts are divided into two major families in mammals: maintenance methyltransferase (Dnmt1) and de novo methyltransferases (Dnmt3a, Dnmt3b, and Dnmt3L) (Bird, 2002).

The flexibility of the Class I structure is further illustrated by existence of a large family of RNA C5-cytosine MTases within this class (Reid, Greene, & Santi, 1999).

Some protein methyltransferases (PMTs) also belong to class I MTases. But the largest group of PMTs, which are the SET-domain protein methyltransferases, belong to the class V MTases. All known SET-domain MTases transfer work on lysine residues within various nuclear proteins involved in chromatin function and transcription regulation, and also in some diverse proteins like Rubisco and cytochrome C (Kozbial & Mushegian, 2005).

Due to the high diversity of substrates for SAM dependent MTase, it is quite challenging to identify the native substrate for a novel MTase (Martin & McMillan, 2002; T. Petrossian & Clarke, 2009). In a recent bioinformatics study (Richon et al., 2011), Mettl8 and its close member mettl2 (Figure 6) are clustered closely with protein arginine methyltransferase (PRMT) family based on the similarity of SAM

binding domain only.

Mettl2, the closest member of Mettl8 as mentioned, has one variant in mouse and two variants in human. Human Mettl2A and Mettl2B are both 378 amino acids with only 5 amino acids different between each other. Mettl2A is encoded by a gene that maps to human chromosome 17q23.2; Mettl2B is encoded by a gene that maps to human chromosome 7q32.1. The two human Mettl2 genes might result from gene duplication which was a possible evolutionary event. Human Mettl2 has similar SANT, SAM, NRB domains and NLS motif to Mettl8, except the S/TQ motif (Figure 6).

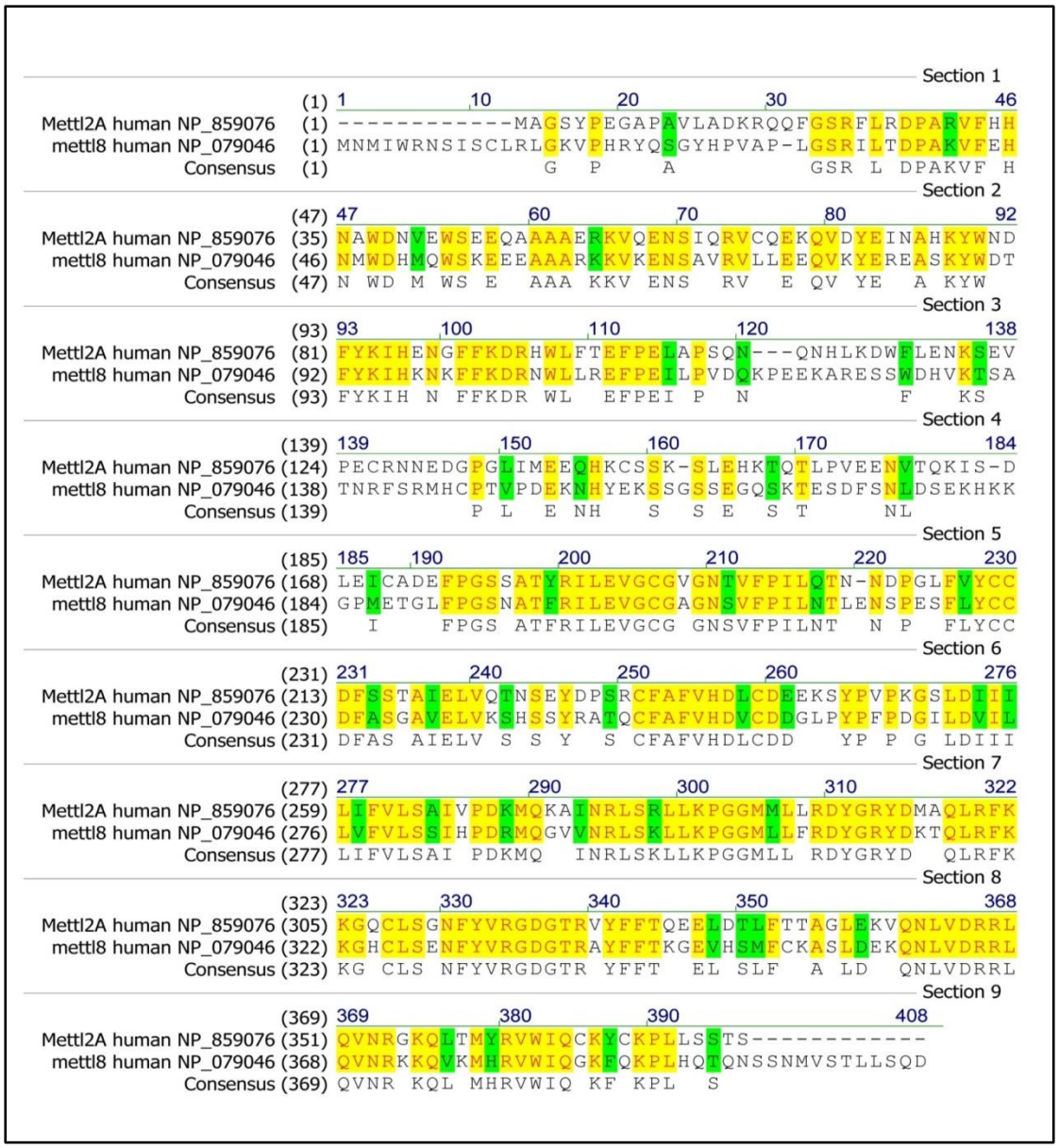

Figure 6. Sequence alignment of human Mettl8 and Mettl2A proteins.

Alignment of human Mettl8 with Mettl2A protein sequence using Vector NTI software showed the high homology between these two proteins.

Identical aa: red text on a yellow background;
Block of Similar aa: black on a light green background;
Non-similar aa: black on a white background.

1.2.3 Methyltransferase like (Mettl) proteins

There are more than 30 genes assigned as methyltransferase like protein (Mettl) genes by the HUGO Gene Nomenclature Committee (HGNC), such as Mettl1, Mettl2A&B, Mettl3, Mettl4, Mettl5 etc., but they do not belong to any specific protein family. Functions of some of the Mettl proteins were revealed, Mettl1 as a 7-methylguanosine-methyltransferase (Alexandrov, Martzen, & Phizicky, 2002), Mettl2's homolog ABP140 as a methyltransferase for 3-methylcytidine at position 32 of tRNAs in *Saccharomyces cerevisiae* (Noma et al., 2011), Mettl3 as N6-adenosine-methyltransferase (Bokar, Shambaugh, Polayes, Matera, & Rottman, 1997), Mettl6's effect in cisplatin sensitivity in lung cancer cells (Huang et al., 2011), Mettl10 methylating lysine residues of eukaryotic elongation factor 1A in *Saccharomyces cerevisiae (Lipson, Webb, & Clarke, 2010)*, Mettl11A as a histone methyltransferase (Richon et al., 2011) and human Mettl14 catalyzing m^6A RNA methylation together with Mettl3 (Liu et al., 2013). However, the majority of Mettl proteins remain poorly studied, and Mettl8 is one of them.

1.2.4 pS/TQ motif

Besides the SAM binding domain, another distinguished and unique feature of human Mettl8 protein is its pS/TQ motif candidate that sits at the very C-terminus.

ATM and its related PIKK family members ATR and DNA-PKcs preferentially phosphorylate their substrates on serine or threonine residues followed by glutamine residue, so-called SQ/TQ (or S/TQ) motif. This motif was first screened out by a

peptide mutagenesis analysis of p53 protein, an established substrate of ATM in response to DNA damage (S. T. Kim, Lim, Canman, & Kastan, 1999).

S/TQ is a minimal essential requirement for all three kinases. But significant differences exist in the co-factor requirements of ATM and ATR compared with DNA-PKcs for optimal *in vitro* activity. ATM and ATR require Mn^{2+}, while DNA-PKcs requires Mg^{2+}, DNA ends, and Ku proteins. In addition, hydrophobic amino acids and negatively charged amino acids immediately N-terminal to serine or threonine are positive determinants and positively charged amino acids in the region are negative determinants for substrate phosphorylation (S. T. Kim et al., 1999).

SQ/TQ cluster domains, termed as SCDs, were found in a large number of ATM/ATR substrates. SCDs are now generally considered as another signature domain characteristic of DNA-damage-response proteins besides BRCT and FHA domains (Traven & Heierhorst, 2005).

As we can see, the C-terminus of Mettl8 sequence STLLSQD fits with all the requirements of being a PIKK substrate, so it could be a novel substrate of ATM or ATR or DNA-PKcs. And it naturally infers to us whether Mettl8 is related to DNA damage.

1.3 DNA damage response (DDR)

Keeping an intact genome from generation to generation is crucial for all life forms. Human cells are constantly exposed to DNA damages from endogenous and exogenous environments tens of thousands of times every day (Ciccia & Elledge, 2010). The endogenous damages can come from cellular metabolic or hydrolytic processes, oxidative stresses and aging (Barnes & Lindahl, 2004). Exogenous insults to DNA integrity include ultraviolet (UV) light, radiation, and DNA-damaging chemicals.

DNA lesions will affect genome replication and transcription. And if left unattended or not repaired correctly, DNA damages will have deleterious effects to genome stability, as they may lead to gene mutations, wider genome aberrations or chromosome instabilities which will affect normal cellular functions and result in diseases such as cancers. Genome instability is one new hallmark of cancer which enables more mutations, allowing tumor cells to survive, proliferate and disseminate (Hanahan & Weinberg, 2011).

To maintain genome stability, life has evolved the DNA-damage response (DDR). DNA damage response involves multi-cascade events to sense the damage, transduce the signal and activate the effectors, either to repair DNA or mount checkpoints on cell cycle progression (Zhou & Elledge, 2000). DDR is highly related to a lot of cellular processes, such as cell cycle, autophagy and apoptosis (Figure 7) (Jackson & Bartek, 2009), and has been increasingly appreciated as guardian of genome

stability (Bartek, Bartkova, & Lukas, 2007; Bartkova et al., 2005; Bartkova et al., 2006). DDR defects will lead to numerous diseases, a complete list of which can be found in a review by Ciccia, A. and Elledge (Ciccia & Elledge, 2010).

Being such a crucial protection mechanism, DDR is present from bacteria to plants to humans. Here only DDR in mammals especially humans will be introduced.

To detect and repair different kinds of DNA lesions, cells have developed six major repair pathways: BER (base excision repair) to correct small chemical alterations, MMR (mismatch repair) to replace mismatched DNA bases with correct ones, NER (nucleotide excision repair) to repair more bulky lesions and intrastrand crosslinks, DR (direct repair) for direct reversal of DNA alkylation damage, HR (homologous recombination) and NHEJ (non-homologous end joining) pathways for DNA double strand break repair (Figure 8) (Postel-Vinay et al., 2012).

There are also other DNA-repair pathways available to guard genome stability, such as Fanconi Anemia/BRCA pathway (Kennedy & D'Andrea, 2005), translesion DNA synthesis and single-strand annealing.

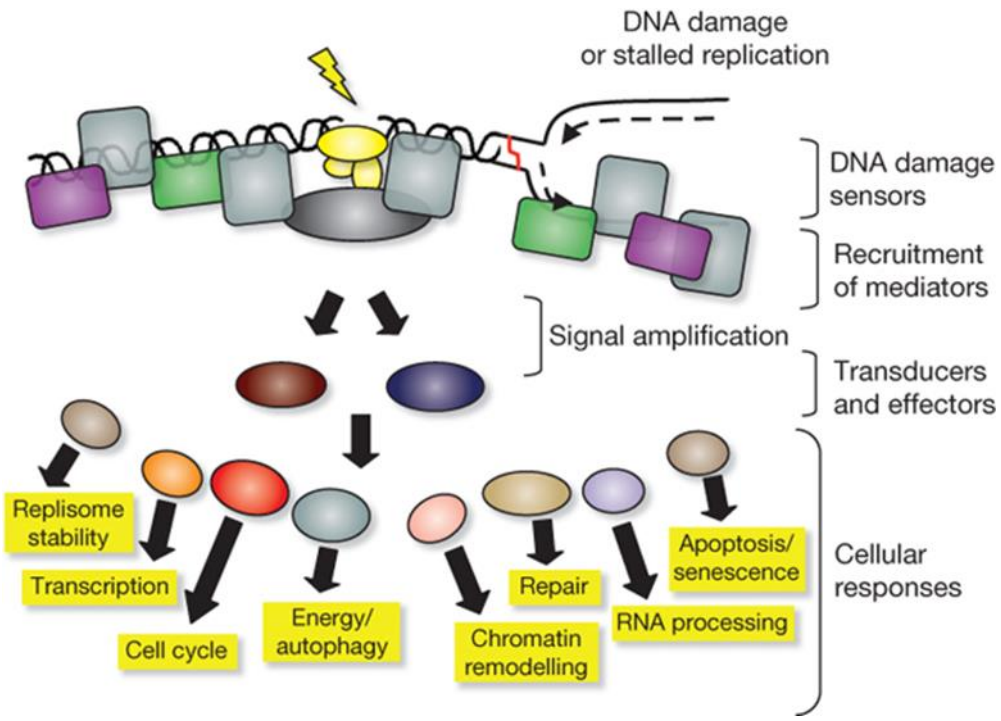

Figure 7. Model for the DDR.

The presence of a lesion in the DNA, which can lead to replication stalling, is recognized by various sensor proteins. These sensors initiate signaling pathways that have an impact on a wide variety of cellular processes.

Figure and caption adapted from (Jackson & Bartek, 2009).

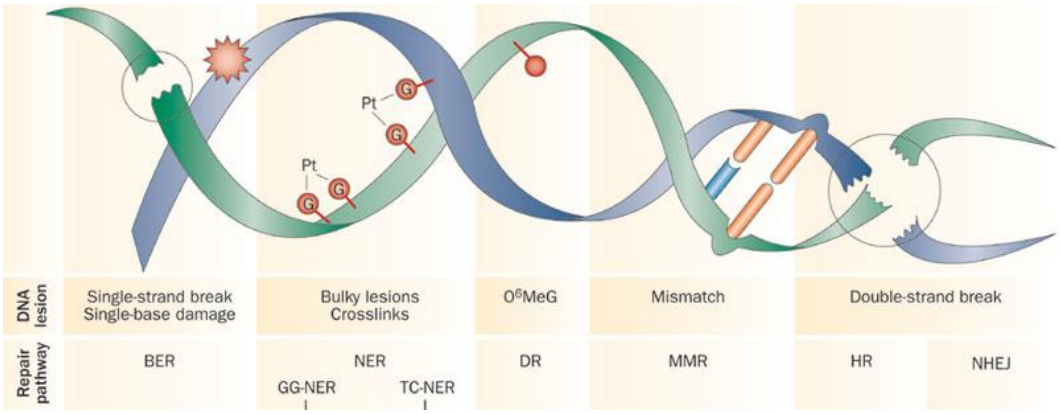

Figure 8. Main DNA lesions and corresponding DNA damage repair pathways.

DNA lesions that affect a single strand without significantly disrupting the helical structure are generally repaired by base excision repair (BER), whereas DNA damage significantly distorting the DNA helix is repaired by nucleotide excision repair (NER). Direct repair (DR) copes with small chemical changes affecting a single base, and mismatch repair (MMR) repairs mismatches in the pairing of DNA caused by replication errors. Finally, homologous recombination (HR) and non-homologous end joining (NHEJ), although distinct pathways, are both involved in the repair of DNA double-strand breaks: HR allows 'error free' repair of the lesion whereas NHEJ is an 'error prone' mechanism that repairs DNA but at the cost of introducing mutations into the genome (Jalal, Earley, & Turchi, 2011). The selection of HR or NHEJ is primarily based on the phase of the cell cycle and the expression, availability and activation of DNA-repair proteins (Shrivastav, De Haro, & Nickoloff, 2008).

Abbreviations: GG-NER, global genome NER; O^6MeG, O^6-methylguanine; TC-NER, transcription-coupled NER.

Figure and caption adapted from (Postel-Vinay et al., 2012).

1.4 Double strand break (DSB) repair signaling and ATM

Among the various kinds of DNA lesions discussed above (Figure 7), DNA double strand break (DSB), which usually arises from ionizing irradiation and chemotherapeutic drugs, is the most deleterious form of damage to chromosome stability, as it will easily lead to chromosome rearrangement and loss if left unrepaired. DNA DSB can also arise from meiotic recombination and immunoglobulin gene rearrangements. To eliminate DSB with minimum alteration in nucleotide sequence, cell has evolved a whole set of complicated machinery which involves a spatiotemporal orchestration of an array of protein factors to sense and repair the damage efficiently.

1.4.1 ATM

ATM (Ataxia telangiectasia mutated), is a big protein with a high molecular weight of about 370 kD. It's a serine/threonine protein kinase belonging to PIKK superfamily. Being an apical kinase in DSB signaling, ATM plays a central role in sensing DNA DSB and coordinating the checkpoint responses. It has two close PIKK family members: ATR (ATM and Rad3 related) and DNAPKcs (DNA dependent protein kinase catalytic subunit), which are believed to play some redundant roles but with some specificity in different damage circumstances.

ATM was first identified as the gene responsible for human autosomal recessive disorder ataxia-telangiectasia which is characterized with hypersensitivity to irradiation, susceptibility of tumor formation, immunodeficiency, neuronal

degeneration, chromosomal instability, and cell cycle abnormalities (Savitsky et al., 1995). Consistently, ATM-deficient mice show many of the same symptoms found in human ataxia-telangiectasia patients and in cells derived from them (Elson et al., 1996; Kuljis, Xu, Aguila, & Baltimore, 1997; Xu et al., 1996; Xu & Baltimore, 1996).

Upon irradiation ATM is rapidly activated by dimer dissociation and auto-phosphorylation at Serine 1981 (Bakkenist & Kastan, 2003). As a key molecule initiating the DSB response, ATM activation mechanism has been intensively investigated and some elements have been revealed: Mre11-Rad50-Nbs1 (MRN) complex is required for recruitment of ATM to the damage site (Uziel et al., 2003) and ATM is acetylated by TIP60 (also known as KAT5) at its C-terminus prior to its autophosphorylation (Sun, Jiang, Chen, Fernandes, & Price, 2005; Sun, Xu, Roy, & Price, 2007), which is recently found to be dependent on H3K9me3 mark and tyrosine phosphorylation of TIP60 by C-Abl (Kaidi & Jackson, 2013). It is accepted that ATM activation requires both the modification of protein complex and chromatin status around the DNA break site, and there is more to be explored given the intrinsic complexity of chromatin structure.

1.4.2 DSB sensing and repair

As introduced before, there are two major repair pathways for DNA double strand break repair: HR (homologous recombination) and NHEJ (non-homologous end joining). Besides general genome maintenance, both of these two pathways are utilized in specialized recombination reactions. NHEJ is crucial for complete V(D)J

recombination and teleomere maintenance, while HR is important for meiosis and interstrand crosslink repair (Ferguson & Alt, 2001). The balance between the two DSB repair pathways is dependent on species, cell types and different cell cycle phases (Shrivastav et al., 2008).There is a detailed, state-of-the-art review on DSB repair pathway choice (Chapman, Taylor, & Boulton, 2012).

Generally, in radiation induced DSB repair, NHEJ pathway is active in all cell cycle phases and can be error-prone as it simply rejoins broken DNA ends with no template, while HR is preferentially active in late S/G2 phases of the cell cycle when a homologous sister chromosome or chromatid is available for direct base-pairing to repair of a DNA DSB without error (Figure 9) (Rothkamm, Krüger, Thompson, & Löbrich, 2003). In mitotic cells, DSB induced DDR is not fully activated until cells enter G1 phase (Giunta, Belotserkovskaya, & Jackson, 2010). Here a general interphase full DSB repair signaling is described.

Within seconds, if DSBs are detected by the Ku70–Ku80 complexes, DNA-PKcs will be recruited to damage sites (Falck, Coates, & Jackson, 2005), which promotes NHEJ. The enzymes involved in NHEJ include Ku, DNA-PKcs, Artemis, XLF (also called Cernunnos), XRCC4, and DNA ligase IV etc. (Figure 9). Poly (ADP-ribose) polymerase 1 (PARP1) competes with Ku protein binding to DSBs to promote HR (Hochegger et al., 2006). After initial accumulation of the MRN complex to DSBs mediated by PARP1 (Haince et al., 2008), ATM is activated followed by phosphorylation of a variant of histone H2A called H2AX at its C-terminal pS/TQ site (termed γH2AX) (Rogakou, Pilch, Orr, Ivanova, & Bonner,

1998). γH2AX is then deposited around DNA double strand breaks, up to 1 mega-base surrounding region (Burma, Chen, Murphy, Kurimasa, & Chen, 2001). This will substantially propagate the damaging signal and serves as a beacon to recruit many mediators to the site, such as mediator of DNA-damage checkpoint 1 (MDC1) (Stewart, Wang, Bignell, Taylor, & Elledge, 2003), Mre11-Rad50-Nbs1 (MRN) complex (Uziel et al., 2003), p53-binding protein 1 (53BP1) (B. Wang, Matsuoka, Carpenter, & Elledge, 2002), BRCA1 (Cortez, Wang, Qin, & Elledge, 1999), and KRAB-associated protein-1 (KAP1) (Goodarzi et al., 2008), all of which are substrates of ATM and form foci-like structure colocalized with γH2AX in the nucleus upon IR. This so-called IRIF (ionizing radiation induced foci) indicates the assembly of complex involving a large number of proteins which provides the platform to execute the DNA repair (Figure 9) and cell cycle checkpoint function. Proteins involved subsequently in the DSB repair include BRCA1/2, replication protein A (RPA), Bloom syndrome protein (BLM), X-Ray repair cross-complementing protein 2/3 (XRCC2/3), MUS81-EME1 complex, RAD51, RAD52, RAD54 and RAD51-B, C, D (Figure 9).

Although recently ATM was reported to be dispensable for HR repair of enzyme-induced euchromatic DSBs, the essential role of ATM in DSB repair is unquestionable as ATM-deficient cells are hypersensitive to DSB, suggesting the existence of ATM-dependent alternative repair pathways other than HR for DSB repair (Rass, Chandramouly, Zha, Alt, & Xie, 2013). ATM is also crucial in facilitating heterochromatin DSBs repair by phosphorylating KAP-1 to make the heterochromatin less compacted and more accessible to repair (Goodarzi et al., 2008).

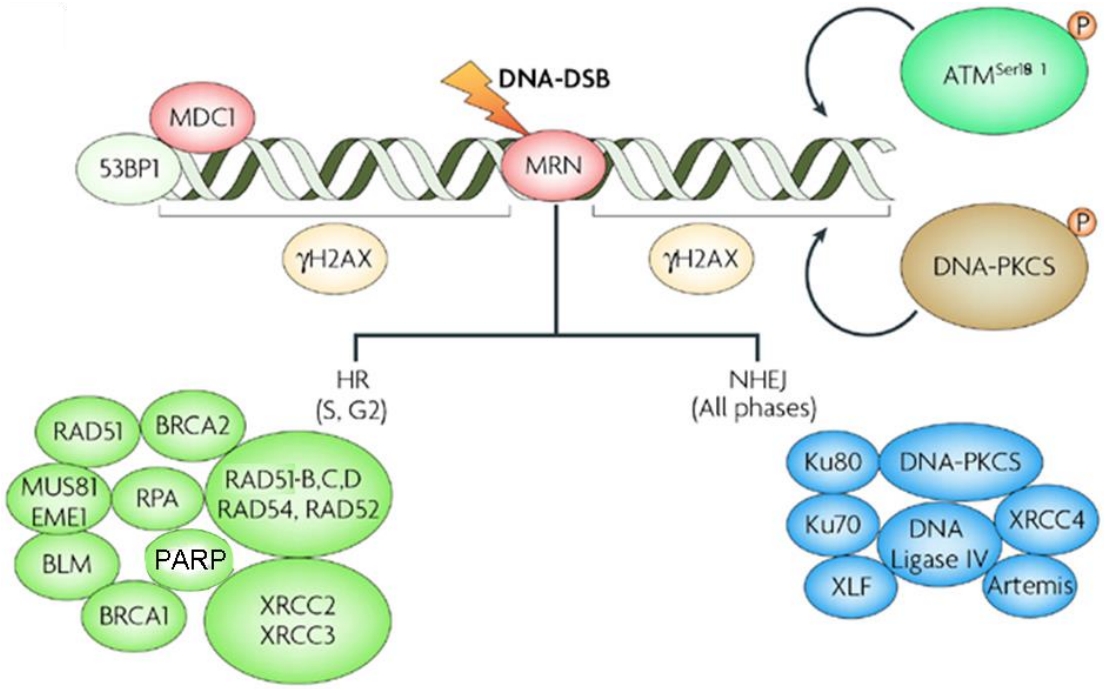

Figure 9. DNA double strand break sensing and repair pathways.

Under normoxic conditions, a DNA double-strand break (DSB) is sensed by the MRN complex. This leads to activation and recruitment of the ATM and DNA-PKcs kinases and phosphorylation of the histone variant H2AX (termed γH2AX, yellow) around the site of the break. Subsequently, a number of DNA damage sensing proteins, such as mediator of DNA damage checkpoint 1 (MDC1) and p53-binding protein 1 (53BP1), and DNA DSB repair proteins involved in HR and NHEJ are recruited within the first 1–6 h of damage recognition to repair the DNA DSB. The NHEJ repair pathway can be used within any phase of the cell cycle and can be error-prone. The HR pathway is preferentially active in the S and G2 phases of the cell cycle when a homologous sister chromosome or chromatid is available for direct base-pairing to effect error-free repair of a DNA DSB.

Abbreviations: PARP, poly (ADP-ribose) polymerase; BLM, Bloom syndrome; EME1, essential meiotic endonuclease 1 homolog 1 (S. pombe); RPA, replication protein A.

Figure and caption adapted from (Bristow & Hill, 2008).

1.5 ATM substrates

The short S/TQ motif is found in a plethora of substrates in response to DNA damage. Among those diversified substrates of ATM, tumor suppressor p53 is well studied. p53 is found to be rapidly phosphorylated at Serine 15 pSQ site in response to IR (Banin et al., 1998), and stabilized via regulation of MDM2-p53 interaction (Chehab, Malikzay, Appel, & Halazonetis, 2000; Hirao et al., 2000; S. Y. Shieh, Ikeda, Taya, & Prives, 1997). This modification is accompanied by p300/PCAF mediated acetylation at its C-terminal stretch (Gu & Roeder, 1997; Ito et al., 2001), which collectively then modulates p53 transactivation ability and turns on downstream target genes required for cell cycle arrest, apoptosis and many other functions. One well-studied effector of p53 is p21 (also called WAF1, CIP1) which can inhibit both the cyclin-dependent G1 kinases and the G2/M-specific CDC2 kinase and thus activate G1 and G2/M cell cycle arrest (Agarwal, Agarwal, Taylor, & Stark, 1995). ATM also phosphorylates the checkpoint kinase to further intertwine the complex network via the checkpoint kinase 1/2 (Chk1/2) mediated phosphorylation on p53 as well as MDM2, and cell cycle regulator CDC25 (Di Leonardo, Linke, Clarkin, & Wahl, 1994).

Given the important function of ATM-p53 in genome stability maintenance (Cao et al., 2006), the mutations compromising this checkpoint are frequently found in different tumors, suggesting this DNA damage response is a barrier against tumorigenesis beyond its early stage (Bartkova et al., 2005) and become attractive target for cancer therapy, which currently heavily depends on DNA damaging agents (Lord & Ashworth,

2012). The efficacy depends on more detailed understanding of the elegant regulation in ATM-p53 interplay (Jiang et al., 2009).

The complex disease phenotypes in both AT patients and ATM-deficient mice suggest that ATM kinase has pleiotropic physiological functions beyond DNA damage repair. Other ATM substrates were demonstrated to be important for chromatin remodeling (Morrison et al., 2007), or gene transcription (Shi et al., 2004; Z. H. Wu, Shi, Tibbetts, & Miyamoto, 2006). Many more putative ATM substrates with functions not fully elucidated yet are predicted to be involved in various aspects of cell life, such as DNA/RNA metabolism, intracellular organization and embryo development (Figure 10) (Shiloh & Ziv, 2013). Many responses that seem to be dependent on ATM are likely to link to unknown substrates of ATM. Therefore, it is important to identify the specific substrates of ATM associated with these functions. On the other hand, studying new substrates of ATM will provide insights into further elucidation of ATM functions.

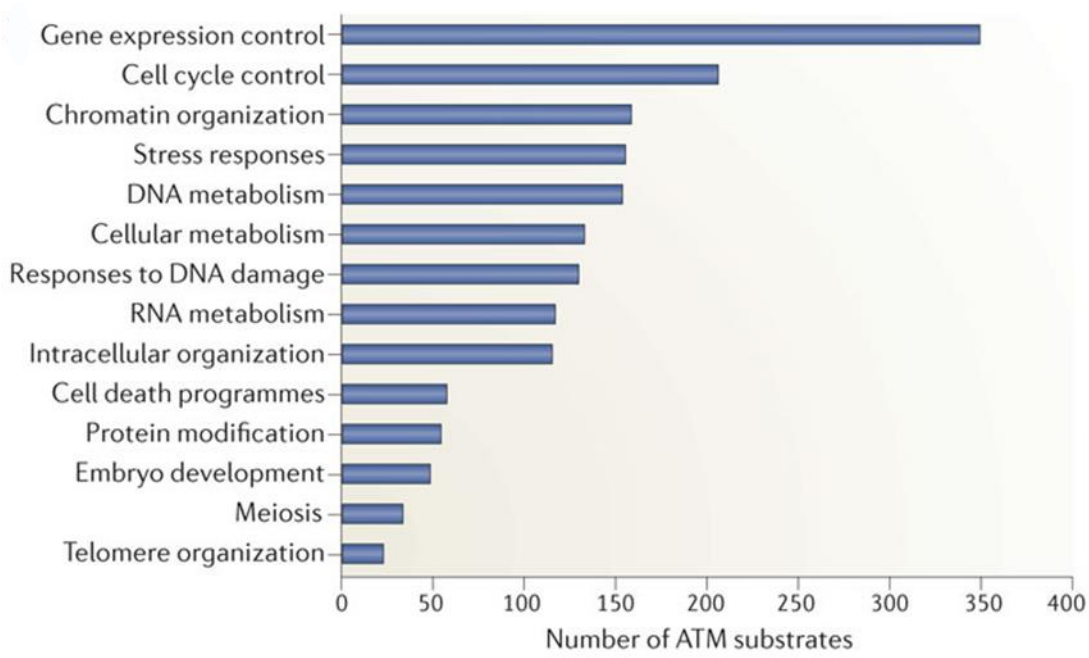

Figure 10. Functional classification of putative ATM substrates.

1,077 proteins were identified in proteomic screens as putative ATM substrates. Initial functional division was made using Gene Ontology annotations, and closely related classes were subsequently assembled into the shown groups. Some of the groups partially overlap.

Figure and caption adapted from (Shiloh & Ziv, 2013).

1.6 Regulation of ATM expression

Given the important role of ATM in diverse physiological processes, much effort was made to study the mechanisms of ATM activation, mutations of ATM and ATM substrates. However, little is known about the regulatory mechanisms of ATM expression.

Although ATM expression is generally stable during cell cycle progress or in response to genotoxic stimuli, it was reported that ATM can be regulated *in vivo* at the transcriptional level (Gueven et al., 2006), it is upregulated during the mitogenic response in peripheral blood mononuclear cells only in protein level (Fukao et al., 1999), there is an increased basal levels of ATM in the FA mutant fibroblast cell lines (Yamamoto et al., 2008) and ATM could be unregulated in both mRNA and protein level upon X-irradiation in lymphoblastoid cell lines only when the ATM genes are wild type (Hirai et al., 2001). Insights of ATM regulation could be gained from studies done in various systems.

1.6.1 MicroRNA and ATM expression

MicroRNAs (miRNAs) are naturally existing, small, non-coding RNA molecules with an important regulatory function of gene expression in multicellular organisms (Bartel, 2004). miRNAs function through base-pairing with complementary sequences within target mRNA molecules, usually resulting in translational repression or transcripts degradation of target genes.

So far, micro RNAs that were reported to be involved in downregulation of ATM include miR-181 in breast cancer (Y. Wang et al., 2011), miR-18a in breast cancer cell and tissues (Song, Lin, et al., 2011) (Guo et al., 2013), miR-18a in colorectal cancer (C. W. Wu et al., 2013), miR-106a in breast cancer (Guo et al., 2013), miR-421 (Hu, Du, Nagabayashi, Seeger, & Gatti, 2010), miR-100 in the human glioma cell line: M059J (Ng, Yan, Zhang, Mo, & Wang, 2010), miR-421 in SKX squamous cell carcinoma (Mansour et al., 2013), and miR-101 in certain tumors (Yan et al., 2010). There is also one contradictory report about miR-18a overexpression leading to upregulation of ATM expression in HCT116 cells (Qased et al., 2013).

1.6.2 Other proteins regulating ATM expression

It was shown that ATM expression can be regulated by Latent Membrane Protein 1 (LMP1) via the NF-κB pathways through direct promoter binding in nasopharyngeal carcinoma cells (Ma et al., 2011).

Fusco etc. (Palmieri et al., 2011) reported that High-mobility group A (HMGA) proteins 1 and 2, two novel substrates of ATM, are two positive regulators of ATM expression and activity by transcriptional activation of ATM promoter, and ATM expression is almost totally abolished in HMGA1/2 double knock out MEF cells.

ATM is transcriptionally regulated by E2F-1, which elevates ATM promoter activity and induces an increase in ATM mRNA and protein levels (Berkovich & Ginsberg, 2003).

There are also negative regulators of ATM expression reported, such as tumor protein D52 (Y. Chen et al., 2013), protein kinase C (PKC) α in human prostate cancer cells *in vitro* and *in vivo* (Truman et al., 2009) and sustained stimulation of cells with EGF in ATM wild type cells (Keating, Gueven, Watters, Rodemann, & Lavin, 2001).

More mechanisms that regulate ATM expression and function wait to be discovered.

1.7 Research aims

Mettl8 first drew our attention as a potential target of Stat3. It became more interesting to us as it has a SAM binding domain which makes it a possible methyltransferase, and an S/TQ motif required for ATM substrate, implicating its potential role in DDR and tumorigenesis.

The aim of our research is to elucidate the function of Mettl8, firstly to study its localization in cells; secondly to confirm whether it is an active methyltransferase and to find its substrate; thirdly to study whether the pSQ motif is indeed phosphorylated by ATM in DDR; fourthly to reveal its cellular role in DNA damage response by overexpression and knockdown/knockout study; finally to assess its role in cell growth, cell transformation and tumorigenesis.

Chapter 2 Materials and Methods

2.1 Antibodies, chemicals and other reagents

2.1.1 Antibodies

Antibodies against Stat3 (C-20), p53 (DO-1), p21 (C-10), Hsp90, HA, α-tubulin, actin were from Santa Cruz; antibodies against Stat3 pY705, ATM pS1981, Chk2 pT68, Phospho-(Ser/Thr) ATM/ATR Substrate, p53 pS15, p53-acetyl K382, Fibrillarin, H2A, H2AX, H2AX pS139 were from Cell Signaling; antibodies against ATM, H3 total, KAP1, KAP1 pS824, H3K9me3, H3K9Ac and H4K20me2 were from Abcam and antibodies against human Mettl8 (HPA035421) and Flag tag (Flag M2) from Sigma.

2.1.2 Chemicals

Table 1. List of chemicals used in this study

Name	Source
5'FU	Calbiochem
AZD7762	Tocris Biosystem
Cisplatin	Sigma
DAPI	Sigma
DMSO	Sigma
Etoposide	Calbiochem
Ku55933	Tocris Biosystem
Mouse OSM	Made in our lab
Wortmannin	Calbiochem

2.1.3 Other reagents

Restriction enzymes and T4 DNA ligase are from NEB.

2.2 Plasmids

For recombinant DNA cloning procedures and plasmid DNA amplification, *E.coli* strain DH5α (Invitrogen) was used as host. Bacteria cells were grown in LB liquid or solid medium with ampicillin (100μg/ml) for selection of positive cells. Mouse Mettl8 was cloned from C57BL/6 E13 embryo liver cDNA pool and cloned into pPyCAGIP vector (courtesy of Dr. Wu Qiang, NUS) by XhoI/NotI. Human Mettl8 was cloned from human lung cancer cell line H2228 and inserted into pPyCAGIP vector by XhoI/NotI with Flag tag at N-terminus and HA tag at C-terminus. Point mutation at Ser405 and deletion mutation at SANT, SAM, NRB motif were carried out following PCR based mutagenesis method (Quikchange). For bacterial expression, human Mettl8 WT and ΔSAM cDNA were subcloned into pGEX6P1 vector by XhoI/EcoRI. pPyCAGIP-Flag-Mettl8-HA was further modified into pPyCAGIP-Flag-Mettl8–HA -T2A-EGFP by insertion of T2A peptide gagggcagaggaagtcttctaacatgcggtgacgtggagg-agaatcctggccca and EGFP cDNA. All plasmids are verified by sequencing. pLKO.1 vectors harboring shRNA against Mettl2, Mettl8 and scramble control were purchased from Sigma and validated.

2.3 Cell culture and treatment

HCT116 (p53 wild type), HEK293T, U2OS and HepG2 cell lines were cultured in Dulbecco's modified Eagle's medium (DMEM) supplemented with 10% fetal-bovine serum (FBS) (Sigma) and antibiotics (100 units/ml penicillin and 100 μg/ml streptomycin). H1650 cells were cultured in RPMI-1640 medium with the same

supplements as above. The cells were incubated at 37 ℃ with a humidified atmosphere of 5% CO_2.

Gamma irradiation is performed in BioBeam 8000 irradiator (Gamma Service Medical GmbH, Leipzig, Germany) with ^{137}Cs as radiation source (dosage at 0.048Gy/sec). UV radiation is performed in UV Stratalinker 2400.

2.4 Transfections and viral transduction

2.4.1 Transfection with Lipofectamine 2000

The manufacturer's protocol (Life Technologies) was followed.

2.4.2 Transfection with calcium phosphate precipitation method

Transfection was done when cells grow to 30%-40% of confluency. 20 μg of plasmid DNA in 450μl autoclaved sterile Milli-Q water was mixed with 50μl of 2.5M freshly-made calcium chloride. Then 500μl of 2×BES buffer [50 mM N,N-bis(2-hydroxyethyl)-2-aminoethanesulfonic acid (BES), 1.5 mM Na_2HPO_4, 280 mM NaCl. Adjust pH to 6.95 with 1 N NaOH] was added and the whole solution was vortexed immediately for 1min followed by a 20 min incubation at room temperature to allow DNA to precipitate. After incubation, the DNA solution was spun down at 250g for 30 sec, pipetted up and down several times, and finally added dropwise evenly to cells in 10 ml culture media in 10 cm dishes. The transfected cells were incubated at 37 ℃ with 2.5% CO_2. After about 16h, media was removed and replaced with 10ml fresh media. Then cells were moved back to 37 ℃ incubator with 5% CO_2 until cells reached full confluency or virus harvest.

2.4.3 Viral transduction

To produce lentiviruses containing shRNA, shRNA-pLKO.1 plasmid or pLKO.1 control plasmid was transiently transfected in 293T packaging cells with 2nd generation packaging plasmid and envelop plasmid for producing viral particles by calcium phosphate precipitation method.

For the viral transduction in cells, Sigma protocol was followed. Briefly, cells to be transduced were seeded at appropriate density on Day 0. The next day lentiviruses were added to cells in growth media containing polybrene (6-8 μg/ml). Media was removed and replaced with fresh growth media on Day 2. After one or two days (cell type dependent) to wait for cells to robustly express puromycin resistant gene, media was removed and replaced with media containing puromycin, whose concentration is cell type dependent. After certain days of puromycin selection (concentration and cell type dependent), media containing dead cells was removed and the remaining cell population was supposed to contain shRNA of interest.

The sequences of the shRNAs used are in Table 2. All the shRNA oligos were purchased from Sigma.

Table 2. List of shRNAs used in this study

Name	Target sequence
Mettl8 shRNA1	GTTGAGGGAATTTCCTGAAAT
Mettl8 shRNA2	GCGAGAGAATCATCATGGGAT
Mettl8 shRNA3	GTGCTACAAATCGTTTCTCAA
Mettl8 shRNA4	GATCGCCGCTTACAAGTTAAT
Mettl8 shRNA5	CTCCTTGTGTCTCCGTTTAAA
Mettl2 shRNA1	GCTAGGCAATTGCAGTTAATA
Mettl2 shRNA2	CCGAGGAAAGCAACTGACAAT
Mettl2 shRNA3	CCACAAATACTGGAATGACTT
Mettl2 shRNA4	CGGGTTTGGATTCAGTGCAAA
Mettl2 shRNA5	ACCTTAAACCACCATTTATTT

2.5 Immunofluorescent staining

Cells grown on cover slips were washed with PBS solution, fixed in 4% paraformaldehyde at room temperature for 20-30 min and permeabilized with 0.2% Triton X-100 in PBS for 10 min. Then cells were blocked with 3% BSA in PBS with 0.1% Triton X-100 for 10 min, followed by incubation with primary antibodies at 4℃ overnight. Then cells were washed three times with 0.1% Triton X-100 in PBS, each time for 10 min and incubated with fluorescence-labeled secondary antibodies in dark at room temperature for 1h. Nuclei were visualized by DAPI staining. Coverslips with cells were mounted onto slides by VECTASHIELD HardSet Mounting Medium (Vector Laboratories, H-1400).

2.6 Microscopy

Image acquisition and analysis was performed on Nikon A1R-A1 confocal microscopy system.

2.7 Flow cytometry

Cells were fixed in ice-cold 70% ethanol at 4℃ overnight. After fixation, the samples were washed twice with cold PBS and resuspended in 0.1ml PBS with 50μg/ml propidium iodide and 20μg/ml RNAse. After incubation for 45 min at room temperate in dark, the samples were diluted by addition of appropriate amount of PBS. The DNA content was determined by a BD LSRⅡ flow cytometer. Data was analyzed using Flowjo software.

2.8 Soft agar colony formation assay

SeaPlaque™ Agarose with low melting temperature (Lonza, 50100) was used in this assay. In triplicate manner, 1.5ml culture medium with 0.6% agarose was first plated into each well of a 6-well plate. After base agarose solidified, another 1.5ml of 0.4% agarose was plated on top in culture medium containing 2500 cells per well. After 20 days colonies grown in soft agar were stained by 1mg/ml Thiazolyl Blue Tetrazolium Bromide (Sigma, M5655) dissolve in water and then scanned in Bio-Rad Gel Doc EZ system. A population with more than 50 cells was counted as one surviving colony. Colonies were counted using Quantity One software.

2.9 Semi-quantitative Real-time PCR

Total RNA was harvested using Trizol reagent (Invitrogen) according to the manufacturer's instructions, purified by the RNeasy mini kit (Qiagen), and then reverse transcribed using the M-MLV Reverse Transcriptase system (Promega). The cDNA products were subjected to semi-quantitative RT–PCR with KAPA SYBR® FAST Universal 2X qPCR Master Mix (KK4600) using a 7300 Real-Time PCR machine (Applied Biosystems). All gene-specific mRNA expression values were normalized against the internal housekeeping gene GAPDH. The sequences of primers used are in Table 3.

Table 3. List of primers used in this study

Gene	Forward primer	Reverse primer
ATM	ATTCCAGCAGACCAGCCAAT	GGTCATCACGGCCCTTAACA
CDH1	CCACCACGTACAAGGGTCAG	TGCCATCGTTGTTCACTGGA
GAPDH (human)	ACCGTCAAGGCTGAGAACGGGA	CCCTGCAAATGAGCCCCAGCC
GAPDH (mouse)	GGTTGTCTCCTGCGACTTCAACAGC	CGAGTTGGGATAGGGCCTCTCTTGC
H2AX	GTCGTGCTTCACCGGTCTAC	TCAGCGGTGAGGTACTCCAG
Mettl2	TGAAGTGTTTCCGGCTCCGGTGT	ACCACTCCACATTGTCCCAGGCAT
Mettl8 (human)	TCCTGGTAGCAATGCCACTTTCAGG	GAGCTCCACAGCTCCAGAAGCA
Mettl8 (human) (ChIP P3)	ACTCCCTTTTCGATCTGCCC	CCGCCTGACGGGAATTGTAG
Mettl8 (mouse)	TTGCCTCTGAAGCTGTGGAACTTGTA	TGCATCCTGTCAGGGTGGATAGATG
Mettl8 (mouse) (ChIP P1)	ACCTCGCGGCCCTCCGTATC	GCTGTTTCTAATACTGCCTGCATGCA
Mettl8 (mouse) (ChIP P2)	CAGACGTTGATTAATTCGCTGCAGTC	GCTGTTTCTAATACTGCCTGCATGCA
p21	CGATGGAACTTCGACTTTGTCA	GCACAAGGGTACAAGACAGTG
Puma	TACGAGCGGCGGAGACAAG	GCACCTAATTGGGCTCCATCT

2.10 Cell fractionation

According to Wysocka et al. (Wysocka, Reilly, & Herr, 2001), briefly, 1×10^7 to 2×10^7 cells were collected, washed with PBS, and resuspended at 4×10^7 cells/ml in buffer A [10 mM HEPES pH 7.9, 10 mM KCl, 1.5 mM $MgCl_2$, 0.34 M sucrose, 10% glycerol, 1 mM dithiothreitol, and protease inhibitor cocktail (Roche)]. Triton X-100 was added to a final concentration of 0.1% (v/v). The resuspended cells were incubated on ice for 8 min, and nuclei (fraction P1) were collected by centrifugation (5 min, 1,300 × g, and 4℃). The supernatant (fraction S1) was clarified by high-speed centrifugation (5 min, 20,000 × g, 4℃), and the supernatant (fraction S2) was collected. The P1 nuclei were washed once in buffer A and lysed for 30 min in buffer B [3 mM EDTA, 0.2 mM EGTA, 1 mM dithiothreitol, and protease inhibitor cocktail (Roche)], and insoluble chromatin (fraction P3) and soluble (fraction S3) fraction were separated by centrifugation (5 min, 1,700 × g, 4℃). The P3 fraction was washed once with buffer B, resuspended in sodium dodecyl sulfate (SDS)-Laemmli buffer and boiled for 10 min.

2.11 Immunoprecipitation

Cell lysate was extracted in lysis buffer [50 mM Tris-HCl pH 7.5, 0.1 mM EGTA, 1% (w/w) Triton X-100, 1 mM sodium orthovanadate, 50 mM sodium fluoride, 5 mM sodium pyrophosphate, 0.27 M sucrose, 0.1% (v/v) 2-mercaptoethanol plus 1 tablet/50 ml of EDTA free complete protease inhibitor cocktail (Roche)]. Protein lysates from cells were centrifuged at 14,000 × g for 5 min at 4 ℃ and the insoluble debris discarded. Protein concentrations were determined using Bio-Rad protein assay

dye. 10 μl of Flag M2 beads (for Flag IP) (Sigma) or 2 μg of relevant antibody coupled to 10 μl of protein G-agarose beads (Thermo Scientific) were washed with 1ml lysis buffer before incubation with 1mg total lysate for 1 h at 4 ℃ on a 1000rpm orbital shaker. Proteins bound to the beads were separated from the supernatant by centrifugation at 15,000 g for 1 min, washed twice with 1 ml of lysis buffer containing 0.5 M NaCl and twice with 1 ml buffer B [50 mM Tris-HCl pH 7.5, 0.27 M sucrose and 0.1% (v/v) 2-mercaptoethanol]. After removing all the remaining supernatant, SDS-Laemmli buffer was added to the beads to denature the antibody and release the immunoprecipitated protein. The samples were boiled for 10 min before being subjected to SDS- PAGE electrophoresis and subsequent Western blotting analysis.

2.12 Western blotting (Immunoblotting)

Appropriate amount of lysate samples were electrophoresed on a polyacrylamide gel of a percentage dependent on the size of the target protein, transferred onto a PVDF membrane in cold room and probed with primary antibodies of interest at 4 ℃ overnight. The following experiment was processed as standard using HRP conjugated secondary antibody (Invitrogen) and enhanced chemiluminescence visualization method (Thermo Scientific).

2.13 Recombinant protein expression and purification

As described previously in Cheung et al (Cheung, Campbell, Nebreda, & Cohen, 2003), BL21 DE3 strain transformed with specific GST tagged expression plasmids were grown to OD_{600nm} of 0.6 and induced for 16 h at 26 ℃ with 40 μM isopropyl–β-D-

thiogalactopyranoside (Sigma). Cells were harvested by centrifugation and resuspended in extraction buffer [50 mM Tris–HCl pH 7.5, 0.1 mM EGTA, 150 mM NaCl, 0.03% (w/v) Brij-35, 5% (v/v) glycerol, 0.1% (v/v) 2-mercaptoethanol, 0.1 mM phenylmethylsulfonyl fluoride, 1 mM benzamidine, 1 mM dithiothreitol]. Before further processing, a small portion of samples were subjected to SDS-PAGE and stained with Coomassie Blue to verify successful induction of target proteins. The harvested cells were subjected to freeze-thaw once and then sonicated for 2 min on ice. Triton X-100 was added to a final concentration of 1% (v/v) and the suspension was left on ice for 30 min. The cell debris was cleared by centrifugation for 30 min at 75,000 × g and the supernatant (termed lysate) was decanted. The lysate (30 ml) was incubated for 1 h at 4 ℃ with 3 ml of a 50% slurry of Glutathione Sepharose 4B (GE healthcare). Then the pellet was washed twice with wash buffer 1 [50 mM Tris–HCl pH 7.5, 0.27 M sucrose, 0.5 M NaCl, 0.1% (v/v) 2-mercaptoethanol], followed by twice with wash buffer 2 [50 mM Tris–HCl pH 7.5, 10 mM NaCl, 0.27 M sucrose, 0.1% (v/v) 2-mercaptoethanol], and eluted with 20 mM glutathione in wash buffer 2. Glutathione was removed by dialysis in wash buffer 2.

2.14 SAM binding assay

10 μg recombinant GST, GST-Mettl8 WT and ΔSAM protein were conjugated to 10 μl Glutathione Sepharose 4B at 4 ℃ for 30min before being incubated with 5μl ^{3}H-SAM (12-18 Ci/mmol (444-666 GBq/mmol)) at 30 ℃ for 30min. After two washes with 0.5ml 100mM Tris-HCl pH7.5, the beads were transferred to scintillation tube and mixed with 2 ml scintillant cocktail (OptiPhase HiSafe 2, Perkin Elmer). The result

was obtained from triplicate reactions on Wallac 1414 Liquid Scintillation counter controlled by the WinSpectral software system.

2.15 Luciferase assay

Mouse mettl8 promoter -1498bp to 0 region was cloned from C57BL/6 adult liver genomic DNA and inserted into pGL4.17 by SacI/BglII sites as pGL4.17-Mettl8b vector. Stat3 binding site at -146bp on reverse strand was mutated from ttccgggag into ggacgggag (named as pGL4.17-Mettl8bM) by site-directed mutagenesis. pGL3-M67-SIE was a gift from Dr. Dominic Voon of NUS. These vectors were transfected together with pRL-TK into Stat3 positive liver cells and after 48h cells were lysed in passive lysis buffer according to manufacturer's instruction (Promega Dual Luciferase kit) and measured manually in triplicate manner.

2.16 Chromatin Immunoprecipitation (ChIP) assay

As described in Lee et al (T. I. Lee, Johnstone, & Young, 2006), briefly $1x10^7$ Stat3 positive liver cells were treated with 10ng/ml murine oncostatin M (OSM) for 0, 30min, 1h and 2h and fixed with formaldehyde and neutralized by glycine. Cells were harvested in cold PBS and nuclear extract prepared as described. After sonication, cleared nuclear lysate was incubated with 2 μg Stat3 antibody conjugated to 20 μl protein G agarose for 16h. After extensive wash DNA was reverse cross-linked and eluted. For H1650 cells, no treatment was done prior to fixation.

2.17 Gene Knockout in cell lines by CRISPR/Cas9

Vector pST1374-NLS-flag-linker-Cas9 containing human-codon-optimized Cas9 and human-gRNA-expression vector MLM3636 were from Addgene. MLM3636 vectors with gRNAs targeting human Mettl8 were self-made in our lab following instructions of Joung Lab.

Cells were transiently transfected with Cas9 plasmid and gRNA expression vectors using lipofectamine with standard protocols (Chapter 2.4.1). Cells were transfected in 24-well plates using 0.5 μg of the Cas9 expression plasmid and 0.3 μg of the RNA expression plasmid. Two days after transfection, cells were trypsinized and replated in 10 cm dishes with a highly diluted passage ratio for single clone selection. After about two weeks, single clones were picked and cultured in individual wells.

The selection of positive clones was done first by western blot analysis of Mettl8 expression. Then genomic DNA of the Mettl8-null clones was extracted by phenol-chloroform method, and then subjected to PCR, TA cloning and sequencing to confirm the mutation of the Mettl8 gene.

2.18 Microarray

Total RNA was harvested and purified by the RNeasy mini kit with on-column DNAse digestion (Qiagen) according to the manufacturer's instructions. The array was done using HumanHT-12 v4 Expression BeadChip Kit by our common facility. The microarray analysis was carried out using R language by our bioinformatician.

Chapter 3 Results

3.1 Mettl8 as a potential methyltransferase

In this chapter, we will show how Mettl8 was screened out and the validation of it as a Stat3 target. As Mettl8 is a poorly studied protein, we started our research by localization study. The ability of Mettl8 to bind SAM molecule is confirmed by *in vitro* assay although the substrate of its potential methyltransferase activity is still unknown.

3.1.1 Mettl8 is a novel target of Stat3

In order to find more targets of Stat3, we carried out the screening in a pair of immortalized mouse liver cells in the presence or absence of Stat3. We created the first cell line without Stat3 by clean-cut genetic approach in the laboratory; it's originated from C57BL/6 mouse with transthyretin (TTR)-Cre driven Stat3 deletion in adult liver. To make a parallel control, Stat3 is reintroduced into the parental Stat3 KO cell to generate Stat3+ liver cell. As shown in Figure 11A, Stat3 is clearly not detectible in original KO cells and expression is restored in the Stat3+ cells. And Stat3 showed expected phosphorylation pattern at Tyrosine 705 when treated with murine oncostatin M (OSM), a potent activator for Stat3, as mentioned in the introduction.

With these cells, we screened about 300 genes by qPCR covering epigenetic factors, growth factors and transcription factors (list of genes available upon request). A number of epigenetic genes showed changed mRNA expression with OSM treatment.

One of them drew our attention: methyltransferase like protein 8 (Mettl8); its mRNA level was upregulated about 1.5-fold in Stat3 KO cells with OSM treatment, while it increased 2.5-fold in Stat3 positive cells (Figure 11B), comparable to the established Stat3 target genes like interferon regulatory factor 1 (IRF1) and suppressor of cytokine signaling 3 (Socs3) which are listed as positive control. Given its novelty, we decided to look further into this gene.

By analyzing promoter sequence of this gene, we found two Stat3 consensus sites, one is very close (-146bp) to TSS (transcription start site) and the other one is at distal region (about 6.2kb upstream). Two AP-1 binding sites are also present at -433 and -989bp, which could be accounted for the induction by OSM in the absence of Stat3, as OSM can also activate MAPK pathway. To further test the regulation of Stat3, we cloned the about 1.5kb promoter region of mouse Mettl8 into pGL4 luciferase reporter vector (pGL4-Mettl8-b), and mutated the proximal Stat3 site (pGL4-Mettl8-bM), as shown in Figure 11C. The primer amplicon corresponding to these two binding sites are listed as P1 (proximal) and P2 (distal).

Firstly Stat3 ChIP experiment was performed to confirm Stat3 binding on P1 but not on P2, as shown in Figure 11D. The binding was induced by OSM treatment dramatically at 30min and dropped after 1h, barely detectible at 2h, as revealed by PCR and qPCR respectively. Secondly, we tested the promoter reporter in the liver Stat3+ cells; the mutation of Stat3 site consistently reduced the activity by 3-fold (Figure 11E). However, this promoter could not be induced further by OSM treatment

(data not shown), indicating that there may be other components required for full Stat3 regulation.

The human Stat3 consensus site on human Mettl8 is also very close (+524bp) to TSS. The primer amplicon corresponding to this binding site is listed as P3 (+446bp to +604bp) (Figure 11F). Human Stat3 ChIP experiment was done using H1650 cells, which is a non-small cell lung cancer cell line with constitutive Stat3 activation (Song, Rawal, Nemeth, & Haura, 2011), so no induce is needed. Stat3 antibody (C-20) has a more than 6-fold increase of binding to Mettl8 promoter compared to that of IgG antibody (Figure 11G). This experiment was done in collaboration with my colleague Miss He Huining.

These data collectively support that Mettl8 is a novel target of Stat3 in both mouse and human, although it is not under exclusive control of Stat3.

A.

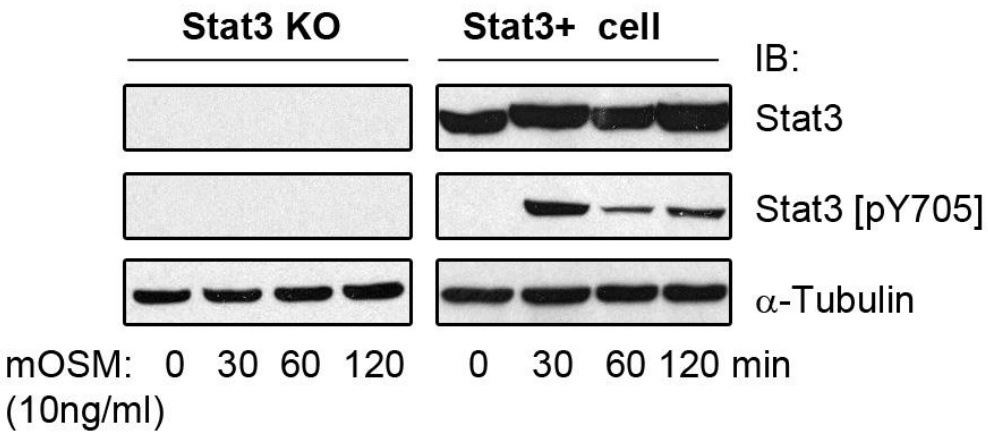
Stat3 KO
Stat3+ cell
IB:
Stat3
Stat3 [pY705]
α-Tubulin
mOSM: 0 30 60 120 0 30 60 120 min
(10ng/ml)

B.

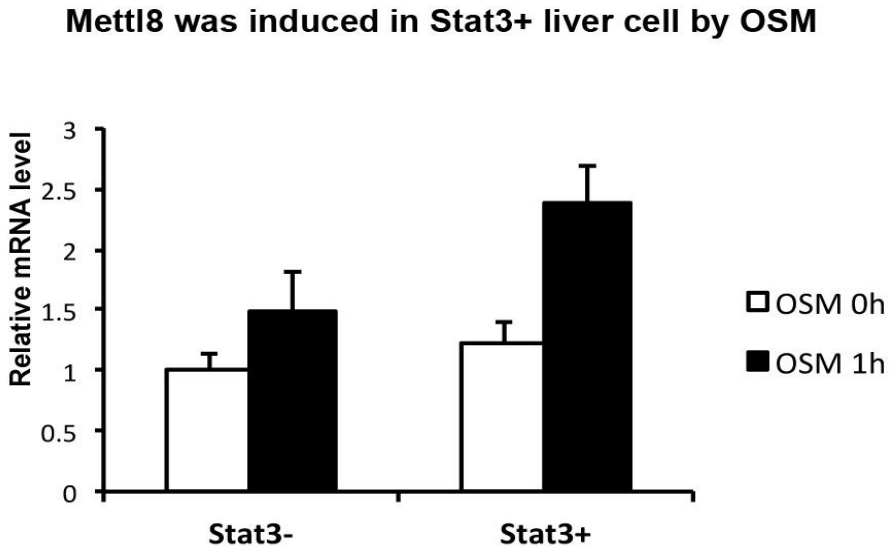
Mettl8 was induced in Stat3+ liver cell by OSM
Relative mRNA level
3
2.5
2
1.5
1
0.5
0
Stat3-
Stat3+
OSM 0h
OSM 1h

C.

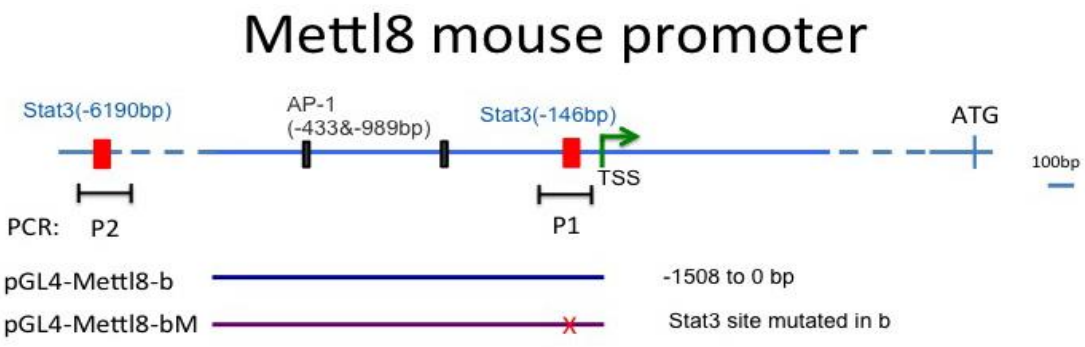
Mettl8 mouse promoter
Stat3(-6190bp)
AP-1
(-433&-989bp)
Stat3(-146bp)
ATG
TSS
100bp
PCR: P2
P1
pGL4-Mettl8-b
-1508 to 0 bp
pGL4-Mettl8-bM
Stat3 site mutated in b

D.

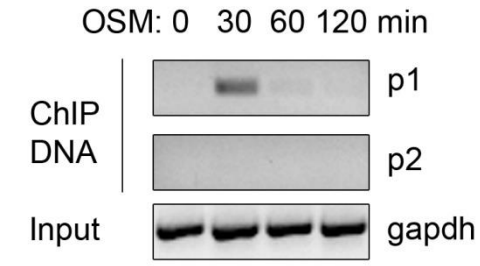
OSM: 0 30 60 120 min
ChIP DNA
Input
p1
p2
gapdh

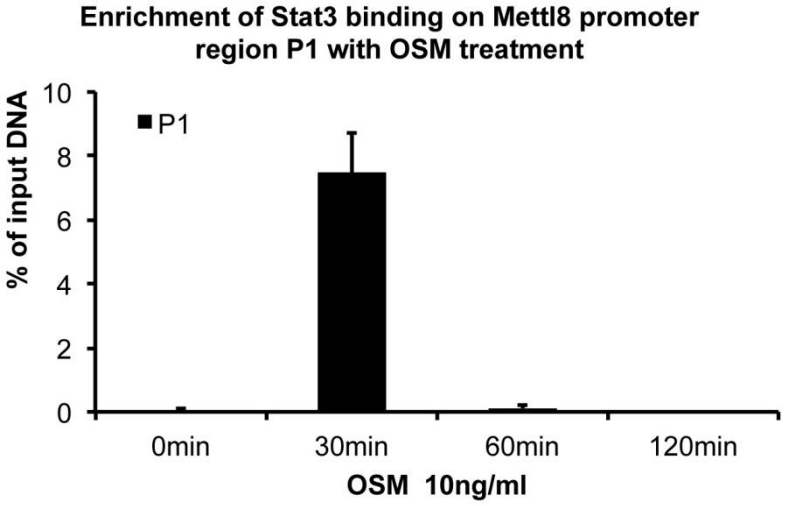
Enrichment of Stat3 binding on Mettl8 promoter region P1 with OSM treatment
% of input DNA
P1
0
2
4
6
8
10
0min
30min
60min
120min
OSM 10ng/ml

E.

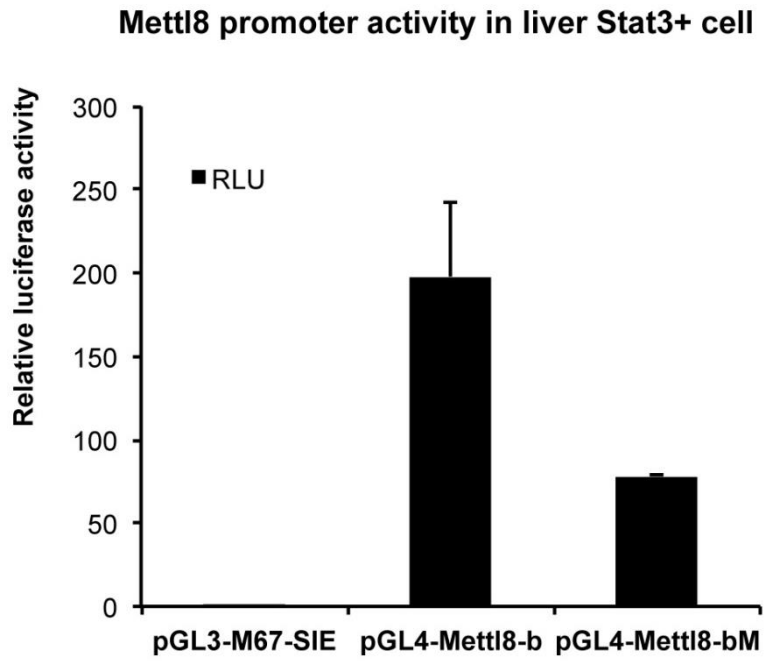
Mettl8 promoter activity in liver Stat3+ cell
Relative luciferase activity
RLU
0
50
100
150
200
250
300
pGL3-M67-SIE
pGL4-Mettl8-b
pGL4-Mettl8-bM

F.

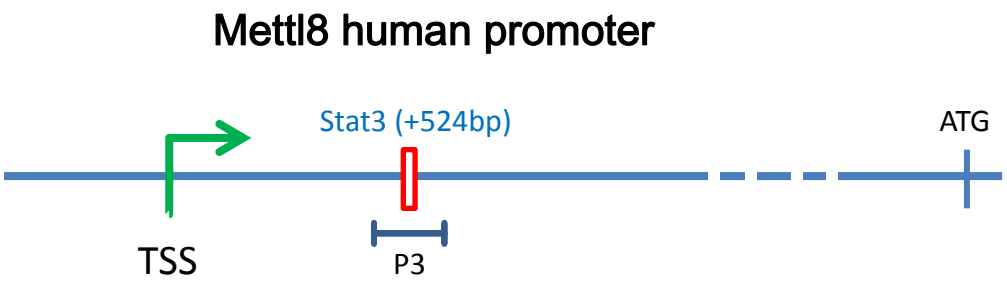
Mettl8 human promoter
Stat3 (+524bp)
ATG
TSS
P3

G.

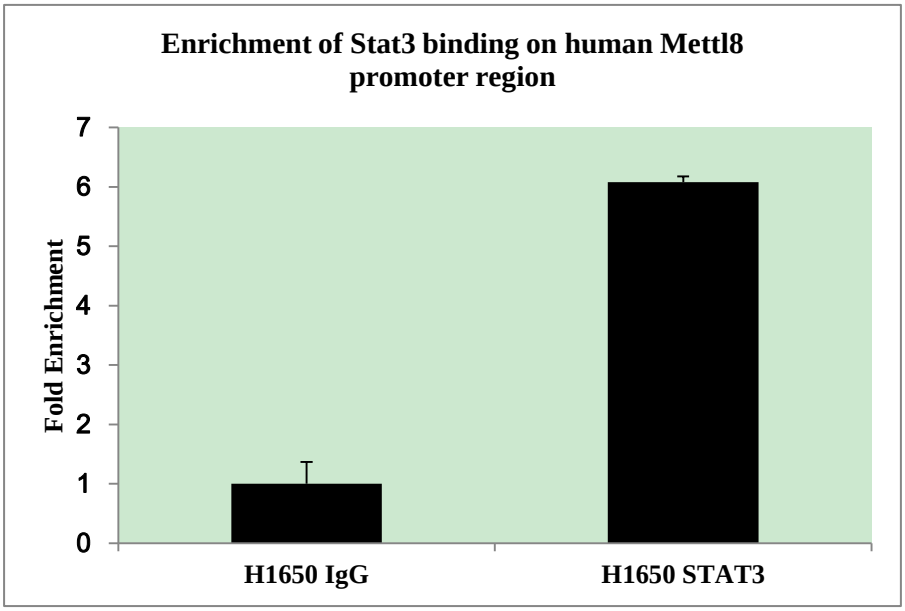
Enrichment of Stat3 binding on human Mettl8 promoter region
Fold Enrichment
0
1
2
3
4
5
6
7
H1650 IgG
H1650 STAT3

Figure 11. Mettl8 is a novel Stat3 target gene.

A) Stat3+ and KO mouse liver cells were established as described in text. 30ug of whole cell lysates were immunoblotted with anti-Stat3, Stat3 pY705 and tubulin antibodies after stimulation with 10ng/ml murine OSM for indicated period.

B) mRNA level of mettl8 is detected by qPCR between untreated and OSM 1h treated Stat3-/+ liver cells.

C) Diagram of mouse mettl8 promoter showing the binding site of Stat3, AP-1, and PCR products surrounding Stat3 binding sites. Two promoter constructs containing wild-type proximal Stat3 site and mutated Stat3 site were listed.

D) Stat3 ChIP was performed with 10^7 Stat3+ liver cells treated with OSM for different time points. Equal amount of eluted DNA was amplified in normal PCR to detect region of two binding site, P1 and P2. A similar sized region on GAPDH gene was amplified against input DNA as internal control (upper panel). The same experiment was carried out with qPCR to show the enrichment of Stat3 binding site as percentage compared to the equal amount of input DNA (lower panel).

E) Luciferase reporting assay was carried out with pGL3-M67-SIE, pGL4-Mettl8-b (wt) and Stat3 binding site mutated vector in Stat3+ liver cell.

F) Diagram of human mettl8 promoter showing the binding site of Stat3 and PCR product surrounding Stat3 binding site.

G) Human Stat3 ChIP was performed with 10^7 H1650 cells. Equal amount of eluted DNA was amplified in qPCR to show the fold enrichment of Stat3 binding to Mettl8 promoter compared to IgG control.

3.1.2 Subcellular localization of Mettl8

Proteins are responsible for performing the vast majority of cellular functions. Cells are highly compartmentalized, restricting most proteins to specific subcellular regions or organelles. The localization of a protein is crucial in determining its activity. For example, a RNA-binding protein would not be able to bind RNA if it were restricted to the cytoplasmic membrane. Thus, determining the subcellular localization of a protein within a cell can provide valuable information about its function.

To better understand the function of Mettl8, we studied its localization in cells by both biochemical fractionation and immunostaining methods.

Mettl8 ΔSAM mutant lost the nuclear localization, compared to the ubiquitous distribution of wildtype protein, when HCT116 stable cells with Flag tagged Mettl8 wild type and ΔSAM mutant proteins were fractionated into nuclear and cytoplasmic fractions using established protocol, shown in Figure 12A. Wild type Mettl8 was detected by Flag antibody in both cytoplasm and nucleus regardless of irradiation, while Mettl8 ΔSAM mutant cannot be found in nuclear fraction, although the part deleted did not contain any nuclear localization signal. Alpha-tubulin served as a cytoplasmic marker.

To further confirm the intracellular localization of WT and mutant Mettl8, wild type or mutant Mettl8 with both Flag and HA tags were transiently overexpressed in U2OS cells by lipofectamine transfection and stained for Mettl8, Flag or HA antibody. All three antibodies provided the same staining patterns (data not all shown) and some

untransfected cells in the field were negatively stained, showing the specificity of the antibodies used.

Wild type Mettl8 showed ubiquitous pattern with slightly stronger localization in nucleus as shown in Figure 12B, regardless of its relative expression level (brightness of Mettl8 signal). We notice there are concentrated positive staining areas in nucleus of Mettl8 wt cells, which resemble nucleolus pattern. Using a nucleolar marker Fibrillarin, we were able to show the colocalization of concentrated Mettl8 signal with nucleolus, suggesting Mettl8 may be related to rRNA processing or ribosome biosynthesis (Figure 12B, left panel). The pS/TQ mutant S405A still possessed the similar pattern as wildtype Mettl8 (Figure 12B, right panel).

Consistent with the fractionation result, ΔSAM mutant cells showed clear exclusion from nucleus region (Figure 12C). Like ΔSAM mutant, ΔNRB mutant is unable to enter nucleus. However, ΔSANT mutant is still able to localize to nucleus (data not shown).

Unfortunately, we did not have a good antibody to detect endogenous Mettl8 to reveal more physiologically relevant information.

A.

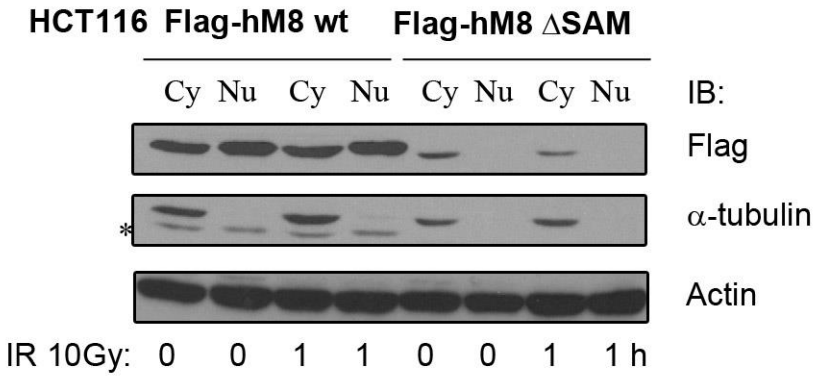
HCT116 Flag-hM8 wt
Flag-hM8 ΔSAM
Cy Nu Cy Nu Cy Nu Cy Nu
IB:
Flag
α-tubulin
*
Actin
IR 10Gy: 0 0 1 1 0 0 1 1 h

B.

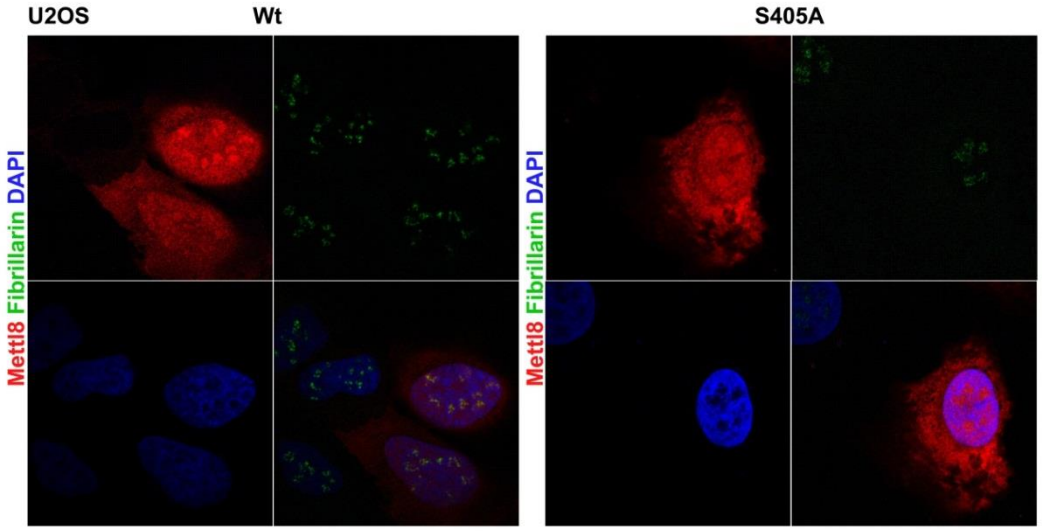
U2OS
Wt
S405A
Mettl8 Fibrillarin DAPI
Mettl8 Fibrillarin DAPI

C.

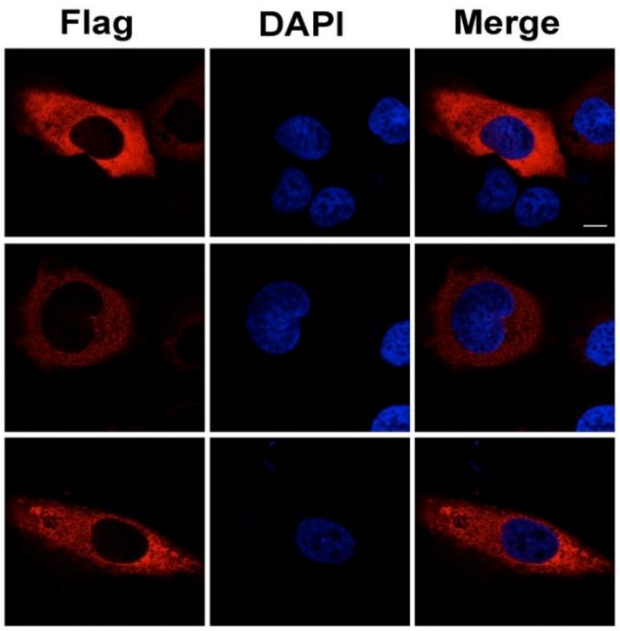
Flag
DAPI
Merge

Figure 12. Subcellular localization of overexpressed wt and mutant Mettl8 proteins.

A) HCT116 cells with stably overexpressed Flag-Mettl8 wt, and ΔSAM mutant were fractionated into cytoplasmic (Cy) and nuclear extract (Nu). Equal amount of lysates were resolved on SDS-PAGE for immunoblotting with anti-Flag, α-tubulin and Actin antibodies. *indicates the remained signal of Flag IB.

B) WT or S405A Flag-Mettl8 were transfected into U2OS cells by lipofectamine and stained for Mettl8 (red) or Fibrillarin (green) antibody and counter stained with DAPI (Blue). One representative picture was shown. The scale bar indicates 10 μm. Slides were visualized using a Nikon A1confocal microscope.

C) Flag-Mettl8 ΔSAM was transfected into U2OS cells by lipofectamine and stained for Flag (red) and counter stained with DAPI (Blue). Three independent pictures were shown in the figure. The scale bar indicates 10 μm. Slides were visualized using a Nikon A1confocal microscope.

3.1.3 Mettl8 is a potential methyltransferase with unknown substrate

As mentioned in the introduction, it is very challenging to identify a substrate for a novel and putative SAM dependent methyltransferase (MTase). However there is an essential function which can be tested rather easily: whether it can bind the methyl donor molecule S-adenosylmethionine (SAM).

For that purpose, GST-tagged wild type and ΔSAM mutant of human Mettl8 were expressed and purified from *E.coli*, as shown in Figure 13A; purification was successful with some degradation product below the major band of GST-Mettl8. Then we tested the ability of Mettl8 to bind SAM, using ^{3}H-labeled SAM. Briefly, immobilized GST, GST-Mettl8 wt and ΔSAM on Glutathione Sepharose 4B beads were incubated with ^{3}H-SAM and measured by standard liquid scintillation method after extensive wash. As shown in Figure 13B, GST beads or GST protein alone showed basal level of background activity, while GST-Mettl8 wt showed 14-fold increase. Mutation of SAM domain disrupted the binding ability of GST-Mettl8 to SAM molecule as the reading was back to background level. More interestingly, autoradiograph of the duplicate binding reaction showed that wt GST-Mettl8 was labeled by ^{3}H-SAM at the size of itself, suggesting that Mettl8 auto-methylation occurred (Figure 13C).

Since later we found Mettl8 forms complex with p53 and core histones (Chapter 3.2.2), we then tested whether they could be methylated by Mettl8 *in vitro*. However, we could not detect any labeling of GST-p53 by Mettl8 (data not shown). Although H2A and H4

could be labeled by Flag-Mettl8 IP from 293T cells, it could be due to contaminants co-purified such as PRMT5 as PRMT5 is readily pulled down by Flag M2 beads (data not shown).

A.

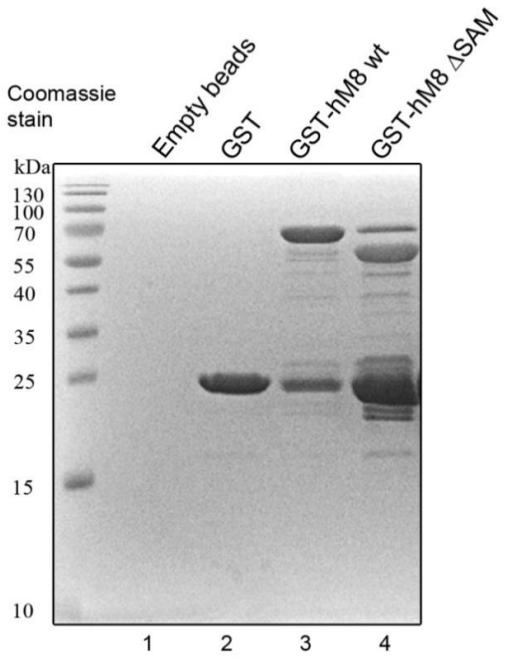
Coomassie stain
Empty beads
GST
GST-hM8 wt
GST-hM8 ΔSAM
kDa
130
100
70
55
40
35
25
15
10
1
2
3
4

B.

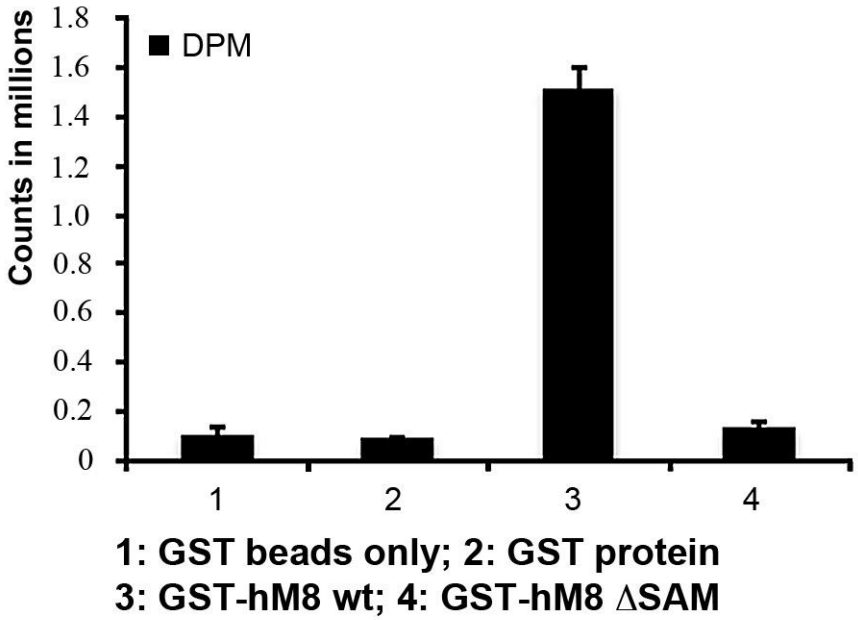
DPM
Counts in millions
1.8
1.6
1.4
1.2
1.0
0.8
0.6
0.4
0.2
0
1
2
3
4
1: GST beads only; 2: GST protein
3: GST-hM8 wt; 4: GST-hM8 ΔSAM

C.

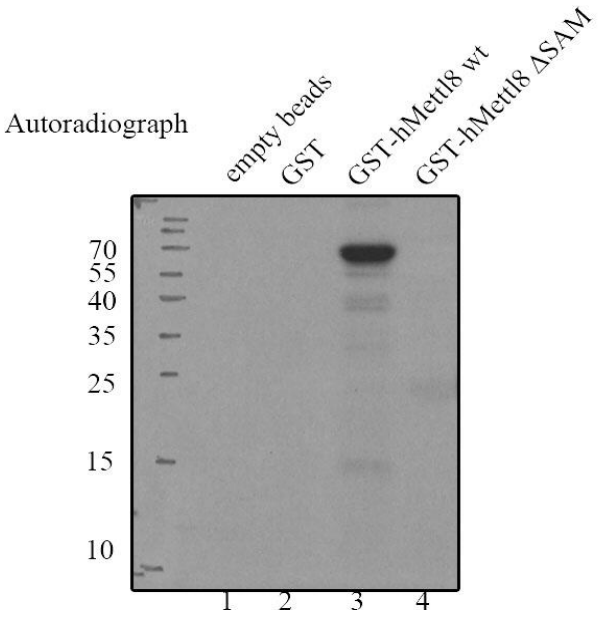
Autoradiograph
empty beads
GST
GST-hMettl8 wt
GST-hMettl8 ΔSAM
70
55
40
35
25
15
10
1
2
3
4

Figure 13. Mettl8 is a potential methyltransferase.

A) GST, GST-Mettl8 wt and ΔSAM mutant were expressed and purified from E.coli BL21 strain by Glutathione Sepharose 4B and resolved on SDS-PAGE. The proteins were visualized by Coomassie staining.

B) Equal amount (10mg) of GST, GST-Mettl8 wt and mutant proteins were conjugated on Glutathione Sepharose 4B beads and incubated with ^{3}H-SAM for 30min at 30℃ with empty beads as control. After extensive wash with 10mM Tris-Cl pH7.5, the beads were transferred to scintillation tubes and measured on liquid scintillation counter in triplicate manner.

C) Similar to B), the beads after incubation with ^{3}H-SAM were resolved on SDS-PAGE and subject to autoradiography at -80℃ for 48h.

All the radioactive work was done by Dr. Liu Xinyu.

3.1.4 Discussion

There are several criteria for identifying a Stat3 target gene. The first one is the presence of an evolutionarily conserved Stat3 binding consensus motif (Ehret et al., 2001) in the promoter or enhancer regions of a gene of interest. This requirement was met in Mettl8 as shown by both gene promoter analysis and ChIP assay and promoter reporter assay experimentally. A second commonly presented form of evidence is that constitutively active mutant form of Stat3 induces the expression of the given gene, which in our case we used OSM treatment instead to activate Stat3, which could indeed induce Mettl8 expression (Figure 11B). Another way of identifying a role for Stat3 in the transcriptional regulation of a particular gene is to show that acute genetic deletion of Stat3 gene results in the loss of target gene expression. Mettl8 mRNA level is similar in Stat3 KO and Stat3+ cells (Figure 11B), suggesting the existence of other transcription factors (TFs) in regulating Mettl8. Whether or not these TFs cooperatively work with Stat3 needs further studies.

The entry and exit of large molecules from the cell nucleus is tightly controlled (Silver, 1991). Transporting most of the nuclear proteins to the cell nucleus of a eukaryotic cell relies on specific nuclear localization signals (NLSs) that are recognized by protein import receptors. NLSs are generally short sequences of 3–20 amino acid residues, normally rich in lysine and arginine (Dingwall & Laskey, 1991). An NLS is a cluster of basic amino acids, which can be monopartite or bipartite. Monopartite NLS contains a single cluster of basic residues, and bipartite NLS contains two clusters of basic residues separated by a 10–12 residue linker. A

consensus sequence that represents the diversity of NLSs is a monopartite NLS sequence where a required lysine residue is followed by two other basic residues in the sequence K-(K/R)-X-(K/R), where X is any amino acid (Hodel, Corbett, & Hodel, 2001). The NLS of mouse Mettl8 protein is LRF***KKGR***CL, which fits the consensus requirement. The NLS of human Mettl8 protein LRF***KKGH***CL has a histidine instead of lysine or arginine, all three of which are basic amino acids. The NLS must be exposed on the protein surface to be accessible for the nuclear protein import receptor complex. And access to a protein's NLS can be regulated by phosphorylation, ligand-induced conformational changes, or intermolecular masking of target sequences (Jans, Xiao, & Lam, 2000). Although Mettl8 ΔSAM or ΔNRB mutant still possesses the NLS, they may have some unknown modification or conformation changes that prevent them from being imported into nucleus.

It is often the case that the initial structural and domain analysis at best indicates a potential function for a given unknown protein, but further identification of a relevant ligand or substrate is impeded by the diversity of possible functions in a specific structural classification of protein family. Although we confirmed the SAM binding activity of Mettl8 protein, it is still challenging to find the substrate. However, given the particular cellular localization of human Mettl8 protein and that its close family member mettl2's homolog ABP140 is a tRNA MTase in *Saccharomyces cerevisiae* (Noma et al., 2011), it is possible that RNA might be the substrate for the methyltransferase activity of Mettl8, which is currently being tested.

3.2 Mettl8 and ATM

3.2.1 Mettl8 is an ATM substrate

As mentioned in the introduction, the C-terminus of Mettl8 sequence STLLSQD fits with all the requirements for being a substrate of the PIKK family. Interestingly, this motif is only present in human Mettl8, but not mouse Mettl8 or human Mettl2, reminiscent of the variance observed of some key factors of DDR such as BRCA1.

To test this possibility, we established stable HCT116 cells with Flag tagged human Mettl8 and treated the cells with various DNA damaging stimulations, such as UV, 5' Fluorouracil (5' FU), cisplatin, etoposide or gamma irradiation at 1 and 10Gy. Indeed, human Mettl8 was found to be phosphorylated at pS/TQ motif with gamma irradiation and etoposide treatment which both cause double strand breaks on DNA, while other DNA damaging agent or treatment did not cause significant pS/TQ phosphorylation, as shown in Figure 14A. Phosphorylation of p53 at Ser15 was found in all stimulation except for UV and this site has been reported to be phosphorylated by different kinases: ATM, ATR and DNAPKcs (Meek, 2009). Phosphorylation of Chk2 at Thr68 was found in cell lysates with DSB only: irradiation and etoposide, which correlated well with ATM activation as shown by ATM autophosphorylation at Ser1981. Similar result was also obtained from 293T cell (data not shown) indicating that this effect is not HCT116 cell specific. As expected, mouse Mettl8 and human Mettl2, which do not have pS/TQ motif, treated with irradiation did not show phosphorylation at pS/TQ motif (data not shown). This result demonstrates that human Mettl8 is readily

phosphorylated in DSB response which predominantly activates ATM at the early time point used here.

We then checked if ATM is the responsible kinase for Mettl8 pS/TQ phosphorylation. Chemical inhibitors of general PIKK Wortmannin, a widely used ATM specific inhibitor Ku55933, along with Chk1/2 inhibitor AZD7762 were used to pretreat HCT116 Flag-Mettl8 stable cells for 1h before gamma irradiation. As shown in Figure 14B, only Wortmannin and Ku55933 pretreated samples showed significantly reduced phosphorylation on KAP1 Ser824 and Chk2 Thr68 which had been proven to be ATM substrate sites. The autophosphorylation of ATM at Ser1981 was only specifically inhibited by Ku55933, but not wortmannin, which is consistent with different mechanisms of these two chemicals: wortmannin covalently modified the phosphate transfer site (Wymann et al., 1996), while Ku55933 is an ATP binding competitor for ATM kinase (Hickson et al., 2004). As expected, pS/TQ of Mettl8 after 10Gy IR was dramatically reduced by pretreatment with wortmannin and Ku55933, suggesting this pSQ motif is indeed phosphorylated by PIKK and ATM is the major responsible kinase. As Ku55933 at 10μM could also inhibit DNAPKcs' activity (IC50 about 5μM) (Hickson et al., 2004), we further tested dose response to Ku55933 on Mettl8 phosphorylation by IR. As shown in Figure 14C, 1μM Ku55933 was sufficient to prevent the phosphorylation of Mettl8, confirming that ATM is the kinase responsible.

To confirm whether Ser 405 on human Mettl8 is the only pS/TQ motif or there exist other sites, we performed site-directed mutagenesis to change Ser 405 into Ala and repeated the experiment in 293T cells. As shown in Figure 14D, upon irradiation

pS/TQ phosphorylation was detected on wild type Mettl8 only, but not S405A mutant. This result points out that Ser 405 is the only pS/TQ motif on Mettl8 and validates the bioinformatics motif analysis result.

To test if the SANT and SAM domain are required for optimal pS/TQ phosphorylation, we generated HCT116 cells with stably expressed Flag mettl8 ΔSANT and ΔSAM. Interestingly, ΔSANT Mettl8 showed pS/TQ phosphorylation as wild type Mettl8 although ΔSANT Mettl8 expression level was much lower than wild type, while ΔSAM Mettl8 cannot be phosphorylated at pS/TQ anymore, as shown in Figure 14E. This difference could be related to their specific subcellular localizations and functions in cell.

Combined with previous results of subcellular localization of Mettl8 WT and ΔSAM mutant (Figure 12), we can conclude that the phosphorylation of pS/TQ motif on Mettl8 should take place in nucleus. Collectively we showed that human Mettl8 is a new substrate of ATM and the phosphorylation site is Ser 405.

A.

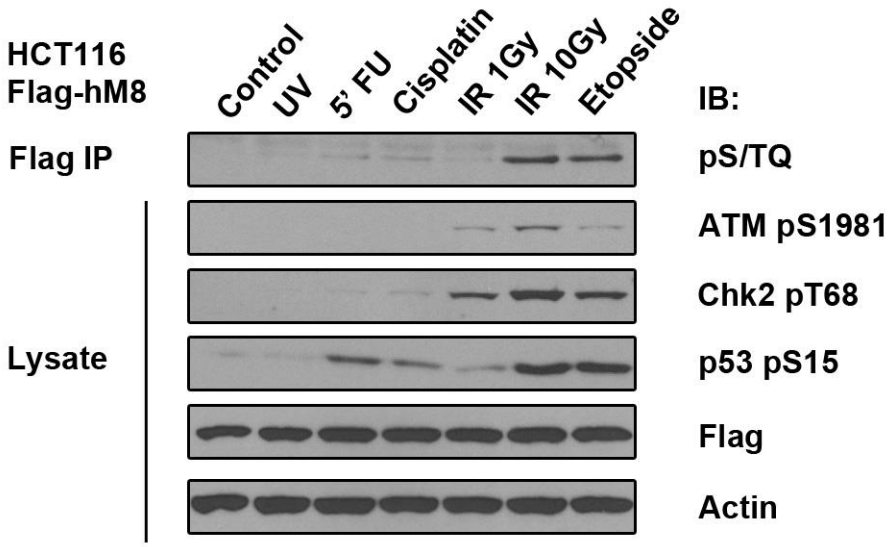
HCT116
Flag-hM8
Control
UV
5' FU
Cisplatin
IR 1Gy
IR 10Gy
Etopside
IB:
Flag IP
pS/TQ
ATM pS1981
Chk2 pT68
Lysate
p53 pS15
Flag
Actin

B.

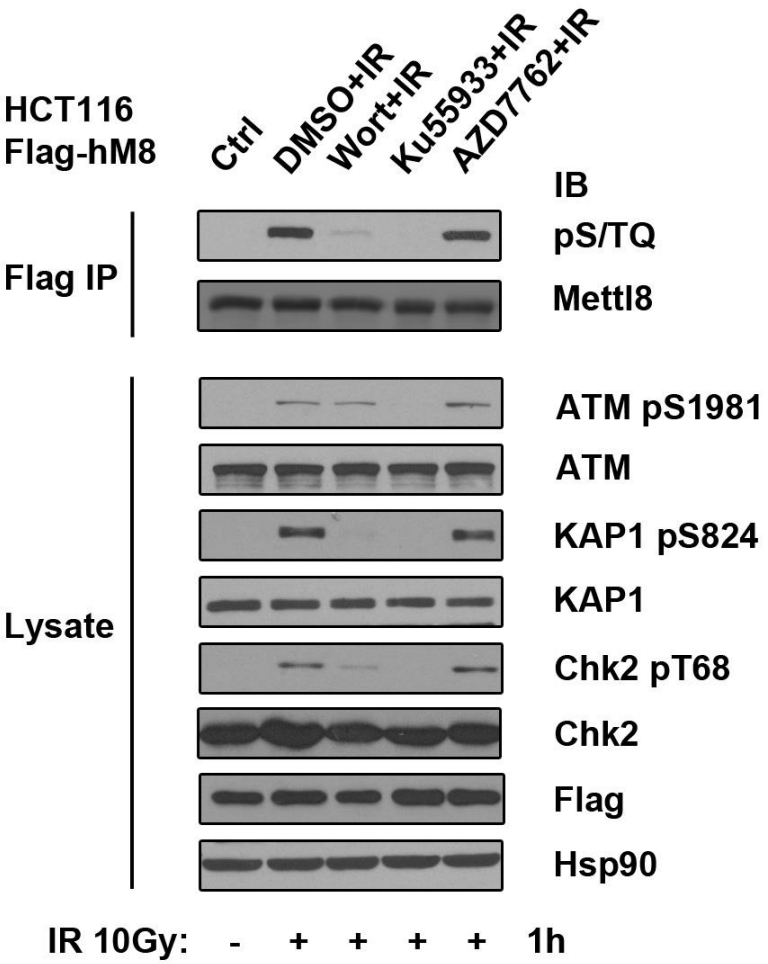
HCT116
Flag-hM8
Ctrl
DMSO+IR
Wort+IR
Ku55933+IR
AZD7762+IR
IB
Flag IP
pS/TQ
Mettl8
ATM pS1981
ATM
KAP1 pS824
KAP1
Lysate
Chk2 pT68
Chk2
Flag
Hsp90
IR 10Gy: - + + + + 1h

C.

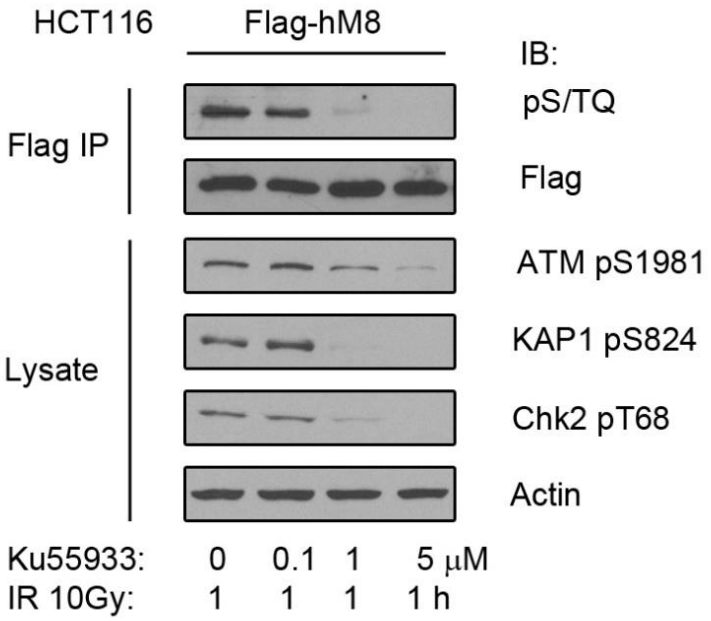
HCT116
Flag-hM8
IB:
Flag IP
pS/TQ
Flag
Lysate
ATM pS1981
KAP1 pS824
Chk2 pT68
Actin
Ku55933: 0 0.1 1 5 μM
IR 10Gy: 1 1 1 1 h

D.

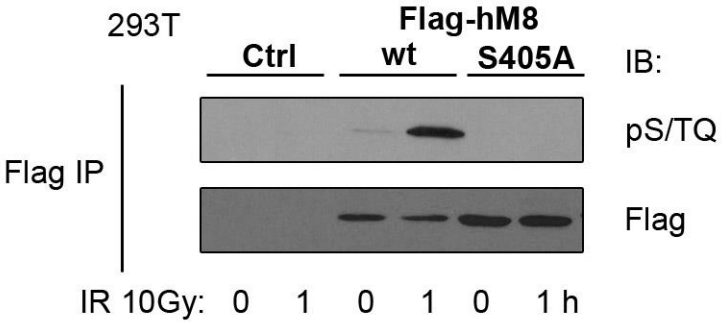
293T
Flag-hM8
Ctrl
wt
S405A
IB:
Flag IP
pS/TQ
Flag
IR 10Gy: 0 1 0 1 0 1 h

E.

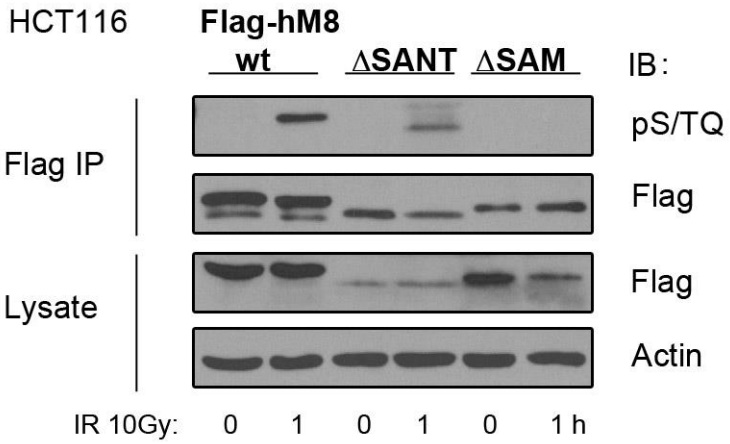
HCT116
Flag-hM8
wt
ΔSANT
ΔSAM
IB:
Flag IP
pS/TQ
Flag
Lysate
Flag
Actin
IR 10Gy: 0 1 0 1 0 1 h

Figure 14. Human Mettl8 is a substrate of ATM.

A) HCT116 stable cells with Flag human Mettl8 protein were treated with various DNA damage agents (UV 100J/m^2, recovered for 6h; 5'FU 25μM, 6h; cisplatin 30μg/ml, 6h; gamma irradiation at 1Gy or 10Gy, recovered for 1h; etoposide 10μM, 6h). Then equal amount of lysates were subjected to Flag IP with M2 beads and washed extensively before being resolved on SDS-PAGE and followed by immunoblotting with anti-pS/TQ motif antibody. The lysates were immunoblotted by indicated antibodies. The result is representative of three independent repeats.

B) Same cells as in A) were pretreated for 1h with Wortmannin (5μM), Ku55933 (10μM), AZD7762 (0.5μM) or DMSO as the vehicle control; then they were irradiated at 10 Gy and harvested 1h later without medium change. Similar to A), equal amount of lysates were subjected to Flag IP and probed for anti-pS/TQ and Mettl8 antibody. The lysate was immunoblotted by antibodies indicated.

C) Same cells as in A) were pretreated for 1h with different doses of Ku55933 as indicated; then they were irradiated at 10 Gy and harvested 1h later without medium change. Similar to A), equal amount of lysates were subjected to Flag IP and probed for anti-pS/TQ and Flag antibody. The lysate was immunoblotted by antibodies indicated.

D) 293T cells transfected with WT Flag-Mettl8 and S405A mutant were irradiated at 10Gy and harvested 1 hour later, together with untransfected cells. Equal amount of lysate were subjected to Flag immunoprecipitation and probed for pS/TQ and Flag antibodies.

E) HCT116 cells with stably overexpressed Flag-Mettl8 WT, ΔSANT, and Δ SAM were irradiated at 10Gy and equal lysates were subjected to Flag IP and probed for pS/TQ and Flag antibodies. The lysates were probed with Flag and Actin antibodies.

3.2.2 Mettl8 binds to ATM, p53 and core histones

Since Mettl8 is a substrate of ATM, it's natural to speculate whether they could form complex. We tried and found it hard to co-express ATM and Mettl8 variants in 293T cells. So Flag-ATM and Mettl8 wt or mutants were expressed separately in 293T cells and some of the cells were treated by 10 Gy irradiation followed by 1h recovery; the lysates were then mixed equally for *in vitro* binding assay. Flag-ATM was immunoprecipitated. Both wt Mettl8 and Mettl8 with mutated or phospho-mimic pSQ site were found to associate with ATM in untreated condition and after irradiation (Figure 15A). We then looked at the reciprocal immunoprecipitation of Flag-Mettl8. Endogenous ATM was detected in resting state and after irradiation (Figure 15B). In both IPs, a very mild reduction of the association between ATM and Mettl8 was found when cells were irradiated. We can conclude that ATM and Mettl8 could form a complex.

As SANT domain has been reported to recruit p300 which is a key co-factor for a number of transcription factors such as p53 and acetylates both histone and p53 (Gu & Roeder, 1997), and ATM was able to bind and phosphorylate p53 (Khanna et al., 1998), we went on to test whether p53 could be associated with Mettl8. In co-immunoprecipitation experiment, endogenous p53 was readily detectible in Flag IP of overexpressed Mettl8 in 293T cells, as shown in Figure 15C. Moreover, phospho-S15 p53 was also found in Flag IP of Mettl8, either wild type or S405A mutant, as shown in Figure 15D, and histone H3 was also found to bind Mettl8, along with other core histones (data not shown). This result is further confirmed in 293T

endogenous IP with Mettl8 antibody (Figure 15E), pointing to a constitutive complex between p53, mettl8 and ATM.

A.

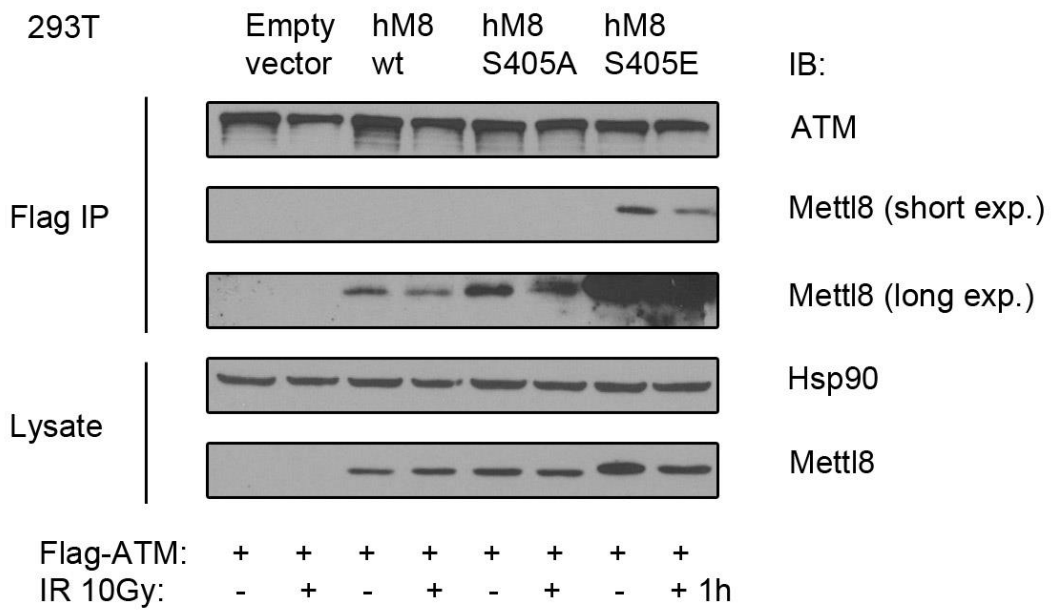
293T
Empty vector
hM8 wt
hM8 S405A
hM8 S405E
IB:
ATM
Flag IP
Mettl8 (short exp.)
Mettl8 (long exp.)
Hsp90
Lysate
Mettl8
Flag-ATM: + + + + + + + +
IR 10Gy: - + - + - + - + 1h

B.

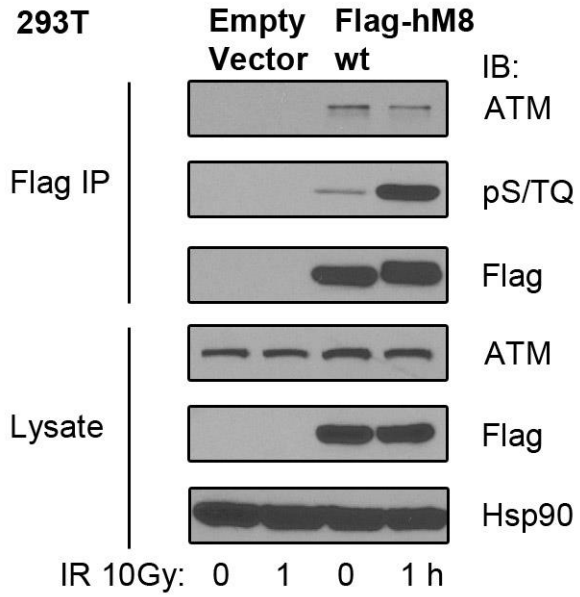
293T
Empty Vector
Flag-hM8 wt
IB:
ATM
Flag IP
pS/TQ
Flag
ATM
Lysate
Flag
Hsp90
IR 10Gy: 0 1 0 1 h

C.

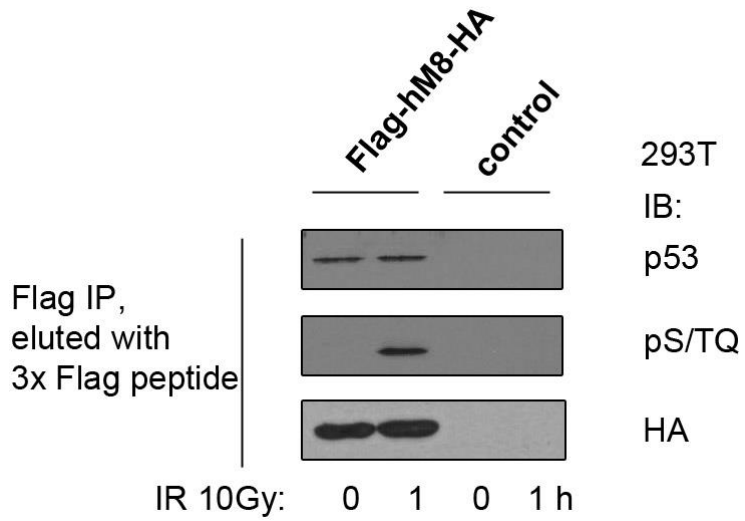
Flag-hM8-HA
control
293T
IB:
p53
pS/TQ
HA
Flag IP,
eluted with
3x Flag peptide
IR 10Gy: 0 1 0 1 h

D.

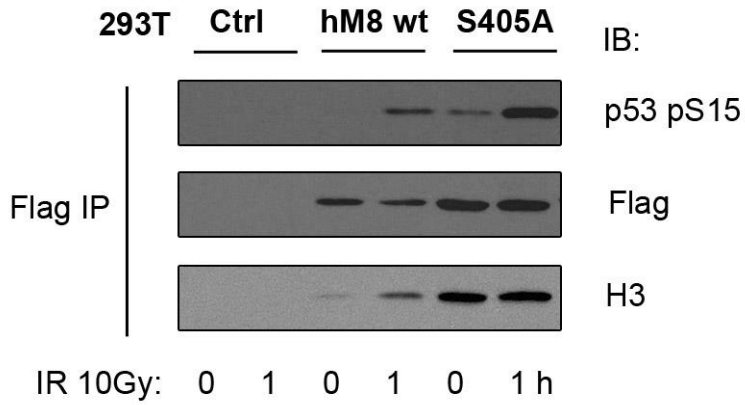
293T
Ctrl
hM8 wt
S405A
IB:
p53 pS15
Flag
H3
Flag IP
IR 10Gy: 0 1 0 1 0 1 h

E.

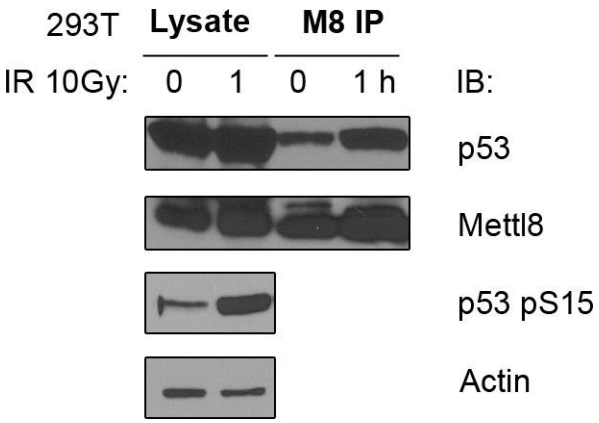
293T
Lysate
M8 IP
IR 10Gy: 0 1 0 1 h
IB:
p53
Mettl8
p53 pS15
Actin

Figure 15. Mettl8 forms complex with ATM, p53 and core histones.

A) 293T cells overexpressed with Flag-ATM or Mettl8-HA variants were treated by IR and left in recovery as indicated. *In vitro* binding of Flag-ATM and Mettl8-HA variants was done by mixing lysates equally as shown in the figure. Flag-ATM was then immunoprecipitated. The lysates from IP were then subjected to IB with ATM and Mettl8 antibodies. 40 μg lysate was checked in immunoblotting for Mettl8 variants expression, with heat shock protein 90 (Hsp90) as loading control.

B) Flag-Mettl8-HA was over-expressed in 293T and immune-purified by M2 beads after irradiation with 10Gy for various time points. The samples were subjected to immunoblotting with ATM, Flag and pS/TQ antibodies. 40 μg lysate was checked in immunoblotting for ATM and Flag expression, with Hsp90 as loading control.

C) Similar to B), lysates immune-purified by M2 beads were eluted with 3X Flag peptide and then subjected to immunoblotting with p53, HA and pS/TQ antibodies.

D) 293T normal cells or overexpressed with wt and S405A mutant of Flag-Mettl8 were irradiated with 10Gy dose and equal amount of lysates were subjected to Flag IP and subsequent immunoblotting with anti-p53 pS15, Flag and histone H3 antibodies.

E) 293T normal cells were irradiated with 10Gy dose and equal amount of lysates were subjected to Mettl8 IP and subsequent immunoblotting with p53 (DO-1) and Mettl8 antibodies. 40 μg lysate of each sample was checked for p53 (DO-1), Mettl8, p53 pS15, and Actin antibodies side by side with IP.

3.2.3 Mettl8 modulates ATM-p53 pathway in response to irradiation

As we have shown that Mettl8 is a substrate of ATM and it forms complex with ATM and p53, both of which belong to the tumor suppressor pathway in response to DNA damage, it will be intriguing to study whether Mettl8 could modulate this pathway. As mentioned in the introduction chapter, p53 is a key factor downstream of DNA damage to execute the cell fate regulation; its stability and transcriptional activation are tightly regulated by phosphorylation at N-terminal Ser 15 by ATM in IR (Cao et al., 2006; Hirao et al., 2002; Matsuoka et al., 2007), and acetylation at C-terminus by p300/PCAF (Ito et al., 2001; Xie et al., 1998).

3.2.3.1 Mettl8 ΔSAM mutant affects ATM-p53 DDR

In a time-course study after 10 Gy of gamma irradiation for stable HCT116 cell lines: empty vector, wild type, SAM mutant as shown in Figure 16A, p53 phosphorylation at Ser 15 in response to IR was enhanced in Mettl8 mutant cells with SAM mutation, compared to wild type and empty vector control. Consistently, acetylation at Lys 382 on p53 also showed similar pattern as phosphorylation on Ser 15. The stability of total p53 did not change as dramatic as Ser15 phosphorylation between Mettl8 mutant and wild type. Chk2 phosphorylation by ATM was changed slightly in mutant cells, in that the activation was much shorter than wild type, however, the intensity was higher. This mild change of Chk2 activation is consistent with total p53 level change in mutant Mettl8 cells, as Chk2 can help stabilize p53 by phosphorylating Ser20 of p53 and disrupting MDM2-p53 binding (S.-Y. Shieh, Ahn, Tamai, Taya, & Prives, 2000).

Strikingly, p21, the established target of p53, was induced significantly in Mettl8 mutant cells, even at basal level without any irradiation in SAM mutant cells. These results suggest that Mettl8 affects the trans-activation ability of p53 by modulating its acetylation and phosphorylation after gamma irradiation.

Since p53 Ser15 is a substrate site of ATM in this situation, we then traced upstream to ATM activation. The autophosphorylation at Ser1981 is hallmark of ATM activation (Bakkenist & Kastan, 2003). Indeed it was upregulated in mutant cells compared to wild type Mettl8 cells, as shown in Figure 16B. Phosphorylation of heterochromatin factor KAP1, another substrate of ATM, was also found to be elevated in mutant cells (Figure 16B), suggesting that Mettl8 may be involved in the heterochromatin repair.

H2AX, a marker for DNA damage was also substantially more activated in SAM mutant cells, compared to empty vector or wild type Mettl8, as shown in Figure 16C, by staining the cells with γH2AX antibody. Brighter and more foci of γH2AX were observed in mutant cells, even without irradiation, which may be due to the much more activated ATM pS1981 in both untreated and irradiated mutant cells (Figure 16B), as it was shown in *in vitro* assay that γH2AX level increases as ATM activation increases (J. H. Lee & Paull, 2004).

To check if the histone marks were changed during this process, the chromatin fraction of HCT116 stable cells with WT Mettl8 or ΔSAM mutant was analyzed for certain markers, as shown in Figure 16D. ATM autophosphorylation and p53

phosphorylation at Serine 15 were found to be stronger in mutant cells, as well as γH2AX, which was consistent with previous result shown in Figure 16 (A, B and C). Global H3K9 acetylation, trimethylation and H4K20 dimethylation mark were not changed between wild type and mutant cells, in line with published data (Tjeertes, Miller, & Jackson, 2009). Strikingly, H2AX total level was much higher in mutant cells compared to wild type, while H2A, H3 core histone were not changed. This is a very interesting result as it may suggest the global level of H2AX isoform in chromatin is affected by Mettl8. This could alter the chromatin structure in some way favoring the more sensitive detection of DNA damaging signals.

To make sure the effect of ΔSAM mutant Mettl8 on ATM-p53 DDR is not a false-positive result in one set of stable cell clones by accident, another independent set of HCT116 stable cells were generated and all the results were reproducible (data not shown).

Next we ask whether pS/TQ motif is required for Mettl8 function to activate ATM kinase, mettl8 wildtype, SAM mutant, S405A or S405E and double mutant of S405 and SAM domain were tested in 293T cells, as shown in Figure 16E. ΔSAM mutant showed enhanced ATM activation compared to wildtype, which is consistent with result obtained from HCT116 cell in Figure 16A, suggesting this is not cell type specific. S405A mutant showed enhanced ATM phosphorylation at 15min after IR, but it quickly diminished from 30 to 60 min after IR. On the contrary, S405E, the phospho-mimic mutant showed reverse effect that ATM activation was delayed but prolonged. S405A and SAM double mutant cells showed even higher activation of

ATM than each single mutant, and the effect was lasting longer. S405E and SAM double mutant showed shorter activation of ATM, which was different from each single mutant phenotype. The other two ATM substrates KAP1 and Chk2 phosphorylation patterns were not changed significantly. These results showed the pS/TQ motif on Mettl8 could affect ATM activation in a distinct manner compared to ΔSAM mutant which was dominant.

In an attempt to scan for genome-wise change in the HCT116 stable cells with Mettl8 ΔSAM mutant, we carried out a whole genome microarray analysis for them. In the list, we found ATM gene is slightly upregulated, along with many other genes (data not shown). To validate the result, we checked the whole cell lysate of stable mutant cells. To our great surprise, as shown in Figure 16F, total H2AX and ATM protein level was upregulated in ΔSAM mutant cells compared to wild type cells. This result was supported further by qPCR analysis, showing that ATM and H2AX was upregulated in ΔSAM cells compared to wild type and empty vector control at unstimulated situation. After 10Gy IR for 24h, the upregulation is not significant between empty vector and ΔSAM mutant cells, while wild type Mettl8 showed certain suppression (Figure 16G).

A.

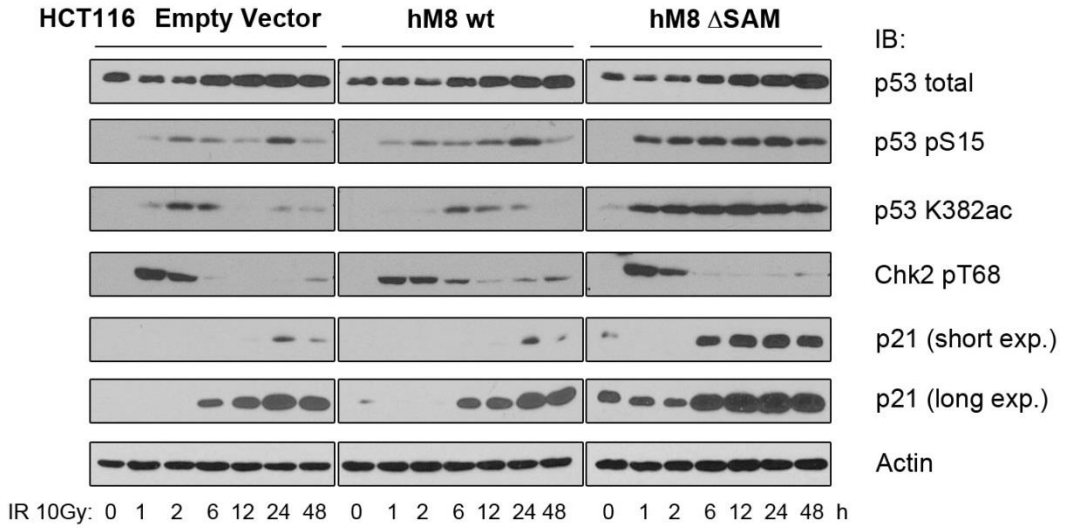
HCT116 Empty Vector
hM8 wt
hM8 ΔSAM
IB:
p53 total
p53 pS15
p53 K382ac
Chk2 pT68
p21 (short exp.)
p21 (long exp.)
Actin
IR 10Gy: 0 1 2 6 12 24 48 0 1 2 6 12 24 48 0 1 2 6 12 24 48 h

B.

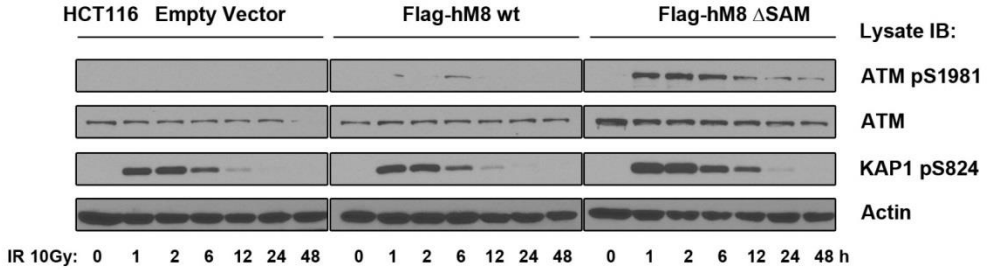
HCT116 Empty Vector
Flag-hM8 wt
Flag-hM8 ΔSAM
Lysate IB:
ATM pS1981
ATM
KAP1 pS824
Actin
IR 10Gy: 0 1 2 6 12 24 48 0 1 2 6 12 24 48 0 1 2 6 12 24 48 h

C.

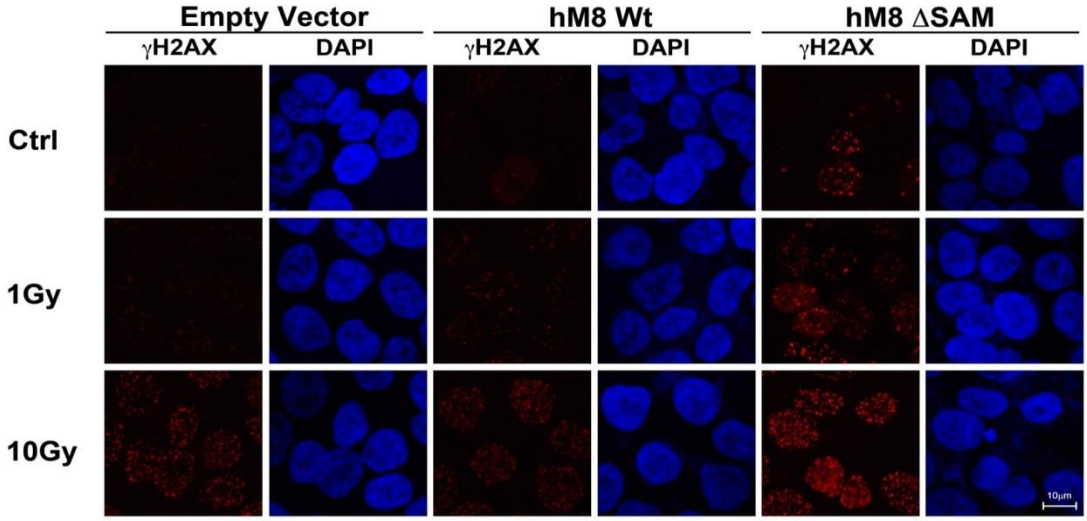
Empty Vector
hM8 Wt
hM8 ΔSAM
γH2AX
DAPI
γH2AX
DAPI
γH2AX
DAPI
Ctrl
1Gy
10Gy
10μm

D.

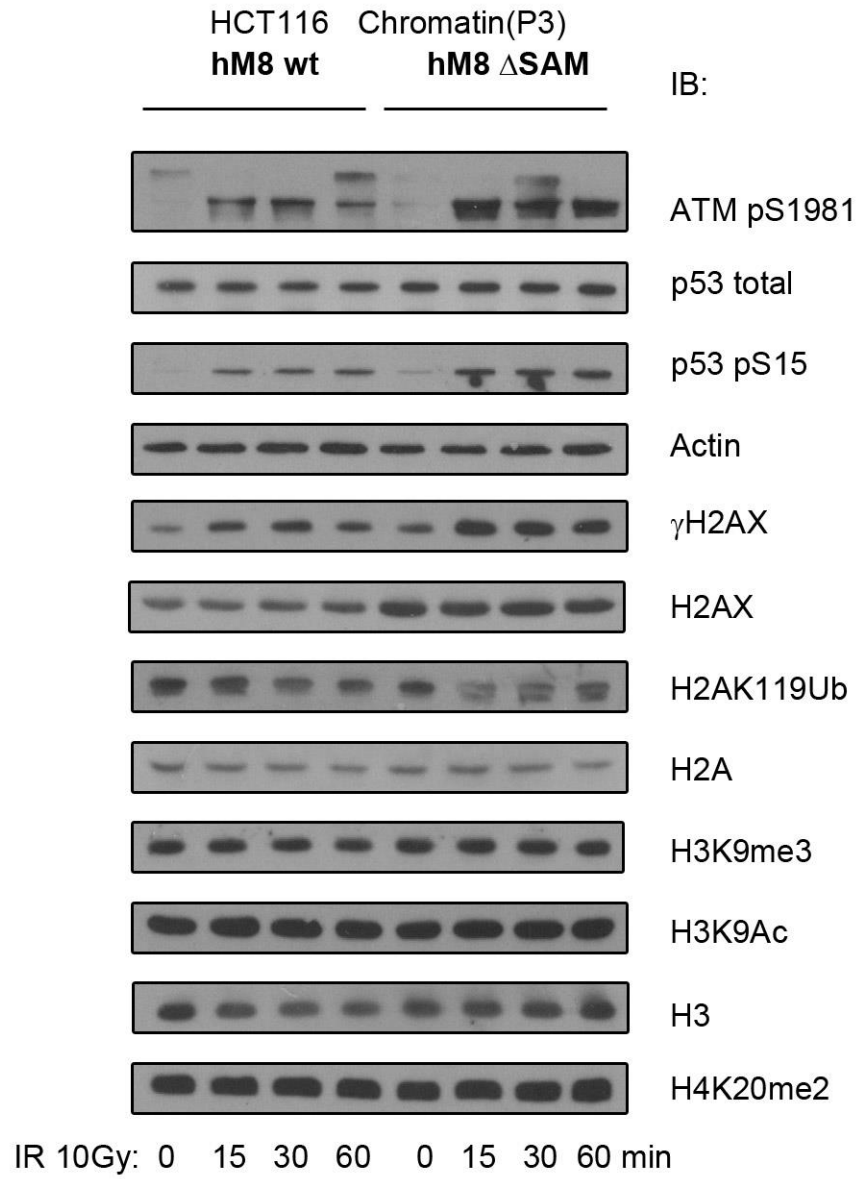
HCT116 Chromatin(P3)
hM8 wt
hM8 ΔSAM
IB:
ATM pS1981
p53 total
p53 pS15
Actin
γH2AX
H2AX
H2AK119Ub
H2A
H3K9me3
H3K9Ac
H3
H4K20me2
IR 10Gy: 0 15 30 60 0 15 30 60 min

E.

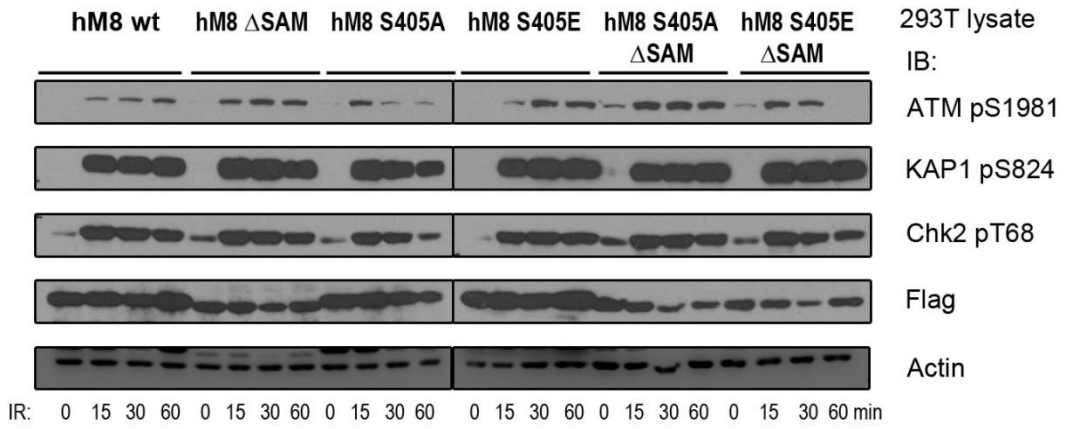
hM8 wt
hM8 ΔSAM
hM8 S405A
hM8 S405E
hM8 S405A ΔSAM
hM8 S405E ΔSAM
293T lysate
IB:
ATM pS1981
KAP1 pS824
Chk2 pT68
Flag
Actin
IR: 0 15 30 60 0 15 30 60 0 15 30 60 0 15 30 60 0 15 30 60 0 15 30 60 min

F.

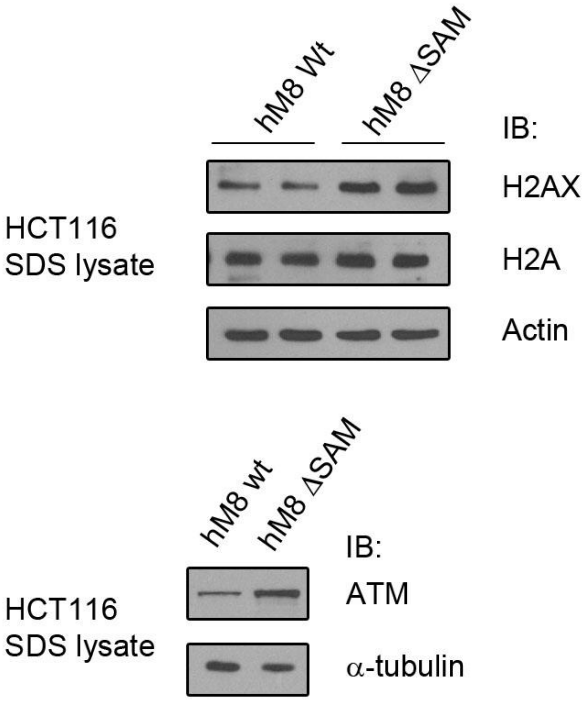
hM8 Wt
hM8 ΔSAM
IB:
H2AX
HCT116
SDS lysate
H2A
Actin
hM8 wt
hM8 ΔSAM
IB:
ATM
HCT116
SDS lysate
α-tubulin

G.

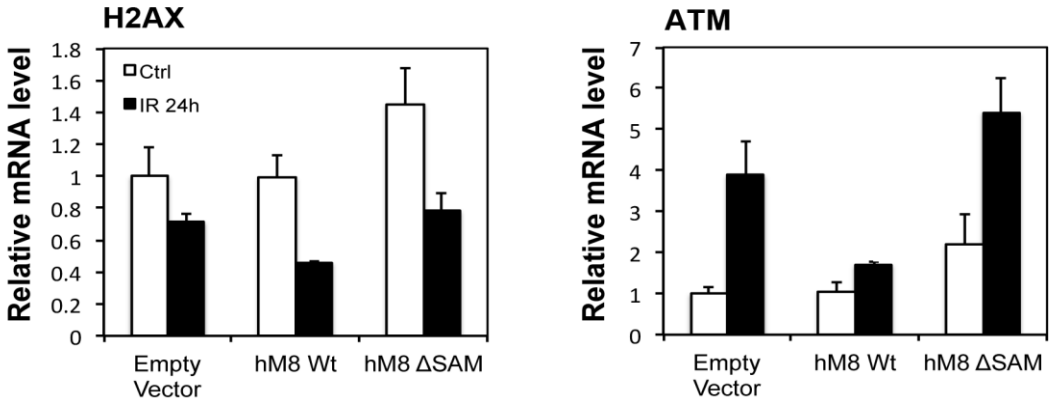
H2AX
Relative mRNA level
Ctrl
IR 24h
Empty Vector
hM8 Wt
hM8 ΔSAM
ATM
Relative mRNA level
Empty Vector
hM8 Wt
hM8 ΔSAM

Figure 16. ΔSAM Mettl8 mutant affects ATM-p53 DDR.

A&B) HCT116 stable clones with Mettl8 variants were irradiated at 10Gy and left in recovery for the time indicated. Equal amount of lysates were resolved on SDS-PAGE and immunoblotted against indicated antibodies. The same lysates were used in Figure A&B.

C) Same cells as in A). Cells were irradiated at 1 or 10Gy and left in recovery for 1h before standard immunostaining procedure with γH2AX antibody and counter stain with DAPI. Images were presented after Z-stack processing by Nikon A1 confocal microscope.

D) The indicated stable cells were irradiated at 10Gy and left in recovery for the time indicated. Chromatin fraction was extracted from the cells. Equal amount of sample was resolved on SDS-PAGE and immunoblotted against indicated antibodies.

E) 293T cells transiently transfected with Mettl8 WT and variants indicated in the figure were irradiated at 10Gy and left in recovery for the time indicated. Equal amount of lysates were resolved on SDS-PAGE and immunoblotted against indicated antibodies.

F) Same cells as in D). Total cell lysates were prepared by solubilizing cells in 1×SDS sample buffer and then subjected to WB with indicated antibodies.

G) Same cells as in A). RNA was extracted and reversed for qPCR analysis with indicated primers.

3.2.3.2 Mettl8&Mettl2 Double knockdown affects ATM-p53 DDR

To validate the results related to ΔSAM mutant Mettl8 in endogenous condition, we established lentivirus mediated shRNA knockdown (KD) cells. Five different shRNAs were tested for Mettl8 and Mettl2 respectively in HCT116 cells. The KD efficiency of Mettl8 shRNAs was evaluated in western blot (Figure 17A); shRNA2 was picked for further experiment. Since we don't have a good Mettl2 antibody to detect endogenous Mettl2, only qPCR was done to select the best shRNA targeting Mettl2 (both Mettl2A&B) (data not shown) and the one with best KD efficiency (shRNA2) was used for further experiment.

There is little enhancement of ATM phosphorylation at Ser1981 as early as 15min after irradiation in Mettl8 KD sample compared to scramble control, however, significant activation of ATM phosphorylation was found in double KD (DKD) samples of both Mettl8 and Mettl2, its close family member (Figure 17B), suggesting that there might be some redundant role between them. Strikingly, phosphorylation of ATM was observed even without irradiation in double KD sample, and total ATM level was also elevated in double KD samples compared to scramble control which is consistent with observations in ΔSAM mutant cells. The specificity and efficiency of knock down was validated by qPCR (Figure 17C).

The mRNA level of ATM and H2AX remained unchanged between double KD cells and scramble control (data not shown).

A.

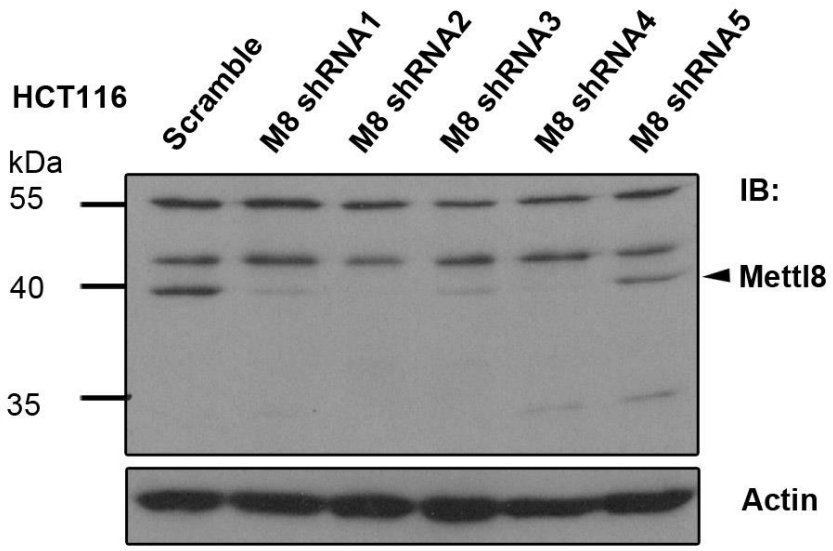
HCT116
Scramble
M8 shRNA1
M8 shRNA2
M8 shRNA3
M8 shRNA4
M8 shRNA5
kDa
55
40
35
IB:
Mettl8
Actin

B.

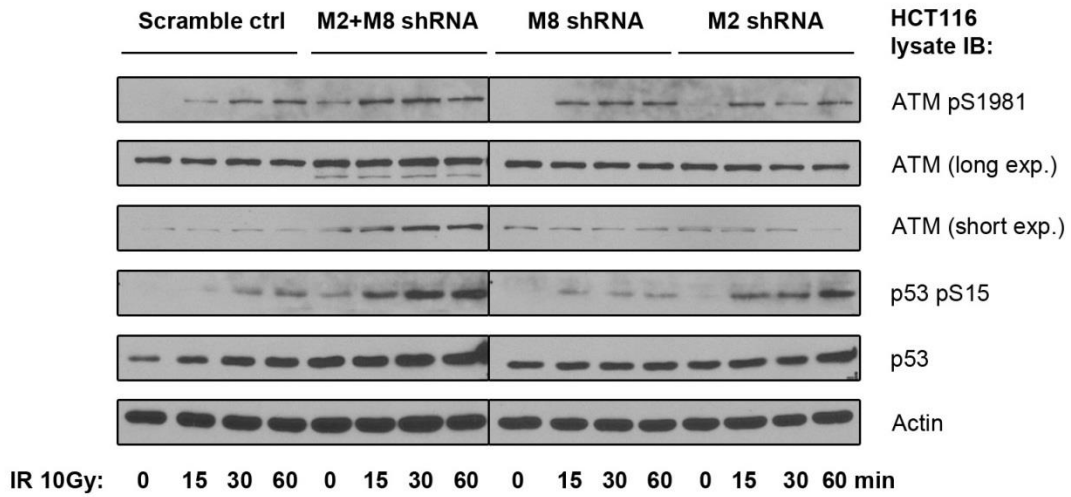
Scramble ctrl
M2+M8 shRNA
M8 shRNA
M2 shRNA
HCT116 lysate IB:
ATM pS1981
ATM (long exp.)
ATM (short exp.)
p53 pS15
p53
Actin
IR 10Gy: 0 15 30 60 0 15 30 60 0 15 30 60 0 15 30 60 min

C.

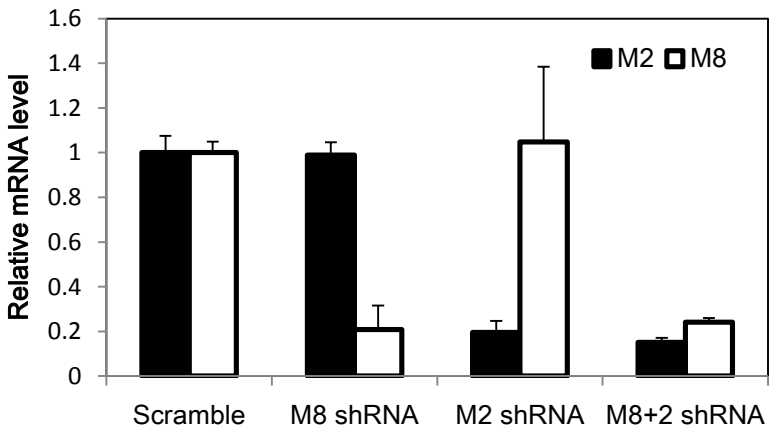
Relative mRNA level
1.6
1.4
1.2
1
0.8
0.6
0.4
0.2
0
M2
M8
Scramble
M8 shRNA
M2 shRNA
M8+2 shRNA

Figure 17. Mettl8 and Mettl2 double KD affects ATM-p53 DDR.

A) HCT116 cells were infected with six kinds of lentiviruses, each harboring one shRNA against Mettl8 or scramble control, for 72 hours. Then cells were harvested in lysis buffer. Equal amount of lysates were resolved on SDS-PAGE for immunoblotting against Mettl8 and Actin antibody.

B) HCT116 cells were infected with lentiviruses harboring shRNA(s) against Mettl8 (M8), Mettl2 (M2), both Mettl8 and Mettl2 (M8+2), or scramble control for 72 hours before irradiation at 10Gy for the time indicated. Equal amount of lysates were resolved on SDS-PAGE for immunoblotting against indicated antibodies.

C) Same cells as in B). RNA was extracted and reversed for qPCR analysis with indicated primers.

3.2.3.3 Mettl8 KO affects ATM-p53 DDR

To further and more thoroughly elucidate the function of Mettl8, Mettl8 knockout (KO) C57BL/6 mouse is being generated from outside source. However, even if we have the Mettl8 KO mouse, we still need a Mettl8 KO human cell line for our ATM and DDR study, as the mouse Mettl8 protein does not have pS/TQ motif.

Again, to validate the results related to ΔSAM mutant Mettl8 in endogenous condition, we used CRISPR/Cas9 technique, a new affordable genome editing tool (Cong et al., 2013; Mali et al., 2013), to generate human cell lines with Mettl8 knockout. Three pairs of guide RNA (gRNA) targeting different regions of the Mettl8 genomic DNA (gDNA) were used to knockout Mettl8 in both HCT116 and 293T cells. The translation start site ATG is located in Exon 2; gRNA 1, 2, 3 targets boundary between intron and Exon 2, Exon 3 and Exon 4 respectively (Figure 18A).

Only one positive stable clone was obtained for each cell line besides control cells: HCT116 with gRNA 3 and 293T with gRNA 1, the knockout effect of which were shown by western blotting and gene sequencing (Figure 18B). The HCT116 positive clone has an 8bp deletion in the Exon 4 coding sequence. The 293T positive clone has a 12bp deletion across the boundary of intron and Exon 2, 6bp before the translation start site ATG, which might result in abnormal mRNA splicing. The Mettl8 protein can no longer be detected in these two positive KO clones.

In all time points after irradiation (15min, 30min and 60min), in both HCT116 and 293T cells, there was significant activation of ATM phosphorylation at S1981, KAP1

pS824, Chk2 pT68 and p53 pS15 in Mettl8 KO samples compared to control (Figure 18C&F). The increase of Chk2 pT68 activation pattern was not observed in ΔSAM mutant HCT116 cells previously (Figure 16A); it is possibly due to the different time points of sample harvest. Strikingly, a dramatic total ATM level elevation was observed in all Mettl8 KO samples with or without irradiation which is consistent with observations in ΔSAM mutant cells and Mettl8&Mettl2 double KD cells.

However, there was only a minor increase of ATM mRNA level in Mettl8 KO cells compared to control cells, suggesting that the upregulation of ATM protein level is not mainly due to positive transcription regulation (Figure 18E). It was the same case with H2AX mRNA and protein level change (Figure 18D&E). H2AX was also more activated in Mettl8 KO cells after irradiation compared to control cells, as shown by probing against γH2AX antibody (Figure 18D), which is consistent with the more activated ATM pS1981 after irradiation in Mettl8 KO cells (Figure 18C). However, p21 expression level and pattern was the same in Mettl8 KO cells and control cells after irradiation; there was even more p21 protein in control cells without irradiation.

After validation of the effect Mettl8 ΔSAM mutant or Mettl8 KO has on ATM and its downstream DDR pathway, we then went further to confirm that the ATM downstream pathway changes were a direct result of ATM activation change, not because of regulation by Mettl8 on each pathway component. As shown in Figure 18G, ATM inhibitor Ku55933 (10μM) pretreatment can eliminate the activation of all the shown ATM substrates, and this result is perfectly consistent between HCT116 Mettl8 overexpression stable cells and Mettl8 KO stable cells.

A.

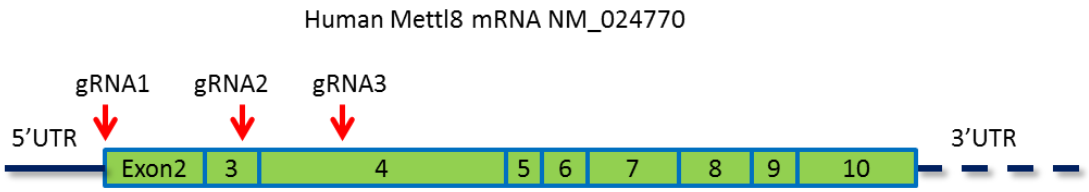

Target	Sequence	Region
gRNA 1	TAACTTTTTAGGTACTGCTT	exon2
gRNA2	CTCAGCTGTGCGAGTCCTTC	exon3
gRNA3	GAAGGCGAGAGAATCATCAT	exon4

B.

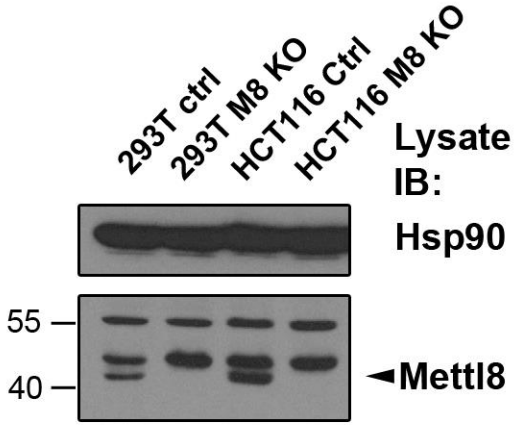

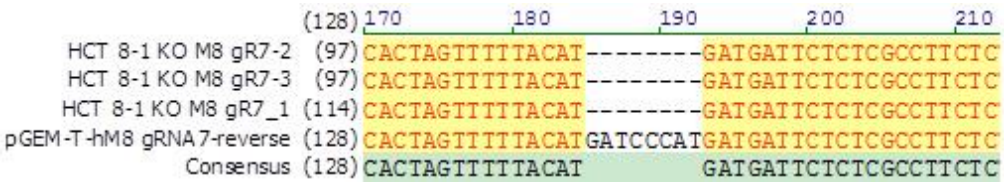

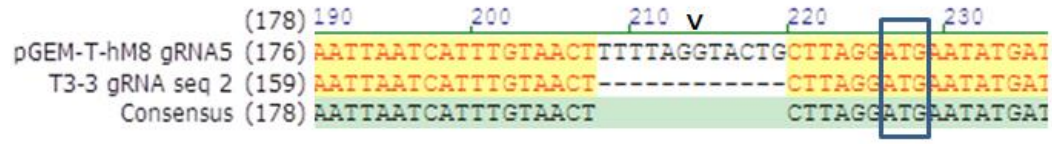

C.

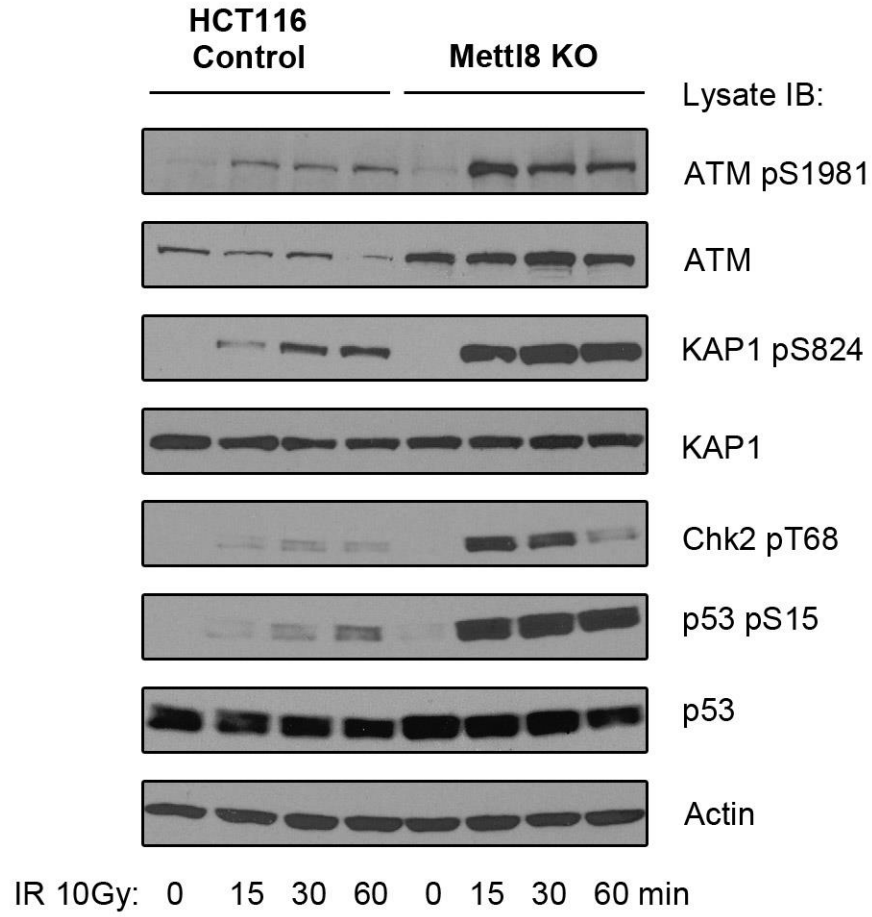
HCT116
Control
Mettl8 KO
Lysate IB:
ATM pS1981
ATM
KAP1 pS824
KAP1
Chk2 pT68
p53 pS15
p53
Actin
IR 10Gy: 0 15 30 60 0 15 30 60 min

D.

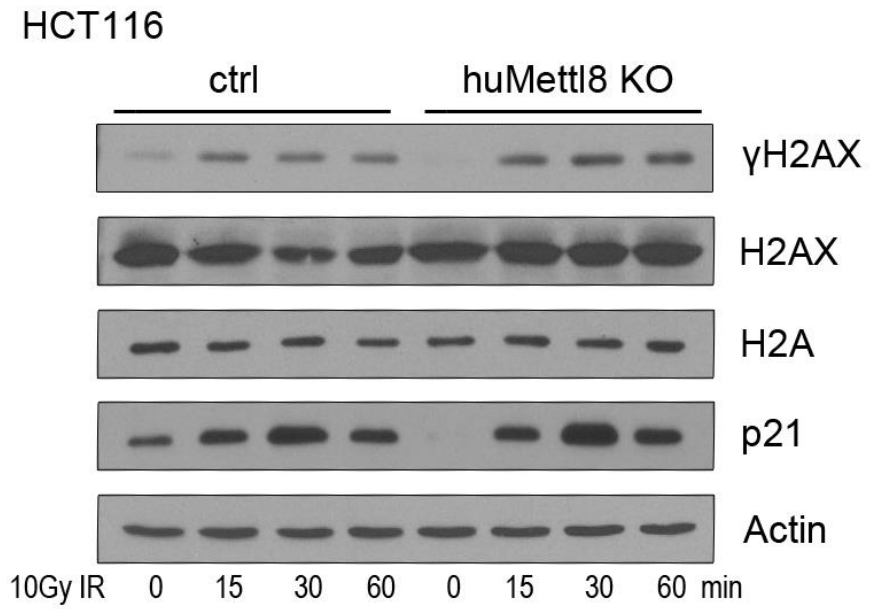
HCT116
ctrl
huMettl8 KO
γH2AX
H2AX
H2A
p21
Actin
10Gy IR 0 15 30 60 0 15 30 60 min

E.

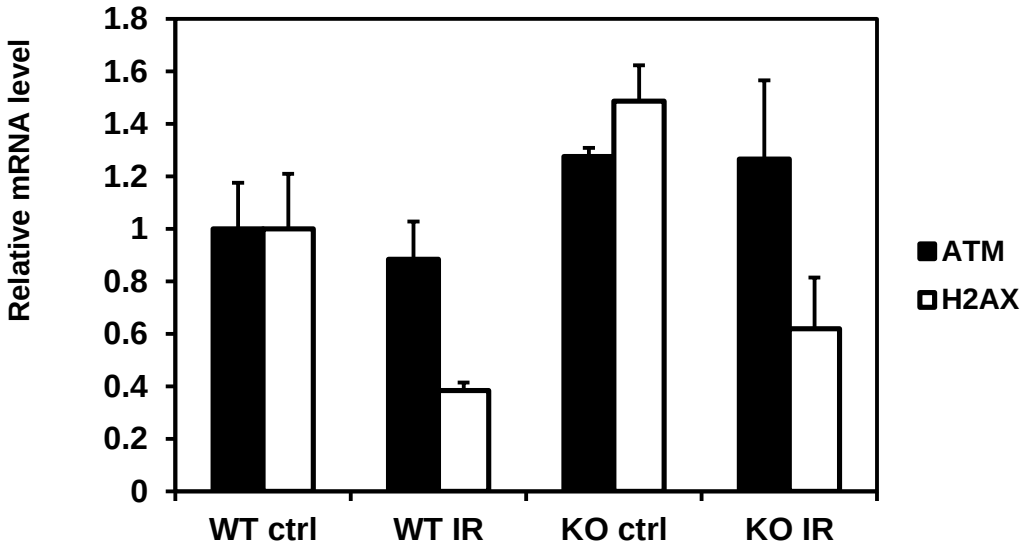
Relative mRNA level
1.8
1.6
1.4
1.2
1
0.8
0.6
0.4
0.2
0
WT ctrl
WT IR
KO ctrl
KO IR
ATM
H2AX

F.

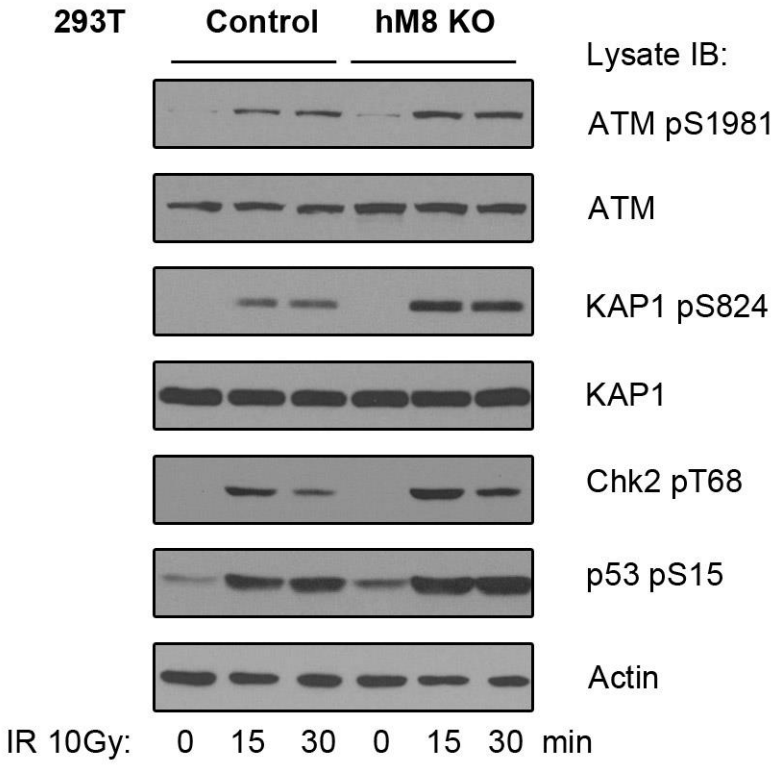
293T
Control
hM8 KO
Lysate IB:
ATM pS1981
ATM
KAP1 pS824
KAP1
Chk2 pT68
p53 pS15
Actin
IR 10Gy: 0 15 30 0 15 30 min

G.

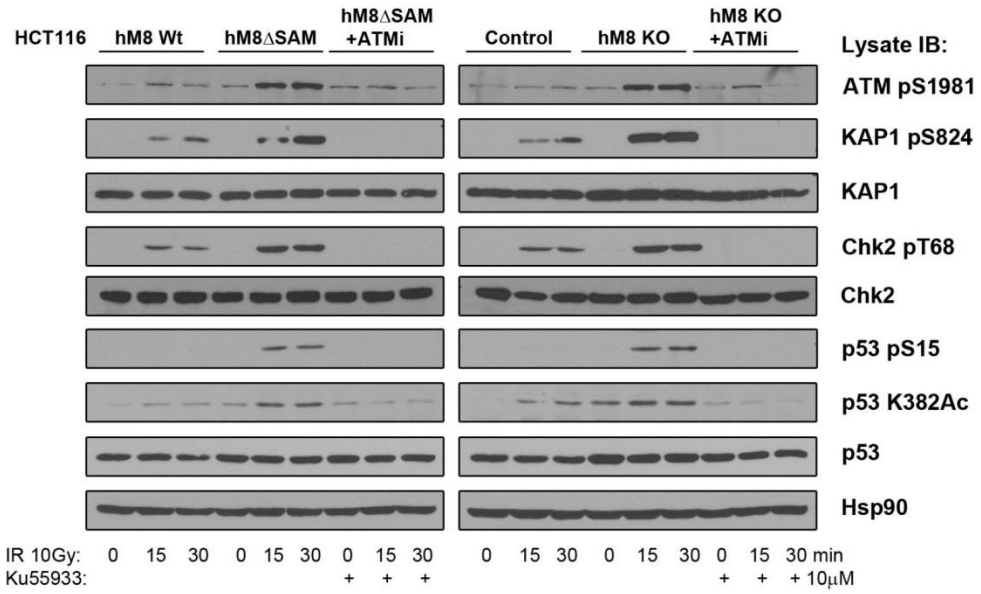
HCT116
hM8 Wt
hM8ΔSAM
hM8ΔSAM +ATMi
Control
hM8 KO
hM8 KO +ATMi
Lysate IB:
ATM pS1981
KAP1 pS824
KAP1
Chk2 pT68
Chk2
p53 pS15
p53 K382Ac
p53
Hsp90
IR 10Gy: 0 15 30 0 15 30 0 15 30 0 15 30 0 15 30 0 15 30 min
Ku55933: + + + + + + + 10μM

Figure 18. Mettl8 knockout affects ATM-p53 DDR.

A) Schematic map of guide RNA (gRNA) target location on the gene of human Mettl8 (upper panel). Sequences of the three gRNAs used (lower panel).

B) Upper panel: Equal amount of lysates from HCT116 and 293T control cells and Mettl8 KO cells were subjected to WB using Mettl8 and Hsp90 (loading control) antibodies.
Middle panel: Sequencing result of HCT116 Mettl8 KO positive clone. Three TA clones (gR7-1,2,3) were sequenced and blasted against intact gDNA sequence.
Bottom panel: Sequencing result of 293T Mettl8 KO positive clone. Three TA clones were sequenced and blasted against intact gDNA sequence. The results were the same. Only one clone (seq 2) is shown. The translation start ATG is shown in a box. The boundary between intron and exon 2 is indicated by a reverse ^ symbol.

C) HCT116 control cells and Mettl8 KO cells were irradiated at 10Gy and left in recovery for the time indicated. Equal amount of lysates were resolved on SDS-PAGE and immunoblotted against the various antibodies listed.

D) Same cells as in C). Total cell lysates were prepared by solubilizing cells in 1×SDS sample buffer and then subjected to WB with indicated antibodies. H2A and Actin were used as loading control.

E) Same cells as in C). Cells were irradiated at 10Gy and left in recovery for 24h, and then were harvested in Trizol. RNA was extracted and reversed for qPCR analysis with indicated primers.

F) 293T control cells and Mettl8 KO cells were irradiated at 10Gy and left in recovery for the time indicated. Equal amount of lysates were resolved on SDS-PAGE and immunoblotted against indicated antibodies.

G) Untreated HCT116 stable cells with WT or ΔSAM Mettl8, and ΔSAM Mettl8 stable cells pretreated with Ku55933 (10 μM) for 1h were irradiated at 10 Gy and left in recovery for the time indicated. Equal amount of lysates were subjected to immunoblotting against antibodies indicated (left). Same experiments were done with Mettl8 KO and control HCT116 cells.

3.2.4 Mettl8 expression in DNA damage response

After establishing Mettl8 as an ATM substrate and its role in regulating ATM-p53 pathway in DDR, we wondered how Mettl8 itself would change in response to DNA damages.

We found that there was no significant change of Mettl8 protein expression level in HCT116 cells within 24 hours in response to 10 Gy IR which caused DSB (Figure 19A). Then we tested Mettl8 protein expression in DNA crosslinks damage induced by different doses of cisplatin in 293T, HCT116 and HepG2 cells. As shown in Figure 19B, Mettl8 expression remained the same when cisplatin concentration increased from 0μM to 30μM in all three cell lines tested. Interesting Mettl8 expression was found to be downregulated by an increase of cisplatin concentration from 30μM to 60μM. In HepG2 cells, Mettl8 expression was not further downregulated when cisplatin concentration went further up to 100 or 150μM. In 293T and HCT116 cells, Mettl8 expression was further suppressed when cisplatin concentration went up from 60μM to 100μM, but did not change between 100μM and 150μM treatment. This result showed that Mettl8 was downregulated in DNA crosslinks damage caused by cisplatin in a dose dependent manner by an unknown mechanism.

Cisplatin is a widely used anticancer agent in the treatment of solid tumors (Basu & Krishnamurthy, 2010). And interestingly upregulation of ATM transcription level was previously reported as a response to DNA crosslinks damage (Yamamoto et al., 2008). Future studies on the role of Mettl8 in cellular response to cisplatin-induced DNA damage may help decide cisplatin sensitivity in cancer therapeutics.

A.

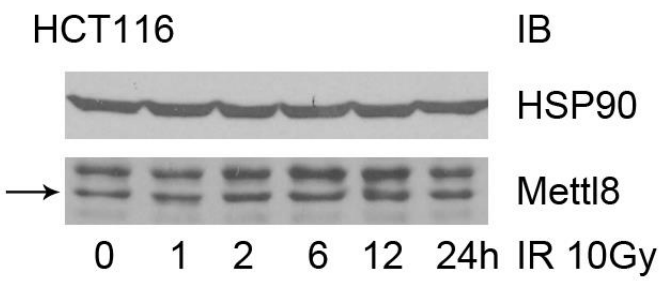

B.

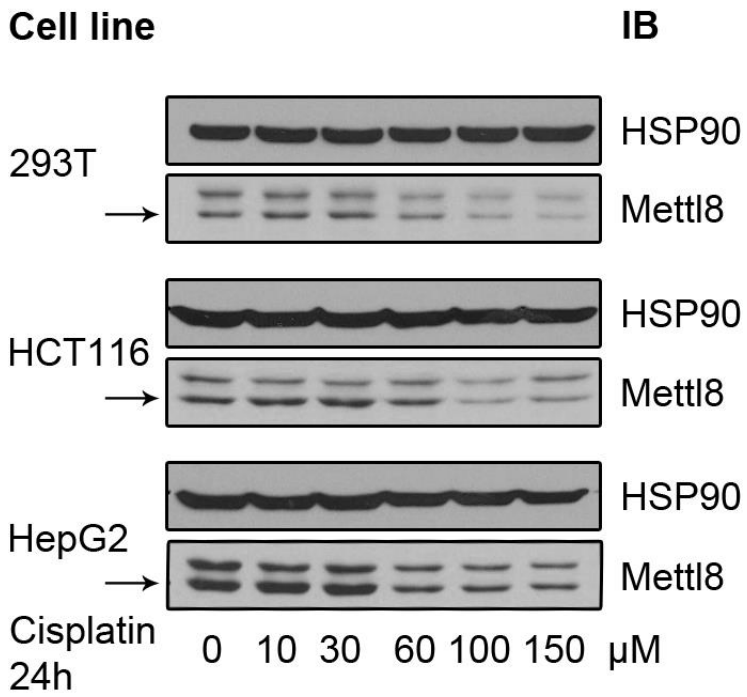

Figure 19. Mettl8 expression level change in different DNA damage response.

A) HCT116 cells were irradiated at 10Gy, and left in recovery for the time indicated. Equal amount of lysates were resolved on SDS-PAGE and immunoblotted against Mettl8 and Hsp90 antibodies.

B) 293T, HCT116 and HepG2 cells were treated with various doses of cisplatin (0, 10, 30, 60, 100, 150μM) for 24h. 40ug lysates were resolved on SDS-PAGE and immunoblotted against Mettl8 and Hsp90 antibodies.

3.2.5 Discussion

In this part, we validated Mettl8 as an ATM substrate and its binding with ATM, p53 and histones. The role of Mettl8 in upregulation of ATM expression and activation, and its downstream pathways was shown consistently under three circumstances: ΔSAM mutant，Mettl8&Mettl2 double KD and Mettl8 KO. By using ATM inhibitor Ku55933, we also showed clearly that the ATM downstream pathway changes were directly affected by ATM. Several mechanisms of ATM activation have been reported in literature, such as the direct recruitment of ATM by MRN complex (J. H. Lee, Goodarzi, Jeggo, & Paull, 2010), and TIP60 mediated acetylation of ATM (Kaidi & Jackson, 2013; Sun et al., 2005). What we found about Mettl8 is a new mechanism for IR induced ATM activation.

Many substrates of ATM are recruited into protein network upon their phosphorylation, showing the coordinating role of ATM to assemble the cascade of signaling events. Some substrate phosphorylation could modulate ATM activation in feedback loop, such as NBS1. In our study, we found S405 mutant of Mettl8 showed certain effect to regulate ATM activation, although the strongest effect was observed in ΔSAM mutant (Figure 16E), as profound as Mettl8 KO and much more profound than Mettl8 KD experiment. The discrepancy could partially be due to insufficient KD of Mettl8 and compensative role from its family member Mettl2.

Our results suggested that in the two cells studied Mettl8 protein level is not crucial in ATM regulation, as neither Mettl8 KD nor Mettl8 wt overexpression had any effect,

unless Mettl8 protein expression was completely abolished by knockout. The SAM mutation only disrupts the binding ability to SAM donor molecule, but leaves the rest part intact which could be responsible for substrate binding. Thus it may be a potent dominant negative mutant. ΔSAM mutant showed substantial effect even at low expression level with the presence of endogenous Mettl8 wt protein which has a much higher protein level, suggesting that the enzymatic function of Mettl8 is critical and dominant negative effect could be more detrimental than protein level change. Whether the SAM domain of Mettl2 protein has similar effect is not covered in the current study, but it is an interesting question for future research.

After we discovered the upregulation of ATM protein level along with ATM hyperactivation, we tried to figure out the underlying mechanism. ATM promoter is under regulation of CpG methylation in HCT116 cells (W. J. Kim, Vo, Shrivastav, Lataxes, & Brown, 2002), however, Mettl8 mutant does not affect the methylation of ATM (data not shown). Although in ΔSAM mutant and Mettl8&Mettl2 double KD HCT116 cells, ATM mRNA level increase was observed in line with protein level increase, the fold change of mRNA level was quite minor compared to that of the protein level. In Mettl8 KO HCT116 cells, this unbalance between ATM mRNA level and protein level was most dramatic, as ATM protein level elevated drastically with ATM mRNA remaining almost unchanged. Thus, it is reasonable to say that the regulation of Mettl8 on ATM is primarily not on a transcriptional level. There was no significant difference of ATM protein stability observed between Mettl8 KO cells and control cells either (data not shown). As introduced in Chapter 1, ATM expression is

tightly regulated by several microRNAs. Whether these microRNAs are changed in our ΔSAM mutant or Mettl8 KO cells is currently under investigation.

There is a minor upregulation of H2AX mRNA level in ΔSAM mutant or Mettl8 KO cells. However, H2AX mRNA upregulation was not found in Mettl8 KD or even Mettl8 and Mettl2 double KD cells, suggesting that there is a different mechanism employed in ΔSAM mutant cells, in line with a more profound change in gene profiling in ΔSAM mutant cells revealed by microarray study compared to Mettl8 single KD cells. Back to the time we did microarray analysis, we didn't know that only Mettl8 and Mettl2 double KD would have significant effect on ATM-p53 pathway and we did not have Mettl8 KO cells, microarray analysis was only done in cells with Mettl8 single KD. Maybe double KD cells or KO cells will have more dramatic change in gene profiling compared to their controls.

ATM and H2AX are important tumor suppressor genes which are colocalized on chromosome 11q and frequently deleted or translocated in certain tumors (Srivastava, Gochhait, de Boer, & Bamezai, 2009). ATM is found to be downregulated in certain tumor models (Bose et al., 2007; Roy, Wang, Makrigiorgos, & Price, 2006; Vo et al., 2004). Therefore, our finding could unveil another potential target for cancer therapy or clinical application.

3.3 Mettl8 regulates cell growth and survival.

Since Mettl8 can modulate ATM-p53 pathway, we then further investigate its physiological significance in cell growth.

As ATM has been shown to be essential for cell checkpoint response, we analyzed the cell cycle profiles of those HCT116 stable clones with Mettl8 wt or ΔSAM mutant overexpressed. As shown in Figure 20C, wild-type Mettl8 cells showed similar profile as empty vector cells at unstimulated condition, while ΔSAM mutant cells showed slightly more accumulation of G2/M population. This trend was more dramatic in the irradiation condition, all three cell lines showed accumulated G2/M cells 24h after 10 Gy gamma irradiation, among which ΔSAM mutant cells showed a significantly highest percentage of G2/M cells. This arrest could be due to upregulated p21 (Figure 16A and Figure 20F) as an established mechanism to prevent damaged cells from migrating into mitosis. However, no significant difference was observed in MTS cell proliferation assay (Figure 20. **Mettl8 is a regulator of cell growth.** or colony formation assay (Figure 20. **Mettl8 is a regulator of cell growth.** between HCT116 stable cells with empty vector, wt or ΔSAM mutant Mettl8. Results of these two assays indicate that the overall growth and survival ability was not affected by overexpression of wt or ΔSAM mutant Mettl8.

The idea of studying the survival and proliferation ability of cells in soft agar was first developed by Hamburger and Salmon in 1977 (Hamburger & Salmon, 1977). The more cancerous cells are the stronger ability they have to grow in

anchorage-independent condition. In the current study, the overexpression of wt or ΔSAM mutant Mettl8 in HCT116 colon cancer cells was assessed in soft agar assay to elucidate its effect on the cells' anchorage-independent growth ability. ΔSAM mutant Mettl8 cells showed much reduced colony number compared to empty vector and wildtype Mettl8 cells (Figure 20D&E), which suggests that overexpression of ΔSAM mutant Mettl8 in cells leads to an attenuated ability in anchorage-independent growth.

Although there is minor upregulation of p21 mRNA in ΔSAM mutant cells, there is no upregulation of Puma, the gene responsible for p53 mediated apoptosis in this situation, especially in the irradiation, suggesting a specific selection of p53 target genes for ΔSAM mutant cells (Figure 20F) which showed different pattern compared to Mettl8 and Mettl2 DKD (Figure 20F). In the DKD cells, there was a drastic elevation of both p21 and Puma mRNA expression even in untreated cells. Consistent with the qPCR result, cell growth and viability were greatly compromised in Mettl8 and Mettl2 DKD cells compared to scramble control cells. If kept in culture for longer time, the survived 'DKD' cells under puromycin selection would finally lose Mettl8 or Mettl2 KD and become single KD cells, indicating that Mettl8 and Mettl2 DKD is lethal to the cells. However, in the Mettl8 KO cells, there was a lower induction fold of both p21 and Puma upon irradiation compared to control cells (Figure 20G), although p53 S15 activation was much higher (Figure 18C). In line with this unusual qPCR result, Mettl8 KO HCT116 cells actually grew faster than

control cells in colony formation assay as shown in Figure 20H, which is in dramatic contrast with the scenarios in ΔSAM mutant cells and DKD cells,.

To try to explain the reduced growth ability of HCT116 ΔSAM mutant cells in soft agar assay, we tested the mRNA level of E-cadherin (CDH1) in the cells. CDH1 is a tumor suppressor as loss of it can lead to cancer cell invasion and tumor metastasis (van Roy & Berx, 2008); it was shown in several cancers including colon cancer (X. Chen et al., 2012). A shown in Figure 20I, ΔSAM mutant cells had almost 3-fold increase of CDH1 mRNA level compared to Mettl8 wt cells, which is in line with soft agar result. In great contrast, Mettl8 KO cells had over 60% decrease of CDH1 mRNA compared to control cells.

A.

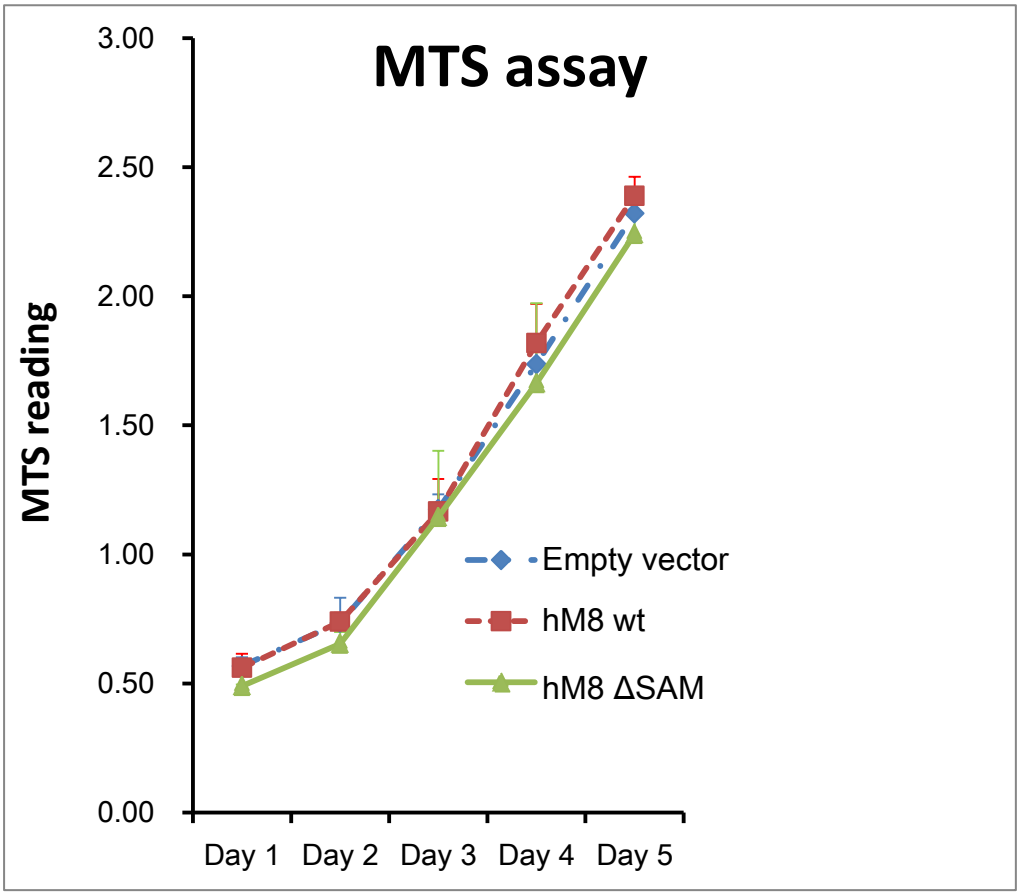
MTS assay
MTS reading
3.00
2.50
2.00
1.50
1.00
0.50
0.00
Day 1
Day 2
Day 3
Day 4
Day 5
Empty vector
hM8 wt
hM8 ΔSAM

B.

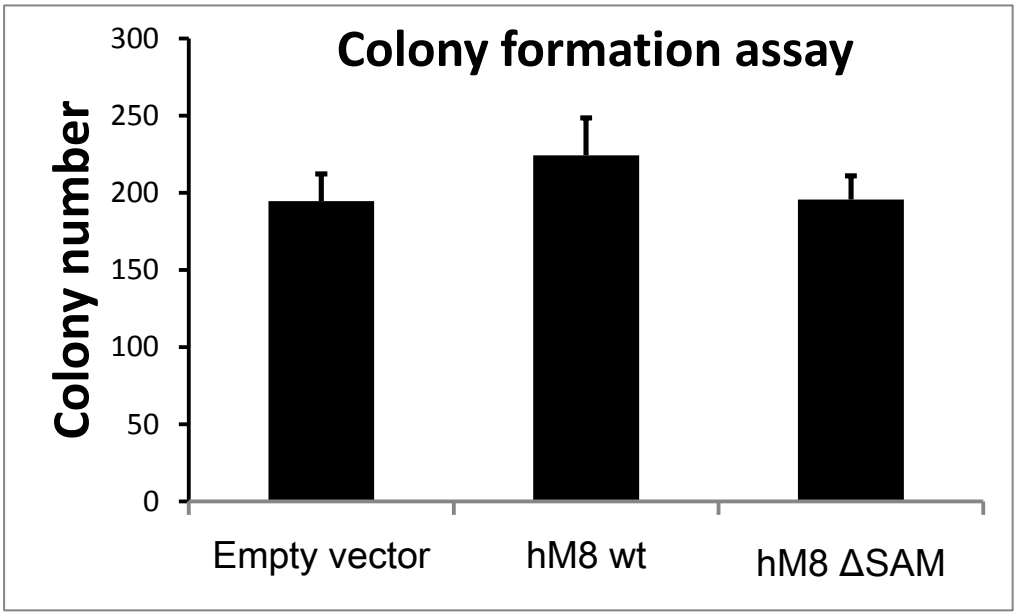
Colony formation assay
Colony number
300
250
200
150
100
50
0
Empty vector
hM8 wt
hM8 ΔSAM

C.

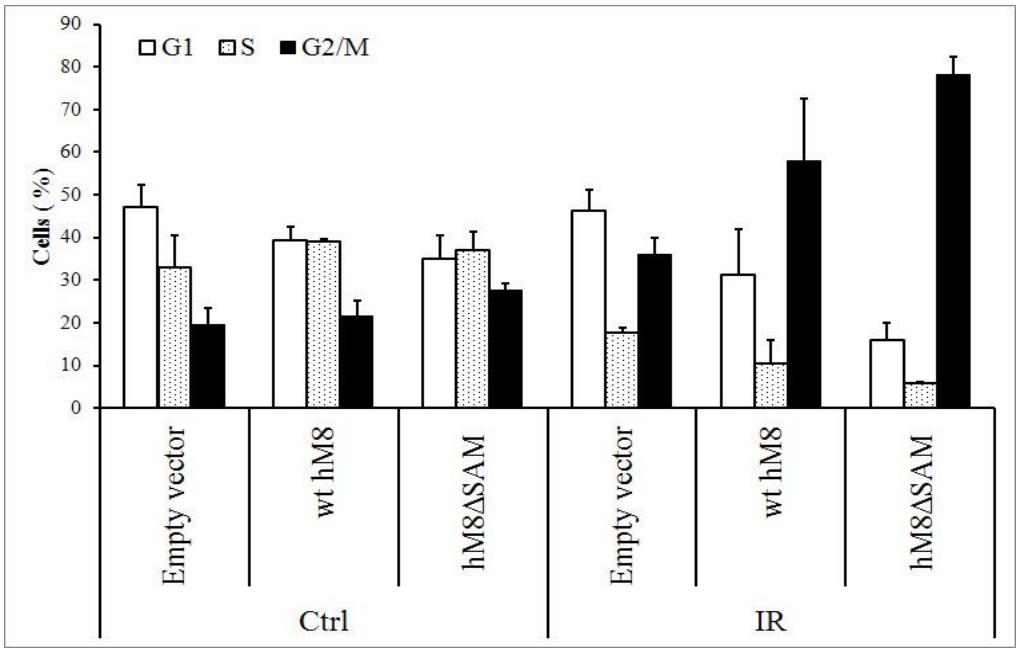
G1
S
G2/M
Cells (%)
90
80
70
60
50
40
30
20
10
0
Empty vector
wt hM8
hM8ΔSAM
Empty vector
wt hM8
hM8ΔSAM
Ctrl
IR

D.

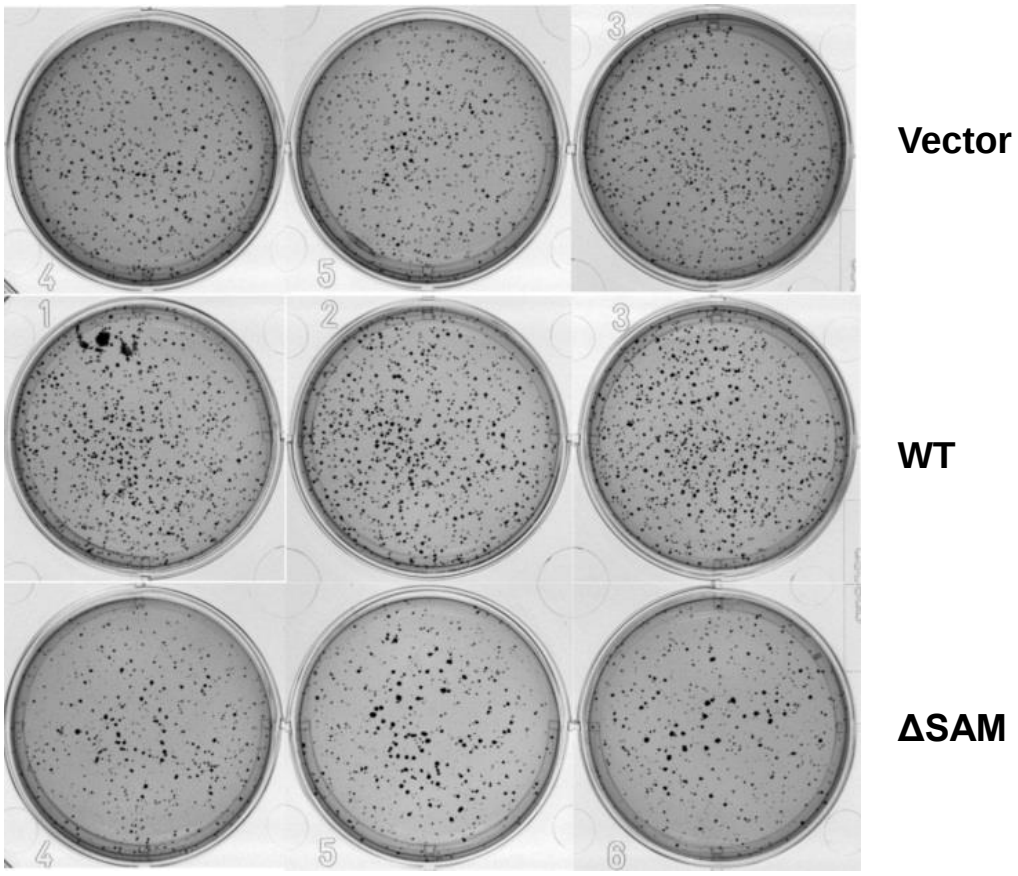
Vector
WT
ΔSAM

E.

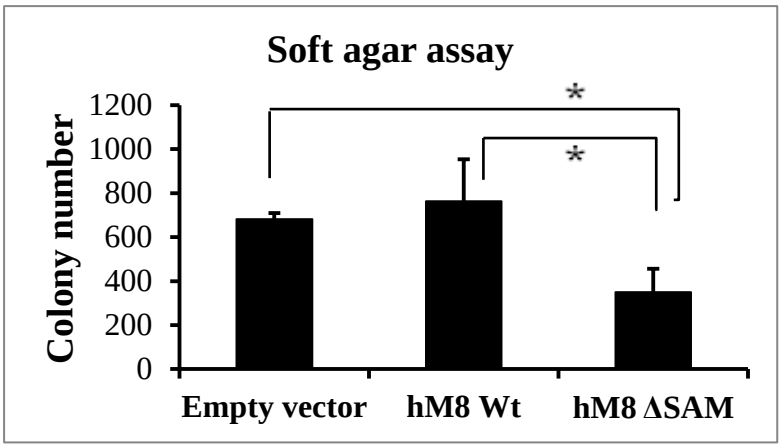
Soft agar assay
Colony number
1200
1000
800
600
400
200
0
*
*
Empty vector
hM8 Wt
hM8 ΔSAM

F.

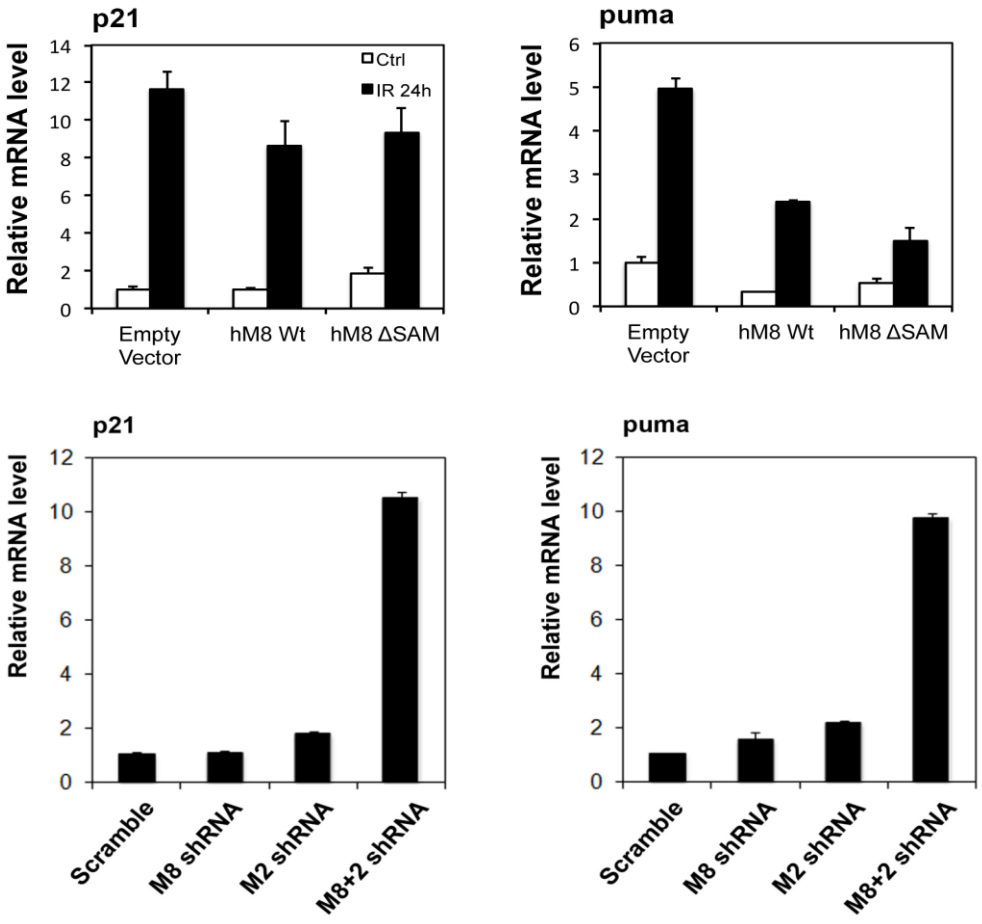
p21
Relative mRNA level
Ctrl
IR 24h
Empty Vector
hM8 Wt
hM8 ΔSAM
puma
Relative mRNA level
Empty Vector
hM8 Wt
hM8 ΔSAM
p21
Relative mRNA level
Scramble
M8 shRNA
M2 shRNA
M8+2 shRNA
puma
Relative mRNA level
Scramble
M8 shRNA
M2 shRNA
M8+2 shRNA

G.

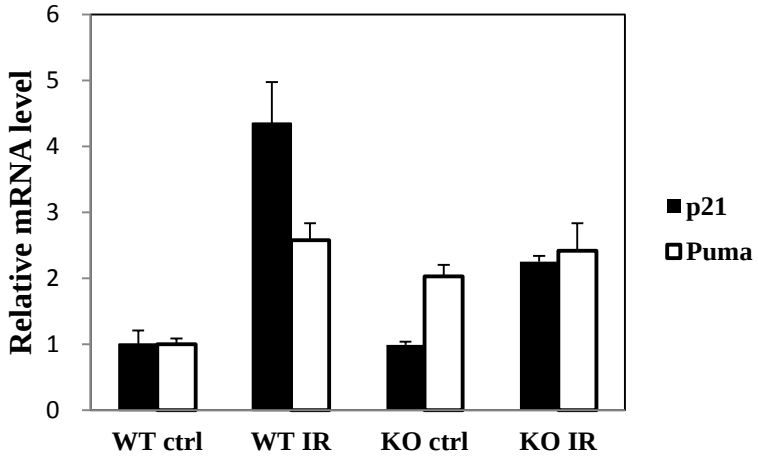
Relative mRNA level
6
5
4
3
2
1
0
WT ctrl
WT IR
KO ctrl
KO IR
p21
Puma

H.

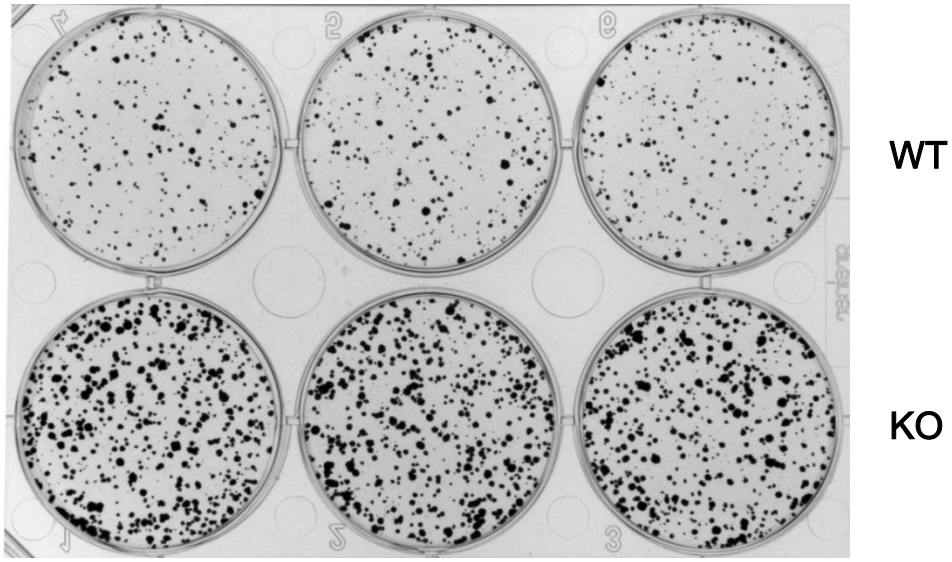
WT
KO

I.

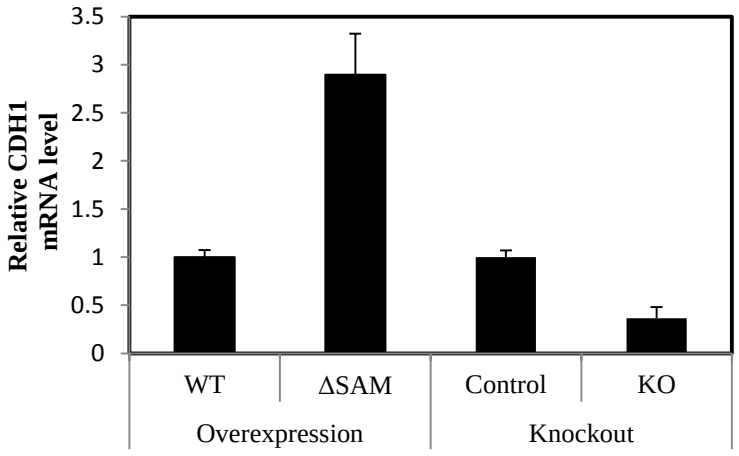
Relative CDH1 mRNA level
3.5
3
2.5
2
1.5
1
0.5
0
WT
ΔSAM
Control
KO
Overexpression
Knockout

Figure 20. Mettl8 is a regulator of cell growth.

A) Growth of HCT116 stable cells with Mettl8 variants was measured using Promega CellTiter 96® AQueous Non-Radioactive Cell Proliferation Assay. The experiment was done three times independently.

B) Quantification of colony formation assay. The colony number shown is average of three independent experiments. HCT116 stable cells with Mettl8 WT or ΔSAM overexpressed were seeded at 500 cells/well in 6-well plates in triplicate manner. After 14 days colonies were stained and scanned in Bio-Rad Gel Doc EZ system. Colonies with more than 50 cells were counted with Quantity One software.

C) HCT116 stable cells with Mettl8 variants were stained with propidium iodide (PI) and profiled for cell cycle by FACS. The experiment was done three times independently. Data was analyzed with FlowJo software.

D) HCT116 stable cells with Mettl8 WT or ΔSAM overexpressed were seeded at 2500 cells/well in 6-well plates in triplicate manner. After 20 days colonies grown in soft agar were stained and scanned in Bio-Rad Gel Doc EZ system. Colonies with more than 50 cells were counted with Quantity One software. The picture is representative of three independent experiments.

E) Quantification of soft agar assay. The colony number shown is average of three independent experiments. * indicates $p<0.05$ by single-tail t-test analysis.

F) HCT116 stable clones with Mettl8 variants were irradiated at 10Gy and left in recovery for 24h (upper panel). HCT116 cells were infected with lentiviruses harboring shRNA(s) against Mettl8 (M8), Mettl2 (M2), both Mettl8 and Mettl2 (M8+2), or scramble control for 72 hours (lower panel). RNA was extracted and reversed for qPCR analysis with indicated primers.

G) HCT116 cells with Mettl8 KO or control were irradiated at 10Gy and left in recovery for 24h. RNA was extracted and reversed for qPCR analysis with indicated primers.

H) HCT116 cells with Mettl8 KO or control were seeded at 500 cells/well in 6-well plates in triplicate manner. After 14 days colonies grown were stained by crystal violet and scanned in Bio-Rad Gel Doc EZ system. The picture is representative of three independent experiments.

I) RNA was extracted from HCT116 stable cells with Mettl8 wt or ΔSAM, and HCT116 cells with Mettl8 KO or control. Then the samples were reversed for qPCR analysis with CDH1 primer.

3.3.1 Discussion

In this chapter, the effect of ΔSAM mutant overexpression, Mettl8&Mettl2 DKD or Mettl8 KO on cell growth and survival was assessed in HCT116 cells.

Our observation of G2/M arrest in HCT116 cells 24h after irradiation is consistent with previous reports (Essmann et al., 2005; Flatmark et al., 2006). The significant higher accumulation of G2/M cells in ΔSAM mutant cells correlates with the hyperactivation of p21 in the same cells, as p21 is an essential gene in cell cycle arrest after DNA damage. p21 overexpression can lead to G1, G2 or S arrest in different circumstances (Gartel & Tyner, 2002) and it is required to sustain G2/M arrest after DNA damage (Bunz et al., 1998; Lossaint, Besnard, Fisher, Piette, & Dulic, 2011; Wendt et al., 2006).

The tumor suppressor p53 is a highly potent transcription factor maintained at low levels under normal circumstances. In response to cellular stress such as DNA damage p53 gets stabilized and activated, the biological outcome of which can be growth arrest, apoptosis and other responses (Vogelstein, Lane, & Levine, 2000). The choice between growth arrest and apoptosis is dependent on a complex range of factors including cell type, stress type, the presence of p53 co-activators and regulators and post-translational modification of p53 (Meek, 2004; Vousden, 2006). The existence of Mettl8 seems to be crucial for p53 regulation of certain downstream targets as Mettl8 KO in cells resulted in a suppressed induction of p21 and Puma even

with higher level of activated p53 present upon IR treatment (Figure 18C&D, Figure 20G).

Epithelial-mesenchymal transition (EMT) is a key biological process involved in development, cancer invasion and metastasis. Although loss of E-cadherin (CDH1) expression is not causal or necessary in EMT (Hollestelle et al., 2013), CDH1 expression is closely associated with EMT and cancer metastasis (Cano et al., 2000; Kalluri & Weinberg, 2009; Onder et al., 2008). We demonstrated that Mettl8 could affect CDH1 level in cells although the underlying mechanism is unknown yet; this implies a possible role of Mettl8 in cancer metastasis and embryonic development.

ATM total level and activation upregulation were consistently observed in ΔSAM mutant cells, DKD cells, and Mettl8 KO HCT116 cells, but the overall output effects on cell growth and survival differ so much (Figure 21). This suggests a role of Mettl8 in other unknown pathways that play a more dominant role in regulating cell growth than ATM-p53 DDR, which requires further investigation.

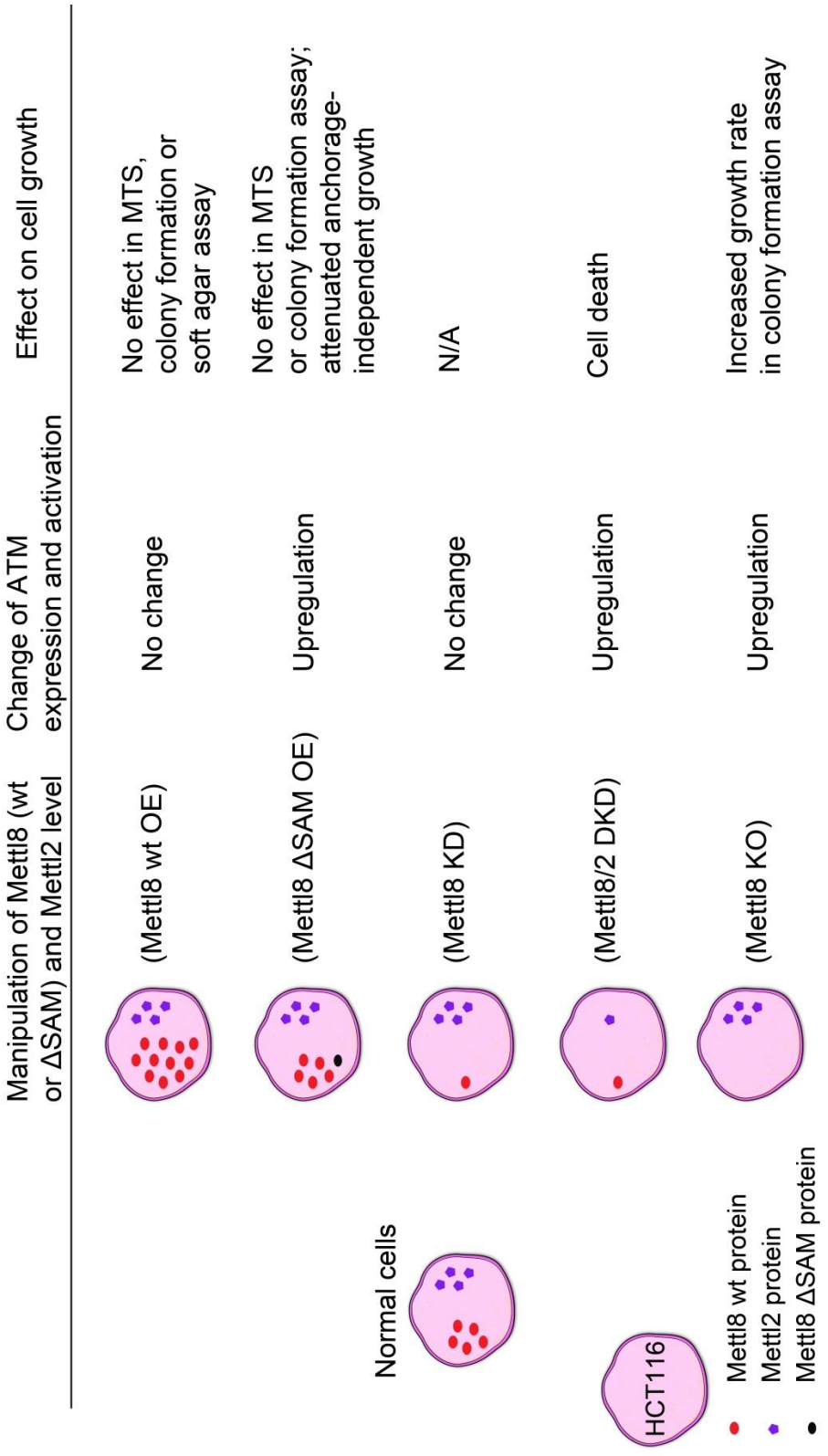

Figure 21. Mettl8 and ATM.

A diagram summary of the experiment results in Chapter 3.2&3.3.

The effect of Mettl8 expression level change on Mettl2 expression was not studied. So Mettl2 protein level was depicted as unchanged in the figure except in the DKD cells. The protein localization was not taken into consideration.

Chapter 4 Conclusions, Discussions and Future Work

Generally we have fulfilled the aim of our research and elucidated some important functions of human Mettl8 protein especially in DDR.

4.1 Mettl8 is novel substrate of ATM and regulates ATM expression and activation.

In a large scale ATM substrates study from Elledge group (Matsuoka et al., 2007), about 700 proteins with pS/TQ motif were identified in pS/TQ IP followed by Mass spectrometry. Many novel substrates were listed in the supplementary data of their paper with unclear functions, expanding our understanding of ATM kinase function beyond DNA damage response. Among those, we found the peptide around Mettl8's Ser405 site, which supports our finding of this unique pS/TQ. However, we not only validated this site in two cell lines but also did further mutagenesis study to confirm this is the only phosphorylation site by ATM in response to IR in which the role of ATM has been established. Our work with chemical inhibitor further consolidated this dependence on ATM (Figure 14B&C) and the cell fractionation work with mutants indicated that this phosphorylation is likely to occur in nucleus where ATM executed its DNA damage response function (Figure 12A&Figure 14E). There is a concern about the human specific feature as this pS/TQ motif is missing in Mettl8 from other organisms, and only the longest isoform of human Mettl8 has this motif. Actually, this situation is also observed in many important mediators of DNA damage response in

that mouse and human homologue indeed show variance in the pS/TQ sites (Matsuoka et al., 2007).

Mettl8 was not found to co-localize with IRIF as shown by γH2AX foci (data not shown), suggesting it may indirectly affect DNA damage response. We shall bear on mind that not all ATM substrates are recruited to such foci; a well-known exception is Chk2 although it plays critical role in checkpoint response elicited by DNA damage.

ATM gene variants and mutations were generally more appreciated and associated with cancer risks in previous studies (Mitui et al., 2009; Shen et al., 2012), especially in breast cancer (Ahmed & Rahman, 2006; Broeks et al., 2008; Khanna & Chenevix-Trench, 2004). However there were also reports about ATM protein level as a useful marker for identifying breast cancer patients at high risk of clinical radiosensitivity (Fang et al., 2010) and the important role of ATM protein level in the maintenance of the shortened telomeres commonly found in prostate cancer cells (Angèle et al., 2004). Our result about Mettl8 and ATM level suggested that loss of Mettl8 protein expression could be a possible reason for increased ATM level in cancer cells.

4.2 Mettl8 is a potential methyltransferase with unknown substrate.

The most conserved feature of Mettl8 is SANT and SAM domain. Mettl8 is named after its SAM binding domain, which suggests it could be a class I SAM dependent methyltransferase. However, it's challenging to identify the exact substrate for any methyltransferase given its diverse candidate atoms to accept methyl group which

could be on DNA, protein or small molecule. We can get some information from mutant phenotype but the final proof is still biochemical assay (T. C. Petrossian & Clarke, 2011). Recently Mettl2 was found to be homolog of a yeast tRNA methyltransferase Trm140. Whether Mettl8 could work similarly on RNA species is under investigation.

In conclusion, in this study Mettl8 is identified as a novel target of Stat3 and a potential methyltransferase with SAM binding activity. And it is also a new substrate of ATM which phosphorylates Mettl8 at S405. Mettl8 mutation on SAM domain or Mettl8 knockout or Mettl8 and Mettl2 double knockdown can promote ATM activation possibly via upregulation of ATM expression level. Hyperactivation of ATM after irradiation in turn phosphorylates p53 and H2AX to initiate DNA damage response. The role of Mettl8 in DNA damage response is established at least in two parts: it is a substrate of ATM and in some unknown manner it regulates ATM level and activation in DSB.

To our knowledge, our work is the first detailed study of one potential methyltransferase as an ATM substrate and its modulating effect on ATM expression and activation. Interestingly several other methyltransferase proteins were listed in the Elledge group's ATM/ATR substrate list (Matsuoka et al., 2007): tRNA (adenine(58)-N(1))-methyltransferase non-catalytic subunit TRM6, histone lysine N-methyltransferase 2D, euchromatic histone-lysine N-methyltransferase 1 and 2 (EHMT1&2), Mettl3, Mettl10d, and Mettl18. It will be very intriguing to study how

other ATM/ATR-substrate MTases interact with ATM/ATR, which is very likely to greatly expand our view of DDR, ATM/ATR and MTase.

4.3 Limitations of the current work

The first limitation of our current work is that the main results about Mettl8 and ATM were obtained in two cell lines: HCT116-WT and 293T. Whether this could apply to other cell lines like human fibroblasts or *in vivo* situations requires further investigation. Although mouse Mettl8 has no pS/TQ motif, it does have a SAM domain for potential methyltransferase activity, so it is also interesting to study Mettl8 and ATM in mouse.

Another limitation is the potential off-target effect of the CRISPR/Cas9 knockout, as CRISPR RNA-guided nuclease was reported to be highly active even with imperfectly matched RNA-DNA interfaces in human cells (Fu et al., 2013). More gRNAs should be tested and rescue experiment can provide extra evidence.

We established Mettl8 as a Stat3 target but we did not do further in-depth studies to find a physiological role for this link. There were reports about Stat3 modulating the DDR pathway (Barry et al., 2010) and involvement of ATM in Stat3 phosphorylation (Y. Zhang et al., 2003), whether Mettl8 plays a role in these regulations is also worth studies.

4.4 Future work

Much remains to be done in order to achieve a full understanding of the mechanism underlying the regulation of Mettl8 on ATM expression and activation and the role of

Mettl8 in other pathways. In order to deepen and broaden our knowledge of Mettl8 and ATM, it is imperative to investigate the following:

i. The miRNA profile of Mettl8 ΔSAM mutant cells and Mettl8 KO cells compared to their respective control.

   As mentioned earlier, the regulation of Mettl8 on ATM expression is not mainly on a transcription level or by protein stability regulation. Since there are many miRNAs reported to regulate ATM expression, it is reasonable to test whether ATM regulating miRNAs are changed in Mettl8 ΔSAM mutant cells and Mettl8 KO cells.

ii. The effect on ATM pathway of Mettl8 with mutation of SANT or NRB domain.

   Besides SAM domain, SANT and NRB domain also execute important functions in Mettl8 protein as shown by the Schuger group (Badri et al., 2008; Jakkaraju et al., 2005). Studying whether disruption of these domains would affect ATM expression or activation is essential for a full understanding of Mettl8's regulation of ATM.

iii. The whole protein and mRNA profile change in Mettl8 KO cells compared to control.

   A view of the global mRNA and protein change induced by Mettl8 KO may help explain the distinct effect of ΔSAM mutant and Mettl8 KO on cell growth, and also provide insights into the function of Mettl8 in other pathways.

iv. The role of Mettl8 in other ATM related functions besides DDR.

v. The relevance of the nucleolar localization of Mettl8 to cell stress response and function of p53.

Nucleolus is more and more appreciated as a central hub in stress response that coordinates cell growth arrest and DNA repair mechanisms (Antoniali, Lirussi, Poletto, & Tell, 2013; Boulon, Westman, Hutten, Boisvert, & Lamond, 2010), and also a stress sensor responsible for p53 level maintenance (Rubbi & Milner, 2003). Given the preferred localization of Mettl8 in nucleolus, its potential enzymatic function as RNA methyltransferase and the regulation of ATM we established, it is intriguing to further investigate the relevance of Mettl8 to nucleolar stress responses.

Bibliography

Agarwal, M. L., Agarwal, A., Taylor, W. R., & Stark, G. R. (1995). p53 controls both the G2/M and the G1 cell cycle checkpoints and mediates reversible growth arrest in human fibroblasts. *Proc Natl Acad Sci U S A, 92*(18), 8493-8497.

Ahmed, M., & Rahman, N. (2006). ATM and breast cancer susceptibility. *Oncogene, 25*(43), 5906-5911. doi: 10.1038/sj.onc.1209873

Alexandrov, A., Martzen, M. R., & Phizicky, E. M. (2002). Two proteins that form a complex are required for 7-methylguanosine modification of yeast tRNA. *RNA, 8*(10), 1253-1266.

Alvarez, J. V., & Frank, D. A. (2004). Genome-wide analysis of STAT target genes: elucidating the mechanism of STAT-mediated oncogenesis. *Cancer Biol Ther, 3*(11), 1045-1050.

Angèle, S., Falconer, A., Foster, C. S., Taniere, P., Eeles, R. A., & Hall, J. (2004). ATM Protein Overexpression in Prostate Tumors: Possible Role in Telomere Maintenance. *American Journal of Clinical Pathology, 121*(2), 231-236. doi: 10.1309/jtkgggkurfx3xmgt

Antoniali, G., Lirussi, L., Poletto, M., & Tell, G. (2013). Emerging Roles of the Nucleolus in Regulating the DNA Damage Response: The Noncanonical DNA Repair Enzyme APE1/Ref-1 as a Paradigmatical Example. *Antioxid Redox Signal*. doi: 10.1089/ars.2013.5491

Badri, K. R., Zhou, Y., Dhru, U., Aramgam, S., & Schuger, L. (2008). Effects of the SANT domain of tension-induced/inhibited proteins (TIPs), novel partners of the histone acetyltransferase p300, on p300 activity and TIP-6-induced adipogenesis. *Mol Cell Biol, 28*(20), 6358-6372. doi: MCB.00333-08 [pii]

10.1128/MCB.00333-08 [doi]

Bakkenist, C. J., & Kastan, M. B. (2003). DNA damage activates ATM through intermolecular autophosphorylation and dimer dissociation. *Nature, 421*(6922), 499-506. doi: 10.1038/nature01368

Banin, S., Moyal, L., Shieh, S., Taya, Y., Anderson, C. W., Chessa, L., . . . Ziv, Y. (1998). Enhanced phosphorylation of p53 by ATM in response to DNA damage. *Science, 281*(5383), 1674-1677.

Barnes, D. E., & Lindahl, T. (2004). REPAIR AND GENETIC CONSEQUENCES OF ENDOGENOUS DNA BASE DAMAGE IN MAMMALIAN CELLS. *Annual Review of Genetics, 38*(1), 445-476. doi: doi:10.1146/annurev.genet.38.072902.092448

Barry, S. P., Townsend, P. A., Knight, R. A., Scarabelli, T. M., Latchman, D. S., & Stephanou, A. (2010). STAT3 modulates the DNA damage response pathway. *Int J Exp Pathol, 91*(6), 506-514. doi: 10.1111/j.1365-2613.2010.00734.x

Bartek, J., Bartkova, J., & Lukas, J. (2007). DNA damage signalling guards against activated oncogenes and tumour progression. *Oncogene, 26*(56), 7773-7779. doi: 10.1038/sj.onc.1210881

Bartel, D. P. (2004). MicroRNAs: Genomics, Biogenesis, Mechanism, and Function. *Cell, 116*(2), 281-297. doi: 10.1016/S0092-8674(04)00045-5

Bartkova, J., Horejsi, Z., Koed, K., Kramer, A., Tort, F., Zieger, K., . . . Bartek, J. (2005). DNA damage response as a candidate anti-cancer barrier in early human tumorigenesis. *Nature, 434*(7035), 864-870. doi: 10.1038/nature03482

Bartkova, J., Rezaei, N., Liontos, M., Karakaidos, P., Kletsas, D., Issaeva, N., . . . Gorgoulis, V. G. (2006). Oncogene-induced senescence is part of the tumorigenesis barrier imposed by DNA damage checkpoints. *Nature, 444*(7119), 633-637. doi: 10.1038/nature05268

Basu, A., & Krishnamurthy, S. (2010). Cellular responses to Cisplatin-induced DNA damage. *J Nucleic Acids, 2010*. doi: 10.4061/2010/201367

Berkovich, E., & Ginsberg, D. (2003). ATM is a target for positive regulation by E2F-1. *Oncogene, 22*(2), 161-167. doi: 10.1038/sj.onc.1206144

Bird, A. (2002). DNA methylation patterns and epigenetic memory. *Genes and Development, 16*(1), 6-21. doi: 10.1101/gad.947102

Bokar, J. A., Shambaugh, M. E., Polayes, D., Matera, A. G., & Rottman, F. M. (1997). Purification and cDNA cloning of the AdoMet-binding subunit of the human mRNA (N6-adenosine)-methyltransferase. *RNA, 3*(11), 1233-1247.

Bose, S., Starczynski, J., Chukwuma, M., Baumforth, K., Wei, W., Morgan, S., . . . Stankovic, T. (2007). Down-regulation of ATM protein in HRS cells of nodular sclerosis Hodgkin's lymphoma in children occurs in the absence of ATM gene inactivation. *J Pathol, 213*(3), 329-336. doi: 10.1002/path.2232

Boulon, S., Westman, B. J., Hutten, S., Boisvert, F.-M., & Lamond, A. I. (2010). The Nucleolus under Stress. *Molecular Cell, 40*(2), 216-227.

Bristow, R. G., & Hill, R. P. (2008). Hypoxia and metabolism: Hypoxia, DNA repair and genetic instability. *Nat Rev Cancer, 8*(3), 180-192. doi: 10.1038/nrc2344

Broeks, A., Braaf, L. M., Huseinovic, A., Schmidt, M. K., Russell, N. S., Van Leeuwen, F. E., . . . Van 'T Veer, L. J. (2008). The spectrum of ATM missense variants and their contribution to contralateral breast cancer. *Breast Cancer Research and Treatment, 107*(2), 243-248. doi: 10.1007/s10549-007-9543-6

Bunz, F., Dutriaux, A., Lengauer, C., Waldman, T., Zhou, S., Brown, J. P., . . . Vogelstein, B. (1998). Requirement for p53 and p21 to Sustain G2 Arrest After DNA Damage. *Science, 282*(5393), 1497-1501. doi: 10.1126/science.282.5393.1497

Burma, S., Chen, B. P., Murphy, M., Kurimasa, A., & Chen, D. J. (2001). ATM phosphorylates histone H2AX in response to DNA double-strand breaks. *J Biol Chem, 276*(45), 42462-42467. doi: 10.1074/jbc.C100466200

Cano, A., Perez-Moreno, M. A., Rodrigo, I., Locascio, A., Blanco, M. J., del Barrio, M. G., . . . Nieto, M. A. (2000). The transcription factor Snail controls epithelial-mesenchymal transitions by repressing E-cadherin expression. *Nat Cell Biol, 2*(2), 76-83.

Cao, L., Kim, S., Xiao, C., Wang, R. H., Coumoul, X., Wang, X., . . . Deng, C. X. (2006). ATM-Chk2-p53 activation prevents tumorigenesis at an expense of

organ homeostasis upon Brca1 deficiency. *EMBO J, 25*(10), 2167-2177. doi: 10.1038/sj.emboj.7601115

Catoni, G. L. (1953). S-Adenosylmethionine; a new intermediate formed enzymatically from L-methionine and adenosinetriphosphate. *The Journal of biological chemistry, 204*(1), 403-416.

Chapman, J. R., Taylor, Martin R. G., & Boulton, Simon J. (2012). Playing the End Game: DNA Double-Strand Break Repair Pathway Choice. *Molecular Cell, 47*(4), 497-510.

Chehab, N. H., Malikzay, A., Appel, M., & Halazonetis, T. D. (2000). Chk2/hCds1 functions as a DNA damage checkpoint in G(1) by stabilizing p53. *Genes Dev, 14*(3), 278-288.

Chen, X., Wang, Y., Xia, H., Wang, Q., Jiang, X., Lin, Z., . . . Hu, M. (2012). Loss of E-cadherin promotes the growth, invasion and drug resistance of colorectal cancer cells and is associated with liver metastasis. *Molecular Biology Reports, 39*(6), 6707-6714. doi: 10.1007/s11033-012-1494-2

Chen, Y., Kamili, A., Hardy, J. R., Groblewski, G. E., Khanna, K. K., & Byrne, J. A. (2013). Tumor protein D52 represents a negative regulator of ATM protein levels. *Cell Cycle, 12*(18), 3083-3097. doi: 10.4161/cc.26146

Cheung, P. C., Campbell, D. G., Nebreda, A. R., & Cohen, P. (2003). Feedback control of the protein kinase TAK1 by SAPK2a/p38alpha. *EMBO J, 22*(21), 5793-5805. doi: 10.1093/emboj/cdg552

Ciccia, A., & Elledge, S. J. (2010). The DNA Damage Response: Making It Safe to Play with Knives. *Molecular Cell, 40*(2), 179-204. doi: 10.1016/j.molcel.2010.09.019

Cong, L., Ran, F. A., Cox, D., Lin, S., Barretto, R., Habib, N., . . . Zhang, F. (2013). Multiplex genome engineering using CRISPR/Cas systems. *Science, 339*(6121), 819-823. doi: 10.1126/science.1231143

Cortez, D., Wang, Y., Qin, J., & Elledge, S. J. (1999). Requirement of ATM-dependent phosphorylation of brca1 in the DNA damage response to double-strand breaks. *Science, 286*(5442), 1162-1166.

Di Leonardo, A., Linke, S. P., Clarkin, K., & Wahl, G. M. (1994). DNA damage triggers a prolonged p53-dependent G1 arrest and long-term induction of Cip1 in normal human fibroblasts. *Genes Dev, 8*(21), 2540-2551.

Dingwall, C., & Laskey, R. A. (1991). Nuclear targeting sequences - A consensus? *Trends in Biochemical Sciences, 16*(12), 478-481.

Ehret, G. B., Reichenbach, P., Schindler, U., Horvath, C. M., Fritz, S., Nabholz, M., & Bucher, P. (2001). DNA binding specificity of different STAT proteins. Comparison of in vitro specificity with natural target sites. *J Biol Chem, 276*(9), 6675-6688. doi: 10.1074/jbc.M001748200 [doi]

M001748200 [pii]

Elson, A., Wang, Y., Daugherty, C. J., Morton, C. C., Zhou, F., Campos-Torres, J., & Leder, P. (1996). Pleiotropic defects in ataxia-telangiectasia protein-deficient mice. *Proceedings of the National Academy of Sciences of the United States of America, 93*(23), 13084-13089. doi: 10.1073/pnas.93.23.13084

Essmann, F., Pohlmann, S., Gillissen, B., Daniel, P. T., Schulze-Osthoff, K., & Jänicke, R. U. (2005). Irradiation-induced Translocation of p53 to Mitochondria in the Absence of Apoptosis. *Journal of Biological Chemistry, 280*(44), 37169-37177. doi: 10.1074/jbc.M502052200

Falck, J., Coates, J., & Jackson, S. P. (2005). Conserved modes of recruitment of ATM, ATR and DNA-PKcs to sites of DNA damage. *Nature, 434*(7033), 605-611. doi: 10.1038/nature03442

Fang, Z., Kozlov, S., McKay, M., Woods, R., Birrell, G., Sprung, C., . . . Clarke, R. (2010). Low levels of ATM in breast cancer patients with clinical radiosensitivity. *Genome Integrity, 1*(1), 9.

Ferguson, D. O., & Alt, F. W. (2001). DNA double strand break repair and chromosomal translocation: lessons from animal models. *Oncogene, 20*(40), 5572-5579. doi: 10.1038/sj.onc.1204767

Flatmark, K., Nome, R., Folkvord, S., Bratland, A., Rasmussen, H., Ellefsen, M., . . . Ree, A. (2006). Radiosensitization of colorectal carcinoma cell lines by histone deacetylase inhibition. *Radiation Oncology, 1*(1), 25.

Fu, Y., Foden, J. A., Khayter, C., Maeder, M. L., Reyon, D., Joung, J. K., & Sander, J. D. (2013). High-frequency off-target mutagenesis induced by CRISPR-Cas nucleases in human cells. *Nat Biotech, 31*(9), 822-826. doi: 10.1038/nbt.2623

Fukao, T., Kaneko, H., Birrell, G., Gatei, M., Tashita, H., Yoshida, T., . . . Lavin, M. F. (1999). ATM is upregulated during the mitogenic response in peripheral blood mononuclear cells. *Blood, 94*(6), 1998-2006.

Gartel, A. L., & Tyner, A. L. (2002). The Role of the Cyclin-dependent Kinase Inhibitor p21 in Apoptosis 1 Supported in part by NIH Grant R01 DK56283 (to A. L. T.) for the p21 research and Campus Research Board and Illinois Department of Public Health Penny Severns Breast and Cervical Cancer grants (to A. L. G.).1. *Molecular Cancer Therapeutics, 1*(8), 639-649.

Giunta, S., Belotserkovskaya, R., & Jackson, S. P. (2010). DNA damage signaling in response to double-strand breaks during mitosis. *J Cell Biol, 190*(2), 197-207. doi: 10.1083/jcb.200911156

Goodarzi, A. A., Noon, A. T., Deckbar, D., Ziv, Y., Shiloh, Y., Lobrich, M., & Jeggo, P. A. (2008). ATM signaling facilitates repair of DNA double-strand breaks associated with heterochromatin. *Mol Cell, 31*(2), 167-177. doi: 10.1016/j.molcel.2008.05.017

Gu, W., & Roeder, R. G. (1997). Activation of p53 sequence-specific DNA binding by acetylation of the p53 C-terminal domain. *Cell, 90*(4), 595-606.

Gueven, N., Fukao, T., Luff, J., Paterson, C., Kay, G., Kondo, N., & Lavin, M. F. (2006). Regulation of the Atm promoter in vivo. *Genes Chromosomes and Cancer, 45*(1), 61-71. doi: 10.1002/gcc.20267

Guo, X., Yang, C., Qian, X., Lei, T., Li, Y., Shen, H., . . . Xu, B. (2013). Estrogen receptor α regulates ATM expression through miRNAs in breast cancer. *Clinical Cancer Research, 19*(18), 4994-5002. doi: 10.1158/1078-0432.CCR-12-3700

Haince, J. F., McDonald, D., Rodrigue, A., Dery, U., Masson, J. Y., Hendzel, M. J., & Poirier, G. G. (2008). PARP1-dependent kinetics of recruitment of MRE11 and NBS1 proteins to multiple DNA damage sites. *J Biol Chem, 283*(2), 1197-1208. doi: 10.1074/jbc.M706734200

Hamburger, A., & Salmon, S. (1977). Primary bioassay of human tumor stem cells. *Science, 197*(4302), 461-463. doi: 10.1126/science.560061

Hanahan, D., & Weinberg, Robert A. (2011). Hallmarks of Cancer: The Next Generation. *Cell, 144*(5), 646-674.

Heinrich, P. C., Behrmann, I., Müller-Newen, G., Schaper, F., & Graeve, L. (1998). Interleukin-6-type cytokine signalling through the gp130/Jak/STAT pathway. *Biochemical Journal, 334*(2), 297-314.

Hickson, I., Zhao, Y., Richardson, C. J., Green, S. J., Martin, N. M. B., Orr, A. I., . . . Smith, G. C. M. (2004). Identification and characterization of a novel and specific inhibitor of the ataxia-telangiectasia mutated kinase ATM. *Cancer Research, 64*(24), 9152-9159. doi: 10.1158/0008-5472.CAN-04-2727

Hirai, Y., Hayashi, T., Kubo, Y., Hoki, Y., Arita, I., Tatsumi, K., & Seyama, T. (2001). X-irradiation induces up-regulation of ATM gene expression in wild-type lymphoblastoid cell lines, but not in their heterozygous or homozygous ataxia-telangiectasia counterparts. *Japanese Journal of Cancer Research, 92*(6), 710-717.

Hirao, A., Cheung, A., Duncan, G., Girard, P. M., Elia, A. J., Wakeham, A., . . . Mak, T. W. (2002). Chk2 is a tumor suppressor that regulates apoptosis in both an ataxia telangiectasia mutated (ATM)-dependent and an ATM-independent manner. *Mol Cell Biol, 22*(18), 6521-6532.

Hirao, A., Kong, Y. Y., Matsuoka, S., Wakeham, A., Ruland, J., Yoshida, H., . . . Mak, T. W. (2000). DNA damage-induced activation of p53 by the checkpoint kinase Chk2. *Science, 287*(5459), 1824-1827.

Hochegger, H., Dejsuphong, D., Fukushima, T., Morrison, C., Sonoda, E., Schreiber, V., . . . Takeda, S. (2006). Parp-1 protects homologous recombination from interference by Ku and Ligase IV in vertebrate cells. *EMBO J, 25*(6), 1305-1314. doi: 10.1038/sj.emboj.7601015

Hodel, M. R., Corbett, A. H., & Hodel, A. E. (2001). Dissection of a nuclear localization signal. *Journal of Biological Chemistry, 276*(2), 1317-1325. doi: 10.1074/jbc.M008522200

Hollestelle, A., Peeters, J. K., Smid, M., Timmermans, M., Verhoog, L. C., Westenend, P. J., . . . Martens, J. W. (2013). Loss of E-cadherin is not a necessity for epithelial to mesenchymal transition in human breast cancer. *Breast Cancer Res Treat, 138*(1), 47-57. doi: 10.1007/s10549-013-2415-3

Hu, H., Du, L., Nagabayashi, G., Seeger, R. C., & Gatti, R. A. (2010). ATM is down-regulated by N-Myc-regulated microRNA-421. *Proceedings of the National Academy of Sciences of the United States of America, 107*(4), 1506-1511. doi: 10.1073/pnas.0907763107

Huang, R. L., Teo, Z., Chong, H. C., Zhu, P., Tan, M. J., Tan, C. K., . . . Tan, N. S. (2011). ANGPTL4 modulates vascular junction integrity by integrin signaling

and disruption of intercellular VE-cadherin and claudin-5 clusters. *Blood, 118*(14), 3990-4002. doi: 10.1182/blood-2011-01-328716

Ito, A., Lai, C. H., Zhao, X., Saito, S., Hamilton, M. H., Appella, E., & Yao, T. P. (2001). p300/CBP-mediated p53 acetylation is commonly induced by p53-activating agents and inhibited by MDM2. *EMBO J, 20*(6), 1331-1340. doi: 10.1093/emboj/20.6.1331

Jackson, S. P., & Bartek, J. (2009). The DNA-damage response in human biology and disease. *Nature, 461*(7267), 1071-1078. doi: 10.1038/nature08467

Jakkaraju, S., Zhe, X., Pan, D., Choudhury, R., & Schuger, L. (2005). TIPs are tension-responsive proteins involved in myogenic versus adipogenic differentiation. *Dev Cell, 9*(1), 39-49. doi: S1534-5807(05)00178-4 [pii]

10.1016/j.devcel.2005.04.015 [doi]

Jalal, S., Earley, J. N., & Turchi, J. J. (2011). DNA repair: from genome maintenance to biomarker and therapeutic target. *Clin Cancer Res, 17*(22), 6973-6984. doi: 10.1158/1078-0432.ccr-11-0761

Jans, D. A., Xiao, C. Y., & Lam, M. H. C. (2000). Nuclear targeting signal recognition: A key control point in nuclear transport? *BioEssays, 22*(6), 532-544. doi: 10.1002/(SICI)1521-1878(200006)22:6<532::AID-BIES6>3.0.CO;2-O

Jiang, H., Reinhardt, H. C., Bartkova, J., Tommiska, J., Blomqvist, C., Nevanlinna, H., . . . Hemann, M. T. (2009). The combined status of ATM and p53 link tumor development with therapeutic response. *Genes Dev, 23*(16), 1895-1909. doi: 10.1101/gad.1815309

Kaidi, A., & Jackson, S. P. (2013). KAT5 tyrosine phosphorylation couples chromatin sensing to ATM signalling. *Nature, 498*(7452), 70-74. doi: 10.1038/nature12201

Kalluri, R., & Weinberg, R. A. (2009). The basics of epithelial-mesenchymal transition. *The Journal of Clinical Investigation, 119*(6), 1420-1428. doi: 10.1172/JCI39104

Kamiya, A., Kinoshita, T., & Miyajima, A. (2001). Oncostatin M and hepatocyte growth factor induce hepatic maturation via distinct signaling pathways. *FEBS Letters, 492*(1-2), 90-94. doi: 10.1016/S0014-5793(01)02140-8

Keating, K. E., Gueven, N., Watters, D., Rodemann, H. P., & Lavin, M. F. (2001). Transcriptional downregulation of ATM by EGF is defective in ataxia-telangiectasia cells expressing mutant protein. *Oncogene, 20*(32), 4281-4290. doi: 10.1038/sj.onc.1204527

Kennedy, R. D., & D'Andrea, A. D. (2005). The Fanconi Anemia/BRCA pathway: new faces in the crowd. *Genes Dev, 19*(24), 2925-2940. doi: 10.1101/gad.1370505

Khanna, K. K., & Chenevix-Trench, G. (2004). ATM and genome maintenance: Defining its role in breast cancer susceptibility. *Journal of Mammary Gland Biology and Neoplasia, 9*(3), 247-262. doi: 10.1023/B:JOMG.0000048772.92326.a1

Khanna, K. K., Keating, K. E., Kozlov, S., Scott, S., Gatei, M., Hobson, K., . . . Lavin, M. F. (1998). ATM associates with and phosphorylates p53: mapping the region of interaction. *Nat Genet, 20*(4), 398-400. doi: 10.1038/3882

Kim, S. T., Lim, D. S., Canman, C. E., & Kastan, M. B. (1999). Substrate specificities and identification of putative substrates of ATM kinase family members. *J Biol Chem, 274*(53), 37538-37543.

Kim, W. J., Vo, Q. N., Shrivastav, M., Lataxes, T. A., & Brown, K. D. (2002). Aberrant methylation of the ATM promoter correlates with increased radiosensitivity in a human colorectal tumor cell line. *Oncogene, 21*(24), 3864-3871. doi: 10.1038/sj.onc.1205485

Kozbial, P., & Mushegian, A. (2005). Natural history of S-adenosylmethionine-binding proteins. *BMC Structural Biology, 5*(1), 19.

Kuljis, R. O., Xu, Y., Aguila, M. C., & Baltimore, D. (1997). Degeneration of neurons, synapses, and neuropil and glial activation in a murine Atm knockout model of ataxia-telangiectasia. *Proceedings of the National Academy of Sciences of the United States of America, 94*(23), 12688-12693. doi: 10.1073/pnas.94.23.12688

Lee, J. H., Goodarzi, A. A., Jeggo, P. A., & Paull, T. T. (2010). 53BP1 promotes ATM activity through direct interactions with the MRN complex. *EMBO J, 29*(3), 574-585. doi: 10.1038/emboj.2009.372

Lee, J. H., & Paull, T. T. (2004). Direct Activation of the ATM Protein Kinase by the Mre11/Rad50/Nbs1 Complex. *Science, 304*(5667), 93-96. doi: 10.1126/science.1091496

Lee, T. I., Johnstone, S. E., & Young, R. A. (2006). Chromatin immunoprecipitation and microarray-based analysis of protein location. *Nat. Protocols, 1*(2), 729-748.

Levy, D. E., & Darnell, J. E. (2002). STATs: transcriptional control and biological impact. *Nat Rev Mol Cell Biol, 3*(9), 651-662.

Lipson, R. S., Webb, K. J., & Clarke, S. G. (2010). Two novel methyltransferases acting upon eukaryotic elongation factor 1A in Saccharomyces cerevisiae. *Archives of Biochemistry and Biophysics, 500*(2), 137-143. doi: 10.1016/j.abb.2010.05.023

Liu, J., Yue, Y., Han, D., Wang, X., Fu, Y., Zhang, L., . . . He, C. (2013). A METTL3-METTL14 complex mediates mammalian nuclear RNA N6-adenosine methylation. *Nat Chem Biol, advance online publication*. doi: 10.1038/nchembio.1432

Loenen, W. A. (2006). S-adenosylmethionine: jack of all trades and master of everything? *Biochem Soc Trans, 34*(Pt 2), 330-333. doi: 10.1042/bst20060330

Lord, C. J., & Ashworth, A. (2012). The DNA damage response and cancer therapy. *Nature, 481*(7381), 287-294. doi: 10.1038/nature10760

Lossaint, G., Besnard, E., Fisher, D., Piette, J., & Dulic, V. (2011). Chk1 is dispensable for G2 arrest in response to sustained DNA damage when the ATM/p53/p21 pathway is functional. *Oncogene, 30*(41), 4261-4274. doi: 10.1038/onc.2011.135

Ma, X., Yang, L., Xiao, L., Tang, M., Liu, L., Li, Z., . . . Cao, Y. (2011). Down-regulation of EBV-LMP1 radio-sensitizes nasal pharyngeal carcinoma

cells via nf-κb regulated ATM expression. *PLoS ONE, 6*(11). doi: 10.1371/journal.pone.0024647

Mali, P., Yang, L., Esvelt, K. M., Aach, J., Guell, M., DiCarlo, J. E., . . . Church, G. M. (2013). RNA-guided human genome engineering via Cas9. *Science, 339*(6121), 823-826. doi: 10.1126/science.1232033

Mansour, W. Y., Bogdanova, N. V., Kasten-Pisula, U., Rieckmann, T., Köcher, S., Borgmann, K., . . . Dahm-Daphi, J. (2013). Aberrant overexpression of miR-421 downregulates ATM and leads to a pronounced DSB repair defect and clinical hypersensitivity in SKX squamous cell carcinoma. *Radiotherapy and Oncology, 106*(1), 147-154. doi: 10.1016/j.radonc.2012.10.020

Martin, J. L., & McMillan, F. M. (2002). SAM (dependent) I AM: the S-adenosylmethionine-dependent methyltransferase fold. *Curr Opin Struct Biol, 12*(6), 783-793.

Matsuoka, S., Ballif, B. A., Smogorzewska, A., McDonald, E. R., 3rd, Hurov, K. E., Luo, J., . . . Elledge, S. J. (2007). ATM and ATR substrate analysis reveals extensive protein networks responsive to DNA damage. *Science, 316*(5828), 1160-1166. doi: 10.1126/science.1140321

Meek, D. W. (2004). The p53 response to DNA damage. *DNA Repair, 3*(8-9), 1049-1056. doi: 10.1016/j.dnarep.2004.03.027

Meek, D. W. (2009). Tumour suppression by p53: a role for the DNA damage response? *Nat Rev Cancer, 9*(10), 714-723. doi: 10.1038/nrc2716

Mitui, M., Nahas, S. A., Du, L. T., Yang, Z., Lai, C. H., Nakamura, K., . . . Gatti, R. A. (2009). Functional and computational assessment of missense variants in the ataxia-telangiectasia mutated (ATM) gene: Mutations with increased cancer risk. *Human Mutation, 30*(1), 12-21. doi: 10.1002/humu.20805

Moat, S. J., & McDowell, I. F. W. (2002). HOMOCYSTEINE IN HEALTH AND DISEASE. *Brain, 125*(3), 682-683. doi: 10.1093/brain/awf065

Morrison, A. J., Kim, J. A., Person, M. D., Highland, J., Xiao, J., Wehr, T. S., . . . Shen, X. (2007). Mec1/Tel1 phosphorylation of the INO80 chromatin remodeling complex influences DNA damage checkpoint responses. *Cell, 130*(3), 499-511. doi: 10.1016/j.cell.2007.06.010

Murray, P. J. (2007). The JAK-STAT Signaling Pathway: Input and Output Integration. *The Journal of Immunology, 178*(5), 2623-2629.

Ng, W. L., Yan, D., Zhang, X., Mo, Y. Y., & Wang, Y. (2010). Over-expression of miR-100 is responsible for the low-expression of ATM in the human glioma cell line: M059J. *DNA Repair, 9*(11), 1170-1175. doi: 10.1016/j.dnarep.2010.08.007

Noma, A., Yi, S., Katoh, T., Takai, Y., Suzuki, T., & Suzuki, T. (2011). Actin-binding protein ABP140 is a methyltransferase for 3-methylcytidine at position 32 of tRNAs in Saccharomyces cerevisiae. *RNA, 17*(6), 1111-1119. doi: 10.1261/rna.2653411

Onder, T. T., Gupta, P. B., Mani, S. A., Yang, J., Lander, E. S., & Weinberg, R. A. (2008). Loss of E-Cadherin Promotes Metastasis via Multiple Downstream

Transcriptional Pathways. *Cancer Research, 68*(10), 3645-3654. doi: 10.1158/0008-5472.can-07-2938

Palmieri, D., Valentino, T., D'Angelo, D., De Martino, I., Postiglione, I., Pacelli, R., . . . Fusco, A. (2011). HMGA proteins promote ATM expression and enhance cancer cell resistance to genotoxic agents. *Oncogene, 30*(27), 3024-3035. doi: 10.1038/onc.2011.21

Petrossian, T., & Clarke, S. (2009). Bioinformatic Identification of Novel Methyltransferases. *Epigenomics, 1*(1), 163-175. doi: 10.2217/epi.09.3

Petrossian, T. C., & Clarke, S. G. (2011). Uncovering the human methyltransferasome. *Mol Cell Proteomics, 10*(1), M110 000976. doi: 10.1074/mcp.M110.000976

Postel-Vinay, S., Vanhecke, E., Olaussen, K. A., Lord, C. J., Ashworth, A., & Soria, J.-C. (2012). The potential of exploiting DNA-repair defects for optimizing lung cancer treatment. *Nat Rev Clin Oncol, 9*(3), 144-155.

Przanowski, P., Dabrowski, M., Ellert-Miklaszewska, A., Kloss, M., Mieczkowski, J., Kaza, B., . . . Kaminska, B. (2013). The signal transducers Stat1 and Stat3 and their novel target Jmjd3 drive the expression of inflammatory genes in microglia. *J Mol Med (Berl)*. doi: 10.1007/s00109-013-1090-5

Qased, A. B., Yi, H., Liang, N., Ma, S., Qiao, S., & Liu, X. (2013). MicroRNA-18a upregulates autophagy and ataxia telangiectasiamutated gene expression in HCT116 colon cancer cells. *Molecular Medicine Reports, 7*(2), 559-564. doi: 10.3892/mmr.2012.1214

Rass, E., Chandramouly, G., Zha, S., Alt, F. W., & Xie, A. (2013). Ataxia telangiectasia mutated (ATM) is dispensable for endonuclease I-Scei-induced homologous recombination in mouse embryonic stem cells. *Journal of Biological Chemistry, 288*(10), 7086-7095. doi: 10.1074/jbc.M112.445825

Reid, R., Greene, P. J., & Santi, D. V. (1999). Exposition of a family of RNA m(5)C methyltransferases from searching genomic and proteomic sequences. *Nucleic Acids Res, 27*(15), 3138-3145.

Richon, V. M., Johnston, D., Sneeringer, C. J., Jin, L., Majer, C. R., Elliston, K., . . . Copeland, R. A. (2011). Chemogenetic Analysis of Human Protein Methyltransferases. *Chem Biol Drug Des, 78*(2), 199-210. doi: 10.1111/j.1747-0285.2011.01135.x

Rogakou, E. P., Pilch, D. R., Orr, A. H., Ivanova, V. S., & Bonner, W. M. (1998). DNA Double-stranded Breaks Induce Histone H2AX Phosphorylation on Serine 139. *Journal of Biological Chemistry, 273*(10), 5858-5868. doi: 10.1074/jbc.273.10.5858

Rothkamm, K., Krüger, I., Thompson, L. H., & Löbrich, M. (2003). Pathways of DNA Double-Strand Break Repair during the Mammalian Cell Cycle. *Molecular and Cellular Biology, 23*(16), 5706-5715. doi: 10.1128/mcb.23.16.5706-5715.2003

Roy, K., Wang, L., Makrigiorgos, G. M., & Price, B. D. (2006). Methylation of the ATM promoter in glioma cells alters ionizing radiation sensitivity. *Biochem Biophys Res Commun, 344*(3), 821-826. doi: 10.1016/j.bbrc.2006.03.222

Rubbi, C. P., & Milner, J. (2003). Disruption of the nucleolus mediates stabilization of p53 in response to DNA damage and other stresses. *The EMBO Journal, 22*(22), 6068-6077. doi: 10.1093/emboj/cdg579

Savitsky, K., Bar-Shira, A., Gilad, S., Rotman, G., Ziv, Y., Vanagaite, L., . . . Shiloh, Y. (1995). A single ataxia telangiectasia gene with a product similar to PI-3 kinase. *Science, 268*(5218), 1749-1753.

Schubert, H. L., Blumenthal, R. M., & Cheng, X. (2003). Many paths to methyltransfer: a chronicle of convergence. *Trends in Biochemical Sciences, 28*(6), 329-335. doi: 10.1016/s0968-0004(03)00090-2

Shen, L., Yin, Z. H., Wan, Y., Zhang, Y., Li, K., & Zhou, B. S. (2012). Association between ATM polymorphisms and cancer risk:a meta-analysis. *Molecular Biology Reports, 39*(5), 5719-5725. doi: 10.1007/s11033-011-1381-2

Shi, Y., Venkataraman, S. L., Dodson, G. E., Mabb, A. M., LeBlanc, S., & Tibbetts, R. S. (2004). Direct regulation of CREB transcriptional activity by ATM in response to genotoxic stress. *Proceedings of the National Academy of Sciences of the United States of America, 101*(16), 5898-5903. doi: 10.1073/pnas.0307718101

Shieh, S.-Y., Ahn, J., Tamai, K., Taya, Y., & Prives, C. (2000). The human homologs of checkpoint kinases Chk1 and Cds1 (Chk2) phosphorylate p53 at multiple DNA damage-inducible sites. *Genes & development, 14*(3), 289-300. doi: 10.1101/gad.14.3.289

Shieh, S. Y., Ikeda, M., Taya, Y., & Prives, C. (1997). DNA damage-induced phosphorylation of p53 alleviates inhibition by MDM2. *Cell, 91*(3), 325-334.

Shiloh, Y., & Ziv, Y. (2013). The ATM protein kinase: regulating the cellular response to genotoxic stress, and more. *Nat Rev Mol Cell Biol, 14*(4), 197-210.

Shrivastav, M., De Haro, L. P., & Nickoloff, J. A. (2008). Regulation of DNA double-strand break repair pathway choice. *Cell Res, 18*(1), 134-147. doi: 10.1038/cr.2007.111

Silver, P. A. (1991). How proteins enter the nucleus. *Cell, 64*(3), 489-497. doi: 10.1016/0092-8674(91)90233-O

Song, L., Lin, C., Wu, Z., Gong, H., Zeng, Y., Wu, J., . . . Li, J. (2011). MiR-18a impairs DNA damage response through downregulation of Ataxia telangiectasia mutated (ATM) kinase. *PLoS ONE, 6*(9). doi: 10.1371/journal.pone.0025454

Song, L., Rawal, B., Nemeth, J. A., & Haura, E. B. (2011). JAK1 activates STAT3 activity in non-small-cell lung cancer cells and IL-6 neutralizing antibodies can suppress JAK1-STAT3 signaling. *Molecular Cancer Therapeutics, 10*(3), 481-494. doi: 10.1158/1535-7163.MCT-10-0502

Srivastava, N., Gochhait, S., de Boer, P., & Bamezai, R. N. (2009). Role of H2AX in DNA damage response and human cancers. *Mutat Res, 681*(2-3), 180-188. doi: 10.1016/j.mrrev.2008.08.003

Stewart, G. S., Wang, B., Bignell, C. R., Taylor, A. M., & Elledge, S. J. (2003). MDC1 is a mediator of the mammalian DNA damage checkpoint. *Nature, 421*(6926), 961-966. doi: 10.1038/nature01446

Struck, A. W., Thompson, M. L., Wong, L. S., & Micklefield, J. (2012). S-adenosyl-methionine-dependent methyltransferases: highly versatile enzymes in biocatalysis, biosynthesis and other biotechnological applications. *Chembiochem, 13*(18), 2642-2655. doi: 10.1002/cbic.201200556

Sun, Y., Jiang, X., Chen, S., Fernandes, N., & Price, B. D. (2005). A role for the Tip60 histone acetyltransferase in the acetylation and activation of ATM. *Proc Natl Acad Sci U S A, 102*(37), 13182-13187. doi: 10.1073/pnas.0504211102

Sun, Y., Xu, Y., Roy, K., & Price, B. D. (2007). DNA damage-induced acetylation of lysine 3016 of ATM activates ATM kinase activity. *Mol Cell Biol, 27*(24), 8502-8509. doi: 10.1128/MCB.01382-07

Takeda, K., Noguchi, K., Shi, W., Tanaka, T., Matsumoto, M., Yoshida, N., . . . Akira, S. (1997). Targeted disruption of the mouse Stat3 gene leads to early embryonic lethality. *Proceedings of the National Academy of Sciences, 94*(8), 3801-3804.

Tjeertes, J. V., Miller, K. M., & Jackson, S. P. (2009). Screen for DNA-damage-responsive histone modifications identifies H3K9Ac and H3K56Ac in human cells. *EMBO J, 28*(13), 1878-1889. doi: 10.1038/emboj.2009.119

Traven, A., & Heierhorst, J. (2005). SQ/TQ cluster domains: concentrated ATM/ATR kinase phosphorylation site regions in DNA-damage-response proteins. *BioEssays, 27*(4), 397-407. doi: 10.1002/bies.20204

Truman, J. P., Rotenberg, S. A., Kang, J. H., Lerman, G., Fuks, Z., Kolesnick, R., . . . Haimovitz-Friedman, A. (2009). PKCα activation downregulates ATM and radio-sensitizes androgen-sensitive human prostate cancer cells in vitro and in vivo. *Cancer Biology and Therapy, 8*(1), 54-63.

Uziel, T., Lerenthal, Y., Moyal, L., Andegeko, Y., Mittelman, L., & Shiloh, Y. (2003). Requirement of the MRN complex for ATM activation by DNA damage. *EMBO J, 22*(20), 5612-5621. doi: 10.1093/emboj/cdg541

van Roy, F., & Berx, G. (2008). The cell-cell adhesion molecule E-cadherin. *Cell Mol Life Sci, 65*(23), 3756-3788. doi: 10.1007/s00018-008-8281-1

Vo, Q. N., Kim, W. J., Cvitanovic, L., Boudreau, D. A., Ginzinger, D. G., & Brown, K. D. (2004). The ATM gene is a target for epigenetic silencing in locally advanced breast cancer. *Oncogene, 23*(58), 9432-9437. doi: 10.1038/sj.onc.1208092

Vogelstein, B., Lane, D., & Levine, A. J. (2000). Surfing the p53 network. *Nature, 408*(6810), 307-310. doi: 10.1038/35042675

Vousden, K. H. (2006). Outcomes of p53 activation - Spoilt for choice. *Journal of Cell Science, 119*(24), 5015-5020. doi: 10.1242/jcs.03293

Wang, B., Matsuoka, S., Carpenter, P. B., & Elledge, S. J. (2002). 53BP1, a mediator of the DNA damage checkpoint. *Science, 298*(5597), 1435-1438. doi: 10.1126/science.1076182

Wang, H., Chen, X., He, T., Zhou, Y., & Luo, H. (2013). Evidence for Tissue-Specific JAK/STAT Target Genes in Drosophila Optic Lobe Development. *Genetics*. doi: 10.1534/genetics.113.155945

Wang, Y., Yu, Y., Tsuyada, A., Ren, X., Wu, X., Stubblefield, K., . . . Wang, S. E. (2011). Transforming growth factor-beta regulates the sphere-initiating stem cell-like feature in breast cancer through miRNA-181 and ATM. *Oncogene, 30*(12), 1470-1480. doi: 10.1038/onc.2010.531

Wendt, J., Radetzki, S., Von Haefen, C., Hemmati, P. G., Güner, D., Schulze-Osthoff, K., . . . Daniel, P. T. (2006). Induction of p21CIP/WAF-1 and G2 arrest by ionizing irradiation impedes caspase-3-mediated apoptosis in human carcinoma cells. *Oncogene, 25*(7), 972-980. doi: 10.1038/sj.onc.1209031

Wu, C. W., Dong, Y. J., Liang, Q. Y., He, X. Q., Ng, S. S. M., Chan, F. K. L., . . . Yu, J. (2013). MicroRNA-18a Attenuates DNA Damage Repair through Suppressing the Expression of Ataxia Telangiectasia Mutated in Colorectal Cancer. *PLoS ONE, 8*(2). doi: 10.1371/journal.pone.0057036

Wu, Z. H., Shi, Y., Tibbetts, R. S., & Miyamoto, S. (2006). Molecular linkage between the kinase ATM and NF-kappaB signaling in response to genotoxic stimuli. *Science, 311*(5764), 1141-1146. doi: 10.1126/science.1121513

Wymann, M. P., Bulgarelli-Leva, G., Zvelebil, M. J., Pirola, L., Vanhaesebroeck, B., Waterfield, M. D., & Panayotou, G. (1996). Wortmannin inactivates phosphoinositide 3-kinase by covalent modification of Lys-802, a residue involved in the phosphate transfer reaction. *Mol Cell Biol, 16*(4), 1722-1733.

Wysocka, J., Reilly, P. T., & Herr, W. (2001). Loss of HCF-1–Chromatin Association Precedes Temperature-Induced Growth Arrest of tsBN67 Cells. *Molecular and Cellular Biology, 21*(11), 3820-3829. doi: 10.1128/mcb.21.11.3820-3829.2001

Xie, G., Habbersett, R. C., Jia, Y., Peterson, S. R., Lehnert, B. E., Bradbury, E. M., & D'Anna, J. A. (1998). Requirements for p53 and the ATM gene product in the regulation of G1/S and S phase checkpoints. *Oncogene, 16*(6), 721-736. doi: 10.1038/sj.onc.1201793

Xu, Y., Ashley, T., Brainerd, E. E., Bronson, R. T., Meyn, M. S., & Baltimore, D. (1996). Targeted disruption of ATM leads to growth retardation, chromosomal fragmentation during meiosis, immune defects, and thymic lymphoma. *Genes and Development, 10*(19), 2411-2422.

Xu, Y., & Baltimore, D. (1996). Dual roles of ATM in the cellular response to radiation and in cell growth control. *Genes and Development, 10*(19), 2401-2410.

Yamamoto, K., Nihrane, A., Aglipay, J., Sironi, J., Arkin, S., Lipton, J. M., . . . Liu, J. M. (2008). Upregulated ATM gene expression and activated DNA crosslink-induced damage response checkpoint in Fanconi anemia: implications for carcinogenesis. *Mol Med, 14*(3-4), 167-174. doi: 10.2119/2007-00122.Yamamoto

Yan, D., Ng, W. L., Zhang, X., Wang, P., Zhang, Z., Mo, Y. Y., . . . Wang, Y. (2010). Targeting DNA-PKcs and ATM with miR-101 sensitizes tumors to radiation. *PLoS ONE, 5*(7). doi: 10.1371/journal.pone.0011397

Ying, Q.-L., Nichols, J., Chambers, I., & Smith, A. (2003). BMP Induction of Id Proteins Suppresses Differentiation and Sustains Embryonic Stem Cell Self-Renewal in Collaboration with STAT3. *Cell, 115*(3), 281-292.

Yu, H., Pardoll, D., & Jove, R. (2009). STATs in cancer inflammation and immunity: a leading role for STAT3. *Nat Rev Cancer, 9*(11), 798-809. doi: 10.1038/nrc2734

Zhang, Q., van der Donk, W. A., & Liu, W. (2012). Radical-mediated enzymatic methylation: a tale of two SAMS. *Acc Chem Res, 45*(4), 555-564. doi: 10.1021/ar200202c

Zhang, Q., Wang, H. Y., Woetmann, A., Raghunath, P. N., Odum, N., & Wasik, M. A. (2006). STAT3 induces transcription of the DNA methyltransferase 1 gene (DNMT1) in malignant T lymphocytes. *Blood, 108*(3), 1058-1064. doi: 10.1182/blood-2005-08-007377

Zhang, Y., Cho, Y. Y., Petersen, B. L., Bode, A. M., Zhu, F., & Dong, Z. (2003). Ataxia telangiectasia mutated proteins, MAPKs, and RSK2 are involved in the phosphorylation of STAT3. *J Biol Chem, 278*(15), 12650-12659. doi: 10.1074/jbc.M210368200

Zhou, B. B. S., & Elledge, S. J. (2000). The DNA damage response: Putting checkpoints in perspective. *Nature, 408*(6811), 433-439. doi: 10.1038/35044005